Design of Novel Polymerization System via Mechanistic Transformation of Active Species during Vinyl Polymerization

Hiroshi AOSHIMA

Design of Novel Polymerization System via Mechanistic Transformation of Active Species during Vinyl Polymerization

ビニル重合における活性種の変換を伴う
新規重合系の設計

Hiroshi AOSHIMA

青嶋 紘

2013

Contents

General Introduction 1

Part I **$FeCl_3$-Mediated Mechanistic Transformation from Living Cationic into Radical Polymerization**

Chapter 1 Iron(III) Chloride/R–Cl/Tributylphosphine for Metal- Catalyzed Living Radical Polymerization: A Unique System with a Higher Oxidation State Iron Complex 23

Chapter 2 A Simple Combination of Higher Oxidation State FeX_3 and Phosphine or Amine Ligand for Living Radical Polymerization of Styrene, Methacrylate and Acrylate 39

Chapter 3 In-Situ Direct Mechanistic Transformation from $FeCl_3$- Catalyzed Living Cationic to Radical Polymerizations 67

Part II **Simultaneous Living Cationic and Radical Polymerization via Interconvertible Dual Active Species**

Chapter 4 Interconvertible Dual Active Species during Vinyl Polymerization: Giving Jekyll-and-Hyde Nature to Dormant Covalent Bond 89

Chapter 5 Interconvertible Concurrent Living Cationic and Radical Polymerization of Various Monomers for Synthesis of Novel Copolymers 107

Part III **Direct Mechanistic Transformation from Living Anionic into Radical Polymerization**

Chapter 6 Direct Mechanistic Transformation from Stereospecific Living Anionic Polymerizations of Methyl Methacrylate to Metal- Catalyzed Living Radical Polymerizaitons 133

List of Publications 151

Acknowledgement 153

General Introduction

Background

Growing Active Species during Vinyl Polymerization

Chain-growth polymerization of vinyl monomers proceeds via successive addition of monomers to an intermediate, which is so-called active species generated from the initiator, leading to the formation of polymer chains (Scheme 1).[1] The active species are mechanistically classified into radical, cation, and anion according to their electronic charge on the carbon atom. The polymer chain generally grows via single active species originating from the initiator whereas type of the active species should be chosen depending on the monomer structure, meaning that there are always limitations of polymerizable monomers for a certain intermediate. For instance, cationic polymerization readily takes place for electron-donating monomers such as vinyl ethers, isobutene, and styrenes, whereas anionic polymerization proceeds only for the monomers bearing conjugated substituents including styrene, (meth)acrylates, and conjugated dienes. On the other hand, radical species enables polymerization of a wide range of monomers including not only styrenes and (meth)acrylates but also vinyl esters. Vinyl ethers cannot be homopolymerized via radical process but undergo radical copolymerization with electron-withdrawing monomers.

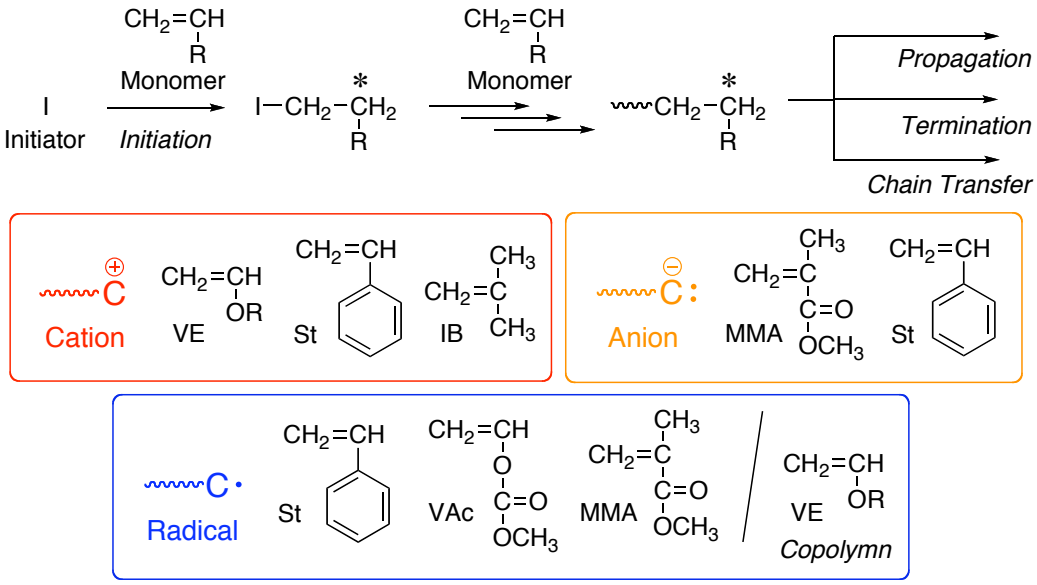

Scheme 1. Growing Active Species of Vinyl Polymerization

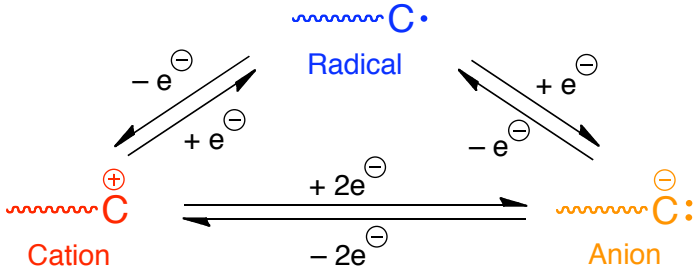

Scheme 2. Mechanistic Transformation of Active Species by Electron Transfer

In principle, an active species can be converted into another type of active species by electron transfer, i.e., radical species is transformed into cationic or anionic counterpart by the one-electron oxidation or reduction, respectively (Scheme 2). Based on this concept, there have been several reports on the in-situ one-time conversion of active species during polymerization by the electron transfer, which consequently affords block copolymers.[2–6] For example, Kamachi et al. demonstrated that the terminal electron-rich radical species in radical polymerization of *p*-methoxystyrene was oxidized into the corresponding carbocation by $Ph_2I^+PF_6^-$, followed by its cationic polymerization.[5] The transformation reaction from cationic into anionic species was also reported by Endo et al., where the cationic species of poly(THF) was converted into anionic one via two-electron reduction induced by SmI_2 for the subsequent block copolymerization of methacrylic monomer.[6]

Living Polymerization

Living polymerization is a chain-growth polymerization, which consists of only initiation and propagation and is free from side reactions, such as chain-transfer and termination (Figure 1). When the initiation is sufficiently faster than the propagation in living polymerization, all the initiator molecules can generate the polymer chains, indicating that one polymer chain is generated from one initiator molecule. As a result, the molecular weight of the obtained polymer is determined by the feed ratio of monomer to initiator and increases in direct proportion to the monomer conversion keeping narrow molecular weight distributions. This method allows

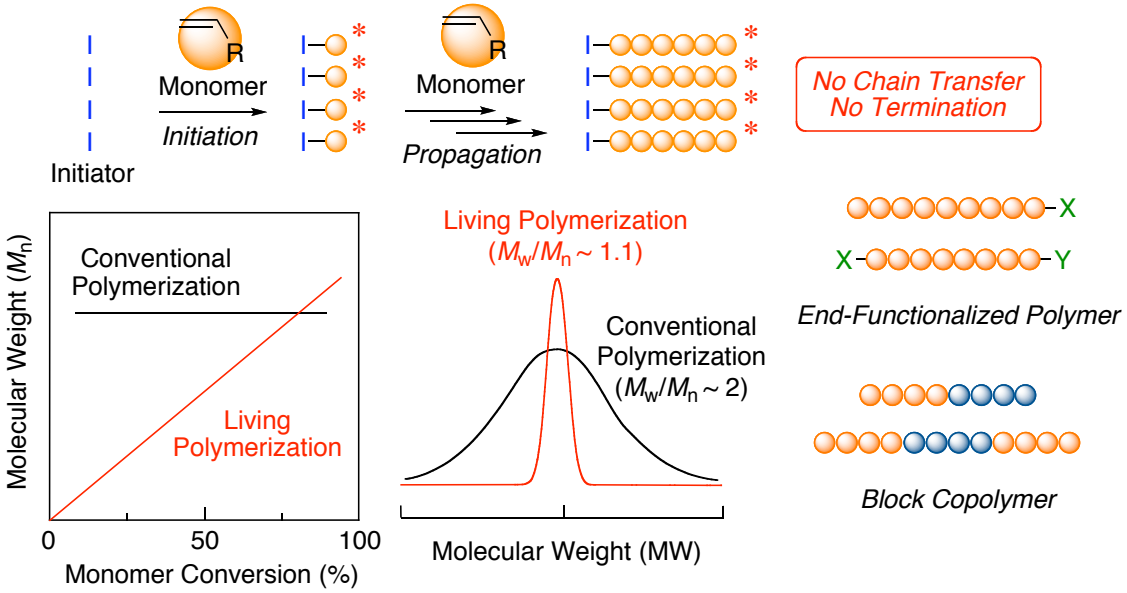

Figure 1. Living Polymerization Schematic

not only the precise control of molecular weight and molecular weight distribution, but also the synthesis of a wide variety of well-defined macromolecular architectures, such as block and end-functionalized polymers.

Living Anionic Polymerization

Living polymerization was first discovered in styrene polymerization via anionic mechanism by Szwarc in 1956.[7] In the anionic polymerization of non-polar monomers, since the growing anionic species are inherently stable, neither termination nor chain-transfer occurs in the absence of impurities, such as water and oxygen.[8,9] In contrast, the anionic polymerization of methyl methacrylate (MMA) is often accompanied by the termination through nucleophillic attack of the propagating enolate anion to antepenultimate or penpenultimate ester carbonyl group forming a cyclic β-ketoester.[10] However, a bulky initiator and a low temperature can suppress the side reactions to result in the polymers with controlled molecular weight.[11] Furthermore, *t*BuMgBr (in toluene)[12] or diphenylhexyllithium (DPHLi) (in THF)[13] effectively induces the stereospecific living anionic polymerization of MMA to produce highly isotactic or syndiotactic PMMA, respectively.

Living Polymerization Based on Dormant Species

Apart from the ideal living anionic polymerizations via such stable anionic species, various approaches have been attempted to overcome the inherent side reactions by using dynamic equilibrium for the unstable growing species.

Consequently, tremendous progresses have been attained in living polymerizations via various active species during the past three decades.[14] Most of these living polymerizations are based on a common concept (Scheme 3), in which the active species at growing terminal is temporally converted into the stable covalent species in dormant state to suppress the side reactions. The dormant terminal can be reversibly activated to generate the growing active species upon some stimuli such as heat, light, catalysts, and another growing chain end. At all events, the fast and reversible activation of the dormant species gives almost equal opportunities for propagation to all dormant terminals to result in the controlled molecular weight and narrow molecular weight distributions. Such a concept has been applied not only for the anionic polymerization, such as group transfer polymerization (GTP)[15], but also for cationic[18–21] and radical polymerizatons[29–33], which had been considered difficult to accomplish for a long term. Details of the living cationic and radical polymerization will be described in the following section.

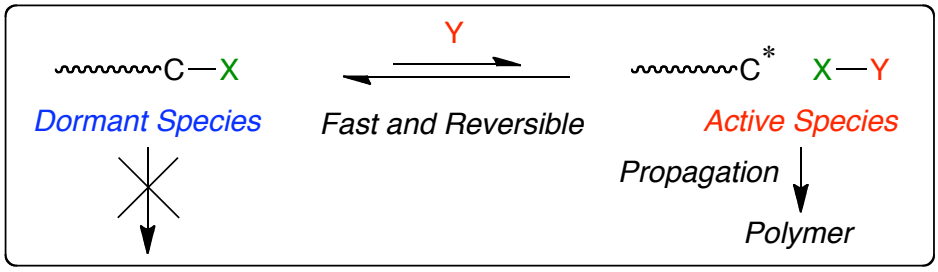

Scheme 3. Reversible Equilibrium between Dormant and Active Species

Living Cationic Polymerization

In general, cationic polymerization involves an inherent drawback in terms of controlling polymerization, i.e., chain transfer via elimination of the β-protons abstracted by monomer and counteranions.[16] In 1984, Higashimura and Sawamoto first discovered living cationic polymerization of vinyl ether with HI/I_2 system based on the concept for reversible activation of dormant species with C–I bond, which is derived from HI and the monomer, by I_2 as a Lewis acid.[17] Since then, various living cationic polymerizations have been developed via similar Lewis-acid assisted two-electron reversible activation of dormant species possessing carbon-halogen and carbon-oxygen bonds (Scheme 4).[18–21] These dormant species are converted into the growing carbocation by Lewis Acid as the catalyst, including Zn(II),[22] Al(III),[23] Sn(IV),[24] Ti(IV),[25] Fe(III),[26] etc. A key to the living cationic polymerizations is the stabilization of unstable carbocation with the nucleophilic counteranion originating from the initiator and Lewis acid or with the added base. For this, the judicious choices of the dormant species derived from initiator, Lewis acid, and additives are important for the living cationic polymerization of various monomers including vinyl ethers and styrenes.

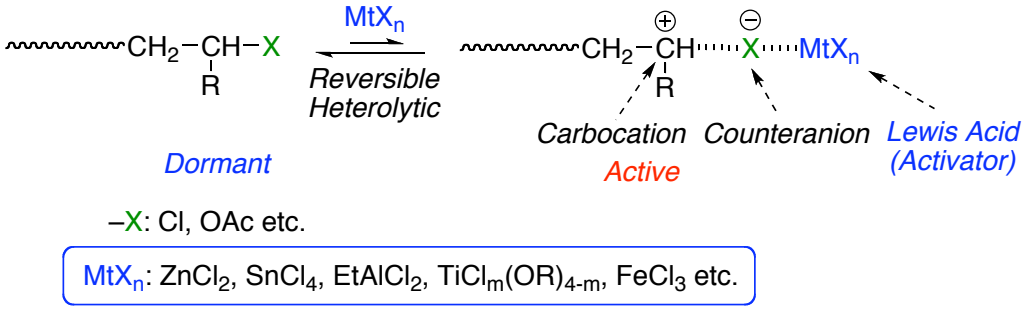

Scheme 4. Living Cationic Polymerization

Living Radical Polymerization

In sharp contrast to the ionic polymerizations, radical polymerization inherently involves bimolecular termination reactions, such as disproportionation and recombination, due to the neutral nature of the growing species.[27,28] Even in such a radical process, the reversible activation of dormant species also led to the discovery of a large variety of living radical polymerizations in the 1990s, i.e., nitroxide-mediated polymerization (NMP),[29] transition metal-catalyzed living radical polymerization or atom transfer radical polymerization (ATRP),[30–32] and reversible addition-fragmentation chain transfer (RAFT) polymerization.[33]

Transition Metal-Catalyzed Living Radical Polymerization or ATRP

Transition metal-catalyzed living radical polymerization was discovered via evolution of metal-catalyzed Kharasch or atom transfer radical addition[34] into radical polymerization as an analogy to living cationic polymerization. In this polymerization, dormant carbon-halogen bond, which is also employed as dormant species in living cationic polymerization, is reversibly activated by transition metal catalyst along with one-electron redox reaction of the metal center (Scheme 5). The transition-metal catalysts effective for this system include Ru(II),[35] Cu(I),[36–38] Fe(II),[39,40] Ni(II),[41,42] Mn(0)[43] etc., which are basically in lower oxidation state to trigger the one electron transfer from the metal to the dormant species. Since the catalyst is the most important component in this polymerization, an appropriate combination of central metals and their ligands as well as the halogens in the dormant species is necessary for controlling the polymerization.

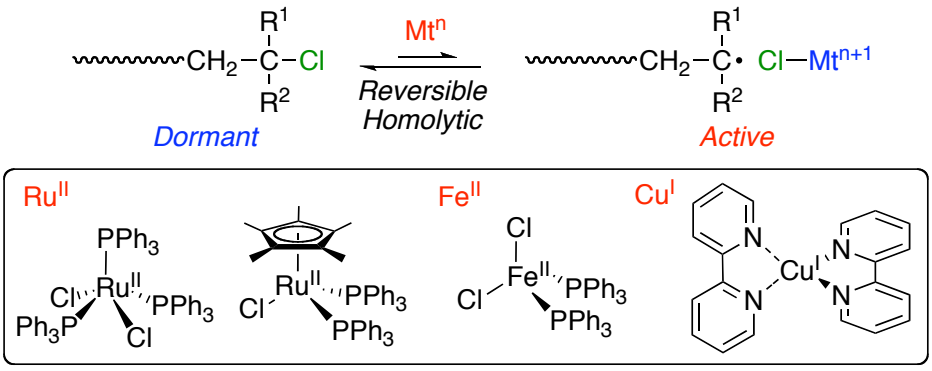

Scheme 5. Transition Metal-Catalyzed Living Radical Polymerization or ATRP

Reversible Addition-Fragmentation Chain Transfer (RAFT) Polymerization

The RAFT polymerization is another effective living radical polymerization with the dithioester compound [R–SC(S)Z], proceeding via one-electron reversible activation of the dormant C-S bond by radical species originating from radical initiator, in which degenerative transfer mechanism works for the control of molecular weight (Scheme 6). For controlling the polymerization, it is most important to design the RAFT agent depending on the monomer structure. In general, the sulfur compounds, such as dithiobenzoate (Z = Ph)[44] and trithiocarbonate (Z = SR')[45] can be used for the living polymerization of conjugated monomers, whereas xanthate (Z = OR)[46] and dithiocarbamete (Z =NR'R'')[47] are effective for controlling the polymerization of unconjugated ones.

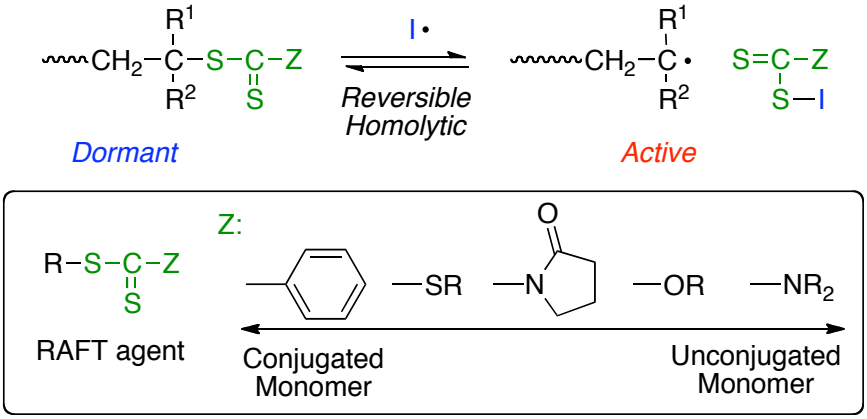

Scheme 6. Reversible Addition-Fragmentation Chain Transfer (RAFT) Polymerization

Objectives

From these backgrounds, the author aims to develop novel living polymerizations accompanying mechanistic transformation of active species through dormant species, in which the stable covalent bond is introduced not only to suppress the side reactions but also to generate various active species by varying the stimulus (Scheme 7). In addition to the one-time mechanistic transformation, the author investigated a novel living copolymerization, which proceeds via interconvertible dual activation of dormant covalent bond by plural catalysts. This

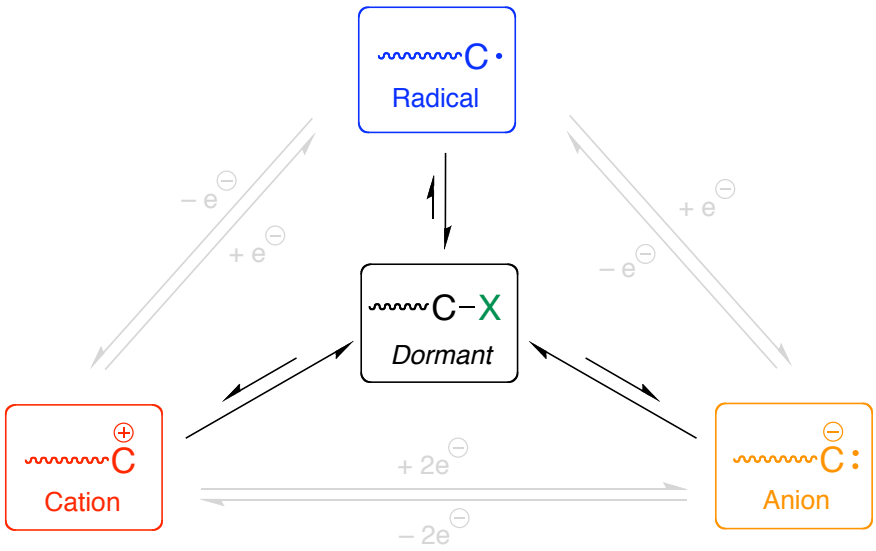

Scheme 7. Mechanistic Transformation through Dormant Species

system overcomes the traditional limitation of the category by active species, which gives a polymer chain grown through different types of active species. The three objectives are listed below.

(1) $FeCl_3$-Mediated Mechanistic Transformation from Living Cationic into Radical Polymerization

(2) Simultaneous Living Cationic and Radical Polymerization via Interconvertible Dual Active Species

(3) Direct Mechanistic Transformation from Living Anionic into Radical Polymerization

(1) $FeCl_3$-Mediated Mechanistic Transformation from Living Cationic into Radical Polymerization

The first objective of this study was directed to the mechanistic transformation from living cationic polymerization into metal-catalyzed living radical polymerization through the dormant C–Cl bond with the same metal catalyst. Recently, dormant carbon-halogen bonds have been used for a mechanistic transformation between growing cationic and radical species.[2,3,48–50] However, in this method, quite different metal catalysts and reaction conditions are necessary for

the two polymerizations. The author thus focused on iron halides ($FeCl_n$) because $FeCl_2$ and $FeCl_3$ catalyze living radical[39,40] and cationic polymerizations,[26] respectively, though their oxidation states are different. For this purpose, Lewis acidic $FeCl_3$, which is considered as inhibitor[51] for radical polymerization, was employed for living radical polymerization in the presence of phosphine and amine ligand [I(a) in Scheme 8]. In addition, the polymerization mechanism was evaluated by spectroscopic analysis of some model reactions. The $FeCl_3$-based system was then applied for direct mechanistic transformation from living cationic to radical polymerization through the common dormant C–Cl bond upon the simple addition of ligand in the same pot [I(b) in Scheme 8].

(2) Simultaneous Living Cationic and Radical Polymerization via Interconvertible Dual Active Species

The second objective of this study was to develop the simultaneous living cationic and radical polymerization via interconvertible dual activation of dormant C–S bond [II in Scheme 8]. Although the dormant C–Cl bond can reversibly generate both the growing carbocation and radical species to enable both living polymerizations, these polymerizations are not compatible in the same reaction system because of the different conditions and catalysts required. Recently, the author's group found that the C–S bond in the trithiocarbonate, which is effective for RAFT radical polymerization, can be cationically and reversibly activated by Lewis acid under the same condition as that for the RAFT radical polymerization.[52] The author thus investigated the simultaneous polymerization via the dormant C–S bond which can be reversibly and non-selectively activated both into growing cationic and radical species by Lewis and radical initiator, respectively.

(3) Mechanistic Transformation from Living Anionic into Radical Polymerization

The final objective of this study is the direct mechanistic transformation from living anionic polymerization into radical polymerization through C–X bond (X = Cl, Br) [III in Scheme 8]. For this, the author investigated the quantitative halogenation of terminal growing anionic species during stereospecific living anionic polymerization of MMA and the subsequent ruthenium-catalyzed living radical polymerization. Although the same procedure for mechanistic transformation has already been reported, the transformation has not been quantitative.[53]

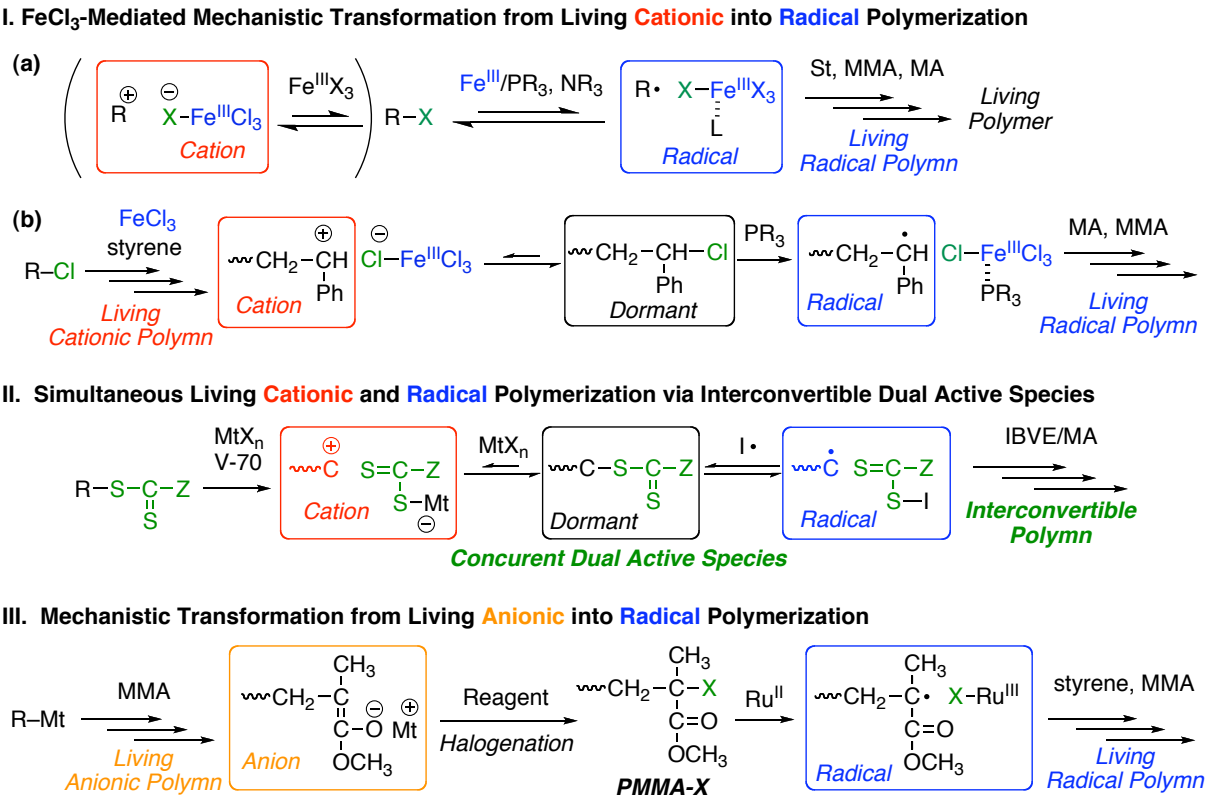

Scheme 8. Novel Polymerization System via Mechanistic Transformation of Active Species

Outline of This Study

The present thesis consists of three parts: **Part I** (Chapter 1–3) deals with the $FeCl_3$-mediated mechanistic transformation from living cationic into radical polymerization via the C–Cl bond. **Part II** (Chapter 4, 5) presents the simultaneous living cationic and radical polymerization via interconvertible dual activation of C–S bond. **Part III** (Chapter 6) focuses on the mechanistic transformation from living anionic into radical polymerization through the C–X bond (X = Cl, Br).

In Part I, ***Chapter 1*** deals with the unprecedented living radical polymerization of styrene using Lewis acidic iron(III) chloride ($FeCl_3$) in the presence of tributylphosphine and a chloride initiator (Scheme 9). Interestingly, only the use of $FeCl_3$ and P*n*Bu_3 without any intentionally added reducing agents or radical initiators induced the polymerization to produce polymers with controlled molecular weights and narrow MWDs. Furthermore, the copolymerization of styrene and MMA resulted in the simultaneous consumption of both monomers at almost the same rate to give copolymers with controlled molecular weights and narrow MWDs, indicating that the $FeCl_3$-catalyzed living radical copolymerization proceeded via homolytic activation of C–Cl bond.

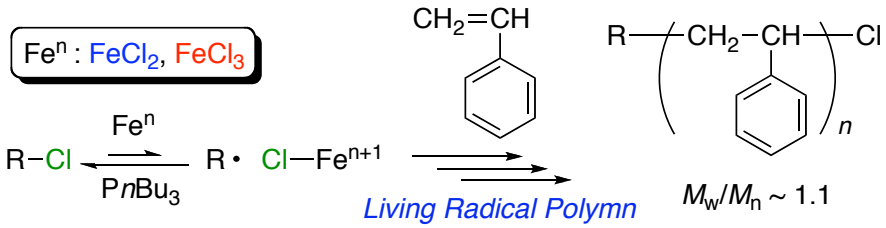

Scheme 9. Living Radical Polymerization of Styrene with R–Cl/$FeCl_n$/P*n*Bu_3

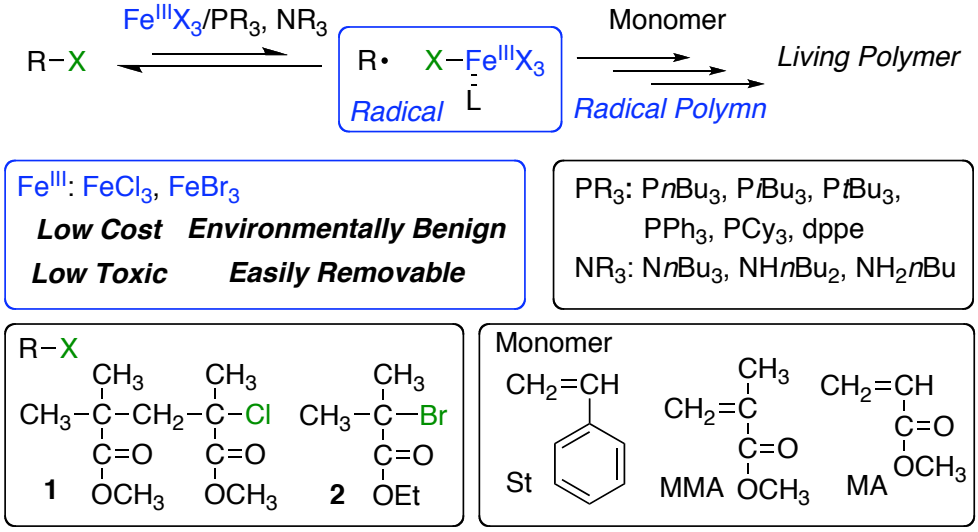

Scheme 10. Living Radical Polymerization of Various Monomers with Fe(III)/PR$_3$ and NR$_3$

Chapter 2 discusses the living radical polymerization of various monomers with FeX$_3$ (X = Cl, Br) and halide initiators in the presence of a series of simple phosphine and amine ligands (Scheme 10). The polymerization of MMA and methyl acrylate (MA) proceeded in a living fashion with the appropriate combination of FeX$_3$ and ligand (e.g., FeCl$_3$/P*t*Bu$_3$ or N*n*Bu$_3$ system for MMA and FeBr$_3$/PPh$_3$ system for MA). In addition, model experiments and stereoscopic analysis of FeCl$_3$ with phosphines and amines suggest that FeCl$_3$ is disproportioned into Fe(III)Cl$_4^-$ anion and Fe(III)Cl$_2^+$ cation, in which the latter species probably works as a real active catalyst in the FeCl$_3$-basded system.

Chapter 3 focuses on the in-situ direct mechanistic transformation from FeCl$_3$-mediated living cationic into radical polymerization via dormant C–Cl bond (Scheme 11). Lewis acidic FeCl$_3$ effectively induced the living cationic polymerization of styrene under appropriate condition, in which the M_n increased in proportion to the monomer conversion. The subsequent addition of the phosphine ligand to the cationic polymerization followed by heating successfully induced the radical polymerization of various monomers via the homolytic activation of C–Cl terminal of the polystyrene. Thus, the mechanistic transformation from living cationic into radical

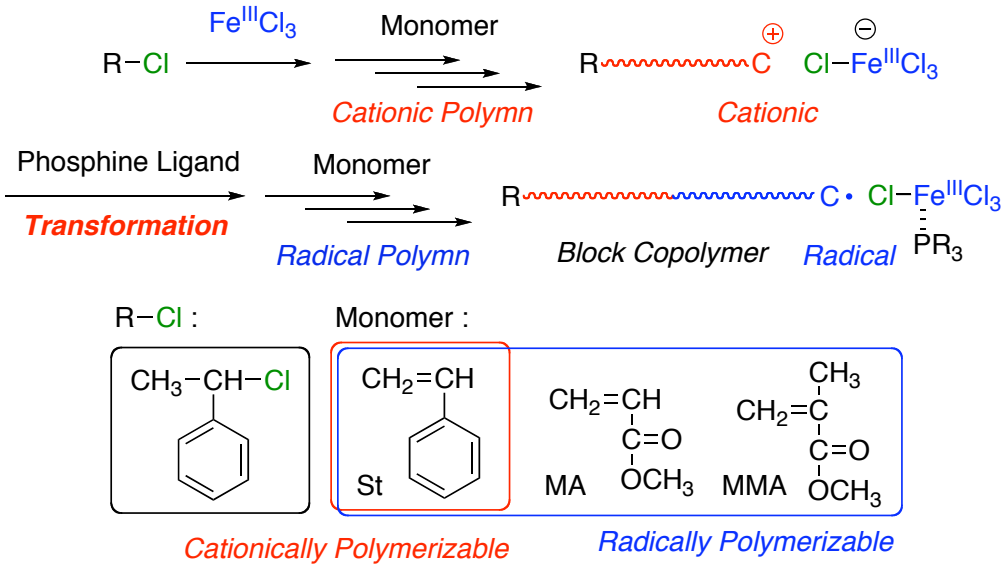

Scheme 11. In-situ Direct Mechanistic Transformation from $FeCl_3$-Mediated Living Cationic into Radical Polymerization

polymerization successfully took place with the $FeCl_3$-based system to afford the one-pot synthesis of various block copolymers.

In Part II, ***Chapter 4*** is directed to simultaneous living cationic and radical polymerization via dual activation of dormant C–S bonds in the presence of both Lewis acid and radical generator (Scheme 12). The copolymerization of isobutyl vinyl ether (IBVE) and MA proceeded in the presence of trithiocarbonate as an initiator using both $EtAlCl_2$ and V-70, in which both IBVE and MA were simultaneously and quantitatively consumed. The M_n of the obtained copolymer agreed well with the calculated value assuming that one molecule of trithiocarbonate generates one polymer chain. The NMR, HPLC, and MALDI-TOF-MS analyses revealed that the polymerization proceeded via interconvertible growing cationic and radical species to generate the copolymer consisting of the cationically and radically polymerizable segments.

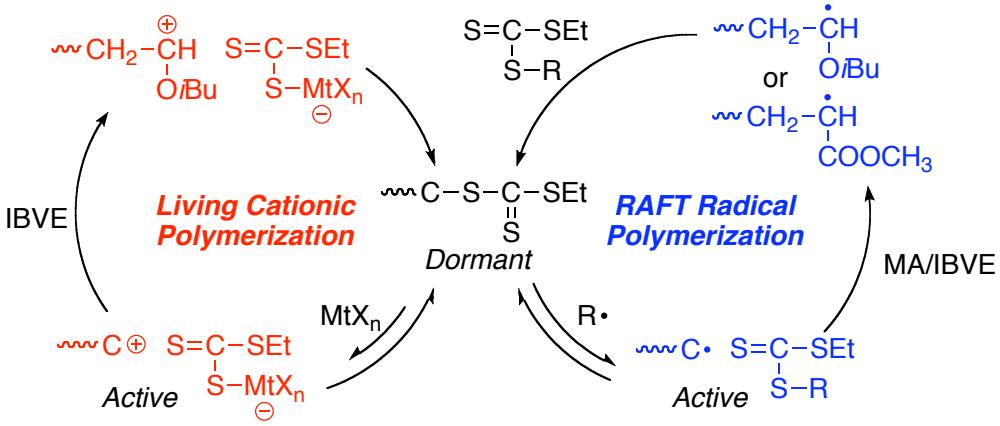

Scheme 12. Simultaneous Living Cationic and Radical Polymerization via Dual Activation of C–S Bonds

Chapter 5 discusses the interconvertible living cationic and radical polymerization of IBVE and (meth)acrylic monomers such as MA, MMA, and acrylonitrile with various initiating systems (Scheme 13). In all cases, the simultaneous polymerization proceeded under appropriate polymerization condition to afford the multiblock copolymers containing both monomer segments via ducal active species. In addition, the choice of RAFT agent and Lewis acid could tune the numbers of interconversion of the two active species per polymer chain in the copolymerization of IBVE and MA.

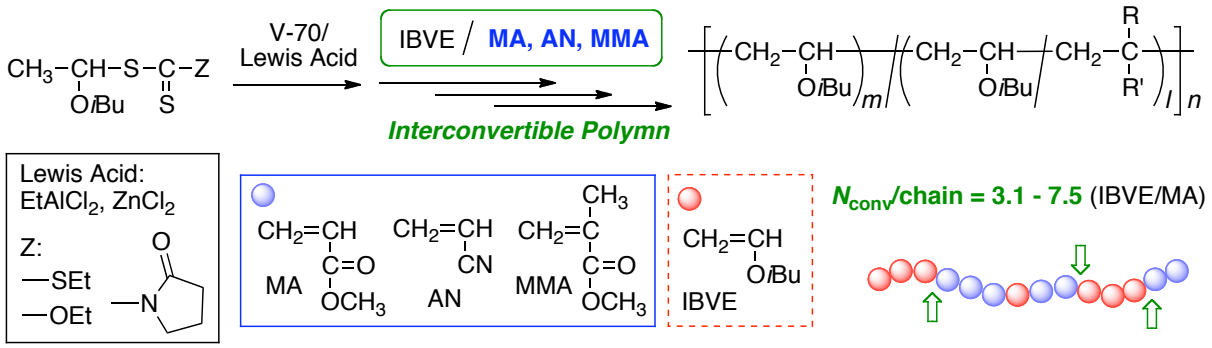

Scheme 13. Synthesis of Novel Multiblockcopolymer by Interconvertible Living Radical and Cationic Polymerization of Various Monomers

In Part III, ***Chapter 6*** deals with the direct mechanistic transformation from living anionic polymerization into radical polymerization via C–X bond (X = Cl or Br) (Scheme 14). Especially, the stereospecific living anion of PMMA was capped by halogen atom, which worked as an initiator for metal-catalyzed living radical polymerization. The quantitative halogeneation of the isotactic or syndiotactic PMMA anion was achieved by using CCl_3Br and CCl_4 as halogen source in the presence of Lewis bases such as 1,8-diazabicyclo[5.4.0]undec-7-ene (DBU). The obtained PMMA with a C–X (X = Cl or Br) bond was then employed in subsequent ruthenium-catalyzed living radical polymerization. Thus, this direct mechanistic transformation was accomplished to produce block copolymers not only consisting of stereoregular PMMA segments and polystyrene but also stereoblock PMMAs with isotactic or syndiotactic and modarate syndiotactic segment.

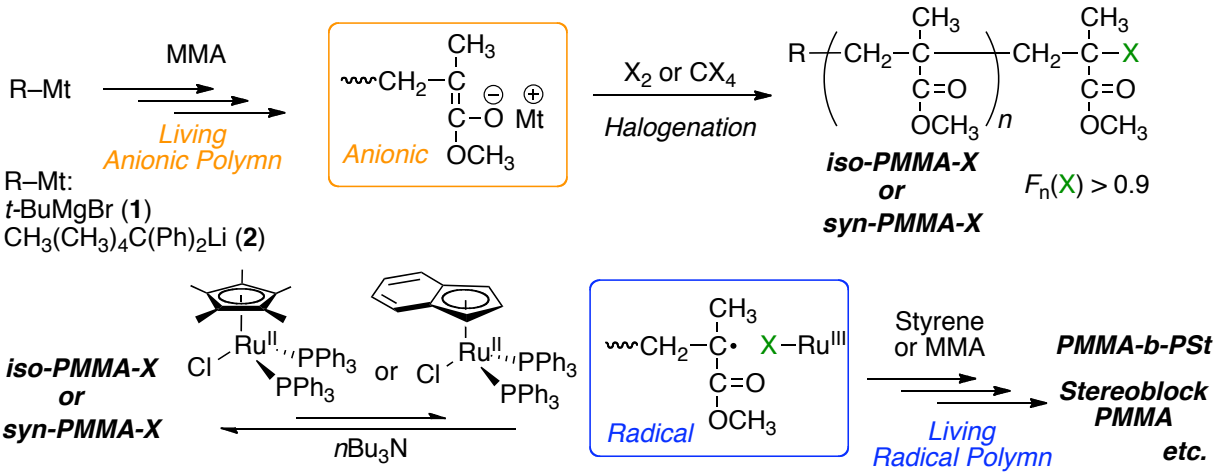

Scheme 14. Direct Mechanistic Transformation from Stereospecific Living Anionic Polymerization of MMA into Metal-Catalyzed Living Radical Polymerization

References

1. Odian, G. *Principles of Polymerization, Fourth Edition*; John Wiley and Sons, Inc., Hoboken, New Jersey, 2004.
2. Yagci, Y.; Tasdelen, M. A. *Prog. Polym. Sci.* **2006**, *31*, 1133–1170.
3. Hadjichristidis, N.; Pitisikalis, M.; Iatrou, H. *Adv. Polym. Sci*. **2005**, *189*, 1–124.
4. (a) Yagci, Y.; Reetz, I. *Prog. Polym. Sci*. **1998**, *23*, 1485–1538. (b) Yagci, Y.; Acar, M.; Hizal, G.; Yildrim, H.; Baysal, B. *Angew. Makromol. Chem*. **1987**, *154*, 169–178. (c) Braun, H.; Yagci, Y.; Nuyken, O. *Eur. Polym. J*. **2002**, *38*, 151–156.
5. (a) Guo, H.-Q.; Kajiwara, A.; Morishima, Y; Kamachi, M. *Macromolecules* **1996**, *29*, 2354–2358. (b) Guo, H.-Q.; Kajiwara, A.; Morishima, Y; Kamachi, M. *Polym. Adv. Technol.* **1997**, *8*, 196–202. (c) Kamachi, M.; Guo, H.-Q.; Kajiwara, A. *Macromol Symp*. **1997**, *118*, 149–161. (d) Kamachi, M.; Guo, H.-Q.; Kajiwara, A. *Macromol. Chem. Phys*. **2002**, *203*, 991–997.
6. (a) Nomura, R.; Narita, M.; Endo, T. *Macromolecules* **1994**, *27*, 4853–4854. (b) Nomura, R.; Endo, T. *Macromolecules* **1994**, *27*, 5523–5526. (c) Nomura, R.; Endo, T. *Macromolecules* **1995**, *28*, 1754–1757.
7. (a) Szwarc, M. *Nature* **1956**, *178*, 1168–1169. (b) Szwarc, M.; Levy, M.; Milkovich, R. *J. Am. Chem. Soc*. **1956**, *78*, 2656–2657.
8. Baskaran, D.; Müller, A. H. E. *Prog. Polym. Sci*. **2007**, *32*, 173–219.
9. Brody, H.; Ladacki, M.; Milkovitch, R.; Szwarc, M. *J. Polym. Sci.* **1957**, *25*, 221–224.
10. (a) Goode, W.E.; Owens, F. H.; Myers, W. L. *J. Polym. Sci*. **1960**, *47*, 75–89. (b) Schreiber, H. *Macromol. Chem*. **1960**, *36*, 86–88. (c) Glusker, D. L.; Lysloff, I.; Stiles, E. *J. Polym. Sci*. **1961**, *49*, 315–334.
11. (a) Hatada, K.; Kitayama, T.; Ute, K. *Prog. Polym. Sci*. **1988**, *13*, 189–276. (b) Hatada, K.; Kitayama, T. *Polym. Int.* **2000**, *49*, 11–47. (c) Baskaran, D. *Prog. Polym. Sci*. **2003**, *28*, 521–581.

12. (a) Goode, W. E.; Owens, F. H.; Fellmann, R. P.; Snyder, W. H.; Moore, J. E. *J. Polym. Sci.* **1960**, *46*, 317–331. (b) Nishioka, A.; Watanabe, H.; Abe, K.; Sono, Y. *J. Polym. Sci.* **1960**, *48*, 241–272. (c) Hatada, K.; Ute, K.; Tanaka, K.; Kitayama, T.; Okamoto, Y. *Polym. J.* **1985**, *17*, 977–980.
13. (a) Freyss, D.; Rempp, P.; Benoit, H. *J. Polym. Sci., Polym. Lett.* **1964**, *2*, 217–222. (b) Cao, Z-K.; Okamoto, Y.; Hatada, K. *Koubunshi Ronbunshu* **1986**, *12*, 857–861. (c) Ohata, M.; Ikeda, S.; Akatani, S.-i.; Isono, Y. *Macromolecules* **1992**, *25*, 5131–5136.
14. *Controlled and Living Polymerizations: From Mechanisms to Materials*; Müller A. H. E.; Matyjaszewski, K., Eds.; Wiley-VCH: Weilheim, Germany, 2008.
15. Webster, O. W. *Adv. Polym. Sci.* **2004**, *167*, 1–34.
16. Matyjaszewski, K., Ed.; *Cationic Polymerizations*; Marcel Dekker: New York, 1996.
17. Miyamoto, M.; Sawamoto, M.; Higashimura, T. *Macromolecules* **1984**, *17*, 265–268.
18. Sawamoto, M. *Prog. Polym. Sci*. **1991**, *16*, 111–172.
19. Puskas. J.E.; Kaszas, G. *Prog. Polym. Sci*. **2000**, *25*, 403–452.
20. Goethals, E. J.; Prez, F. D. *Prog. Polym. Sci*. **2007**, *32*, 220–246.
21. (a) Aoshima, S.; Yoshida, T.; Kanazawa, A.; Kanaoka, S. *J. Polym. Sci. Part A: Polym. Chem*. **2007**, *45*, 1801–1813. (b) Aoshima, S.; Kanaoka, S. *Chem. Rev*. **2009**, 129, 5245–5287. (c) Kanazawa, A.; Kanaoka, S.; Aoshima, S. *Chem. Lett.* **2010**, *39*, 1232–1237.
22. (a) Sawamoto, M.; Okamoto, C.; Higashimura, T. *Macromolecules* **1987**, *20*, 2693–2697. (b) Kamigaito, M.; Sawamoto, M.; Higashimura, T. *Macromolecule* **1991**, *24*, 3988–3992. (c) Kamigaito, M.; Sawamoto, M.; Higashimura, T. *Macromolecule* **1992**, *25*, 2587–2591.
23. (a) Aoshima, S.; Higashimura, S. *Polym. Bull*. **1986**, *15*, 417–423. (b) Aoshima, S.; Higashimura, T. *Macromolecules* **1989**, *22*, 1009–1013.
24. (a) Ishihama, Y.; Sawamoto, M.; Higashimura, T. *Polym. Bull*. **1990**, *24*, 201–206. (b) Kamigaito, M.; Sawamoto, M.; Higashimura, T. *Macromolecules* **1993**, *26*, 1643–1649.
25. (a) Kaszas, G.; Puskas, J. E.; Chen, C. C.; Kennedy, J. P. *Polym. Bull*. **1988**, *20*, 413–419.

(b) Kamigaito, M.; Sawamoto, M.; Higashimura, T. *Macromolecules* **1995**, *28,* 5671–5675.

26. Kanazawa, A.; Hirabaru, Y.; Kanaoka, S.; Aoshima, S. *J. Polym. Sci., Part A: Polym. Chem.* **2006**, *44*, 5795–5800.
27. Moad, G.; Solomon, D. H. *The Chemistry of Radical Polymerization, Second Edition*; Elsevier, Oxford, UK, 2006.
28. Matyjaszewski, K.; Davis, T. P., Eds.; *Handbook of Radical Polymerization*; Wiley Interscience, New York, 2002.
29. (a) Hawker, C. J.; Bosman, A. W.; Harth, E. *Chem. Rev*. **2001**, *101*, 3661–3688. (b) Studer, A.; Schulte, T. *Chem. Rec*. **2005**, *5*, 27–35. (c) Sciannamea, V.; Jérôme, R.; Detrembleur, C. *Chem. Rev*. **2008**, *108*, 1104–1126. (d) Grubbs, R. B. *Polym. Rev*. **2011**, *51*, 104–137.
30. (a) Sawamoto, M.; Kamigaito, M. *J. Macromol. Sci. Pure Appl. Chem*. **1997**, *A34*, 1803–1814. (b) Kamigaito, M.; Ando, T.; Sawamoto, M. *Chem. Rev*. **2001**, *101*, 3689–3745. (c) Kamigaito, M.; Ando, T.; Sawamoto, M. *Chem. Rec*. **2004**, *4*, 159–175. (d) Ouchi, M.; Terashima, T.; Sawamoto, M. *Acc. Chem. Res*. **2008**, *41*, 1120–1132. (e) Ouchi, M.; Terashima, T.; Sawamoto, M. *Chem. Rec*. **2009**, *109*, 4963–5050. (f) Kamigaito, M. *Polym. J.* **2010**, 42, 105–120.
31. (a) Matyjaszewski, K.; Xia, J. *Chem. Rev*. **2001**, *101*, 2921–2990. (b) Tsarevsky, N. V.; Matyjaszewski, K. *Chem. Rev*. **2007**, *107*, 2270–2299. (c) Braunecker, W. A.; Matyjaszewski, K. *Prog. Polym. Sci*. **2007**, *32*, 93–146. (d) di Lena, F.; Matyjaszewski, K. *Prog. Polym. Sci*. **2010**, *35*, 959–1021. (e) Matyjaszewski, K. *Macromolecules* **2012**, *45*, 4015–4039.
32. Rosen, B. M.; Percec, V. *Chem. Rev*. **2009**, *109*, 5069–5119.
33. (a) Moad, G.; Rizzardo, E.; Thang, S. H. *Aust. J. Chem.* **2005**, *58*, 379–410. (b) Moad, G.; Rizzardo, E.; Thang, S. H. *Polymer* **2008**, *49*, 1079–1131. (c) Moad, G.; Rizzardo, E.; Thang, S. H. *Acc. Chem. Res*. **2008**, *41*, 1133–1142. (d) Moad, G.; Rizzardo, E.; Thang, S. H. *Aust. J. Chem.* **2009**, *62*, 1402–1472. (e) Moad, G.; Rizzardo, E.; Thang, S. H. *Aust. J.*

Chem. **2012**, *65*, 985–1076. (f) Keddie, D. J.; Moad, G.; Rizzardo, E.; Thang, S. H. *Macromolcules* **2012**, *45*, 5321–5342.

34. (a) Kharasch, M. S.; Jensen, E. V.; Urry, W. H. *Science* **1945**, *102*, 128. (b) Iqbal, J.; Bhatia, B.; Nayyar, N. K. *Chem. Rev.* **1994**, 94, 519–554.
35. Kato, M.; Kamigaito, M.; Sawamoto, M.; Higashimura, T. *Macromolecules* **1995**, *28*, 1721–1723.
36. Wang, J.-S.; Matyjaszewski, K. *J. Am. Chem. Soc*. **1995**, *117*, 5614–5615.
37. Pecec, V.; Barboiu, B. *Macromolecules* **1995**, *28*, 7970–7972.
38. Haddleton, D. M.; Jasieczek, C. B.; Hannon, M. J.; Shooter, A. J. *Macromolecules* **1997**, *30*, 2190–2193.
39. Ando, T.; Kamigaito, M.; Sawamoto, M. *Macromolecules* **1997**, *30,* 4507–4510.
40. Matyjaszewski, K.; Wei, M. Xia, J.; McDermott, N. E. *Macromolecules* **1997**, *30*, 8161–8164.
41. Granel, C.; Dubois, Ph.; Jérôme, R.; Teyssié, P. *Macromolecuels* **1996**, *29*, 8576–8582.
42. Uegaki, H.; Kotani, Y.; Kamigaito, M.; Sawamoto, M. *Macromolecules* **1997**, *30*, 2249–2253.
43. (a) Koumura, K.; Satoh, K.; Kamigaito, M. *Macromolecules* **2008**, *41*, 7359–7367. (b) Koumura, K.; Satoh, K.; Kamigaito, M. *Macromolecules* **2009**, *42*, 2497–2504. (c) Koumura, K.; Satoh, K.; Kamigaito, M. *J. Polym. Sci., Part A: Polym. Chem.* **2009**, *47*, 1343–1353. (d) Koumura, K.; Satoh, K.; Kamigaito, M. *Polym. J.* **2009**, *41*, 595–603.
44. Chiefari, J.; Chong, Y. K.; Ercole, F.; Krstina, J.; Jeffery, J.; Le, T. P. T.; Mayadunne, R. T. A.; Meijs, G. F.; Moad, C. L.; Moad, G.; Rizzardo, E.; Thang, S. H. *Macromolecules* **1998**, *31*, 5559–5562.
45. Mayadunne, R. T. A.; Rizzardo, E.; Chiefari, J.; Krstina, J.; Moad, G.; Postma, A.; Thang, S. H. *Macromolecules* **2000**, *33*, 243–245.
46. Charmot, D.; Corpart, P.; Adam, H.; Zard, S. Z.; Biadatti, T.; Bouhadir, G. *Macromol. Symp.*

2000, *150*, 23–32.

47. Destarac, M.; Charmot, D.; Franck, X.; Zard, S. Z. *Macromol. Rapid Commun.* **2000**, 21, 1035–1039.
48. Matyjaszewski, K.; Teodorescu, M.; Acar, M. H.; Beers, K. L.; Coca, S.; Gaynor, S. G.; Miller, P. J.; Paik, H-j. *Macromol. Symp*. **2000**, *157*, 183–192.
49. (a) Coca, S.; Matyjaszewski, K. *Macromolecules* **1997**, *30,* 2808–2810. (b) Coca, S.; Matyjaszewski, K. *J. Polym. Sci., Part A: Polym. Chem*. **1997**, *35*, 3595–3601. (b) Chen, X.; Ivan, B.; Kops, J.; Batsberg, W. *Macromol. Rapid. Commun*. **1998**, *19*, 585–589. (c) Lu, J.; Liang, H.; Li, A.; Cheng, Q. *Eur. Polym. J*. **2004**, *40*, 397–402.
50. (a) Toman, L.; Janata, M.; Spěváček, J.; Vlček, P.; Látalová, P.; Masař, B.; Sikora, A. *J. Polym. Sci., Part A: Polym. Chem*. **2004**, *42*, 6096–6108. (b) Toman, L.; Janata, M.; Spěváček, J.; Vlček, P.; Látalová, P.; Sikora, A.; Masař, B. *J. Polym. Sci., Part A: Polym. Chem*. **2005**, *43*, 3823–3830.
51. (a) Bamford, C. H.; Jenkins, A. D.; Johnston, R. *Nature* **1956**, *177*, 992. (b) Bamford, C. H.; Jenkins, A. D.; Johnston, R. *Proc. R. Soc.* **1957**, *239A*, 214–229.
52. Kumagai, S.; Nagai, K.; Satoh, K.; Kamigaito, M. *Macromolecules* **2010**, *43*, 7523–7531.
53. (a) Masař, B.; Vlček, P.; Kříž, J. *J. Appl. Polym. Sci.* **2001**, *81*, 3514–3522. (b) Liu, F.; Liu, B.; Luo, B.; Ying, SK. *Chem. Res. Chin. U*. **2000**, *16*, 72–77.

Part I

$FeCl_3$-Mediated Mechanistic Transformation from Living Cationic into Radical Polymerization

Chapter 1

Iron(III) Chloride/R–Cl/Tributylphosphine for Metal-Catalyzed Living Radical Polymerization: A Unique System with a Higher Oxidation State Iron Complex

Abstract

Iron(III) chloride ($FeCl_3$), a higher oxidation state iron species, was employed for the metal-catalyzed living radical polymerization of styrene in the presence of tributylphosphine as the ligand and H–$(MMA)_2$–Cl [$Me_2C(CO_2Me)CH_2C(CO_2Me)(Me)Cl$] as the initiator without any added reducing agents or radical initiators. The polymerization smoothly proceeded without an induction period in toluene at 100 °C to produce polymers with controlled molecular weights, which increased in direct proportion to the monomer conversion and were in good agreement well with the calculated values, and narrow molecular weight distributions (MWDs) ($M_w/M_n \leq 1.1$). The polymerization rate was almost half that of iron(II) chloride under the same conditions. The obtained polymer possessed one initiator moiety at the α-end and almost one chlorine atom at the ω-end. The copolymerization of styrene and methyl methacrylate resulted in the simultaneous consumption of both monomers at almost the same rate to give copolymers with controlled molecular weights and narrow MWDs, indicating that the $FeCl_3$-catalyzed living radical copolymerization proceeded via a radical mechanism. Similar controlled/living radical polymerizations of styrene with methyl and butyl acrylates were also possible using the R–Cl/$FeCl_3$/P*n*Bu_3 initiating system.

Introduction

Recent advances in the controlled/living radical polymerization have been making significant impacts on not only polymer science, but also other wide areas related to the polymeric materials based on the controlled polymer structures.[1–7] One of the most widely employed and efficient living radical polymerizations is the one based on a metal catalyst that generates the growing radical species from the carbon–halogen polymer terminal via the reversible redox reaction of the metal center. The various effective central metals, such as Ru(II),[8] Cu(I),[9–11] Ni(II),[12,13] Fe(II),[14–33] and so forth, give one electron upon the formation of the radical species from the dormant carbon–halogen covalent bond and thus should be basically in a low oxidation state.

However, these metal complexes in a low oxidation state are generally sensitive to air or oxygen, especially in solution, which may render them difficult to practically use. Thus, when using metal catalysts for living radical polymerization, it requires careful handling and procedures including the removal of oxygen and oxidants not only from the reaction systems, but also from the transportation packages. This problem can be resolved by using a higher oxidation state metal species, such as Cu(II), in the presence of reducing agents or radical generators, which in situ change the metals into a lower oxidation state so that they can be active for the carbon–halogen dormant terminal.[34–44] Another problem for the metal catalysts is the possible toxicity of the metals, which may remain in the polymer products because of the difficulty in the complete removal. This can be more or less overcome by the development of highly active catalysts, which can efficiently work even at a low concentration, or by the use of reducing agents, which can reactivate the oxidized metal species, because the use of a small amount of the metal catalysts diminishes the contamination of metals in the products.[37–39] However, the best solution would be the use of a nontoxic metal, such as iron, as well as an easily removable metal catalyst. Iron catalysts are highly promising in all the chemical and industrial areas from the viewpoint of being environmentally benign and naturally abundant in nature,[45] and thus the development of

effective iron-based catalytic systems are still required.

Under such circumstances, there are now many iron-based catalysts for the living radical polymerization, which are mostly iron(II) halides with various phosphorous and/or nitrogen-based ligands, including phosphine, amine, bipyridine, diamine, diimine, aminopyridine, iminopyridine, bisoxazoline, pyridylphosphine, triamine, diaminopyridine, diiminopyridine, and so forth.[14–33] Alternatively, iron(III) halides were employed in conjunction with similar ligands in the presence of a radical initiator like 2,2'-azobisisobutyronitrile (AIBN), in which Fe(III) was reduced to Fe(II) via the reaction with the initiating radical species (R·) along with the formation of an alkyl halide (R–X).[35–43]

However, there are no reports on the direct use of the Fe(III) complex as a catalyst for living radical polymerizations without any intentionally added reducing agents, because a higher oxidation state iron(III) complex is believed to be inactive for the homolytic activation of the dormant C–X bond.[46] This chapter reports the unprecedented living radical polymerization using iron(III) chloride[47] in the presence of a phosphine ligand (P*n*Bu$_3$) and a chloride initiator without any added reducing agents or radical initiators (Scheme 1).[48]

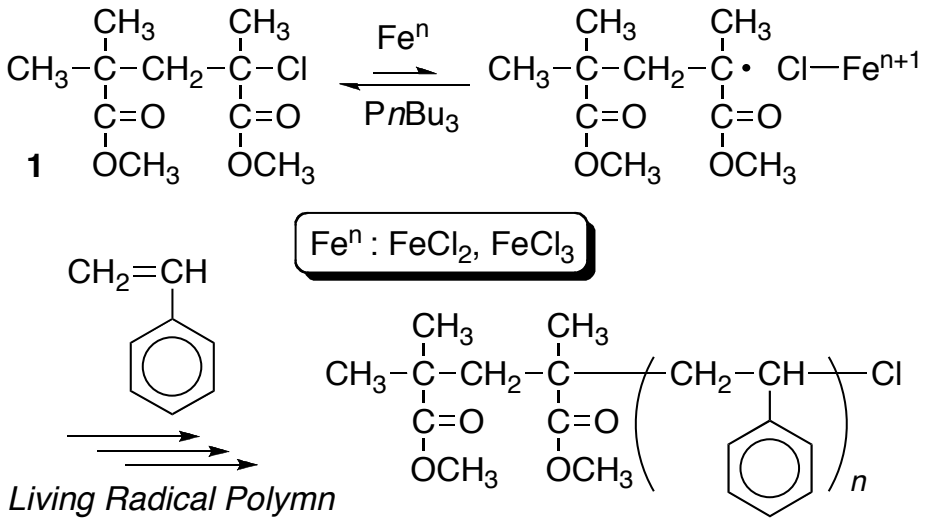

Scheme 1. Living Radical Polymerization of Styrene with R–Cl/FeCl$_n$/P*n*Bu$_3$.

Experimental Section

Materials

Styrene (KISHIDA, 99.5%), methyl methacrylate (MMA; TCI; >98%), methyl acrylate (MA; TCI; >99%), and butyl acrylate (BA; KANTO, >99%) were distilled over calcium hydride under reduced pressure before use. $FeCl_2$ (Aldrich; 99.99%), $FeCl_3$ (Aldrich; >99.99%], and P*n*Bu_3 (KANTO; >98%) were used as received and handled in a glove-box (VAC Nexus) under a moisture- and oxygen-free argon atmosphere (O_2 < 1 ppm). $Me_2C(CO_2Me)CH_2C(CO_2Me)(Me)Cl$ (**1**) was prepared according to the literature.[49] Toluene was distilled over sodium benzophenone ketyl and bubbled with dry nitrogen over 15 min just before use. All other reagents were purified by usual methods.

Polymerization

Polymerization was carried out under dry nitrogen in baked glass tubes equipped with a three-way stopcock. Typically, a mixture of $FeCl_3$ (176 mg, 1.08 mmol) and P*n*Bu_3 (0.54 mL, 2.16 mmol) in toluene (10.3 mL) was stirred for 12 h at 80 °C to give a homogeneous purple solution. After the solution was cooled to room temperature, 0.7 mL of the $FeCl_3$ solution (0.10 mol/L) was added into styrene (3.20 mL, 28.0 mmol) and toluene (2.64 mL) mixture. And then a toluene solution (0.60 mol/L) of 1 (0.46 mL, 0.28 mmol) was added. The solution was evenly charged in seven glass tubes, and the tubes were sealed by flame under a nitrogen atmosphere. The tubes were immersed in thermostatic oil bath at 100 °C. In predetermined intervals, the polymerization was terminated by cooling the reaction mixtures to –78 °C. Monomer conversion was determined from the concentration of residual monomer measured by gas chromatography, with toluene as an internal standard (528 h, 91% conversion). The quenched reaction mixture was diluted with toluene (30 mL), washed with dilute citric acid or hydrochloric acid solution and water to remove complex residues, evaporated to dryness under reduced pressure, and vacuum-dried to give the product polymers (0.38 g; M_n = 11,100, M_w/M_n = 1.19).

Measurements

^{1}H NMR spectrum was recorded on a Varian Gemini 2000 spectrometer (400 MHz). The number-average molecular weights (M_n) and molecular weight distributions (MWDs: M_w/M_n) of the polymers were measured by size-exclusion chromatography using THF, at a flow rate 1.0 mL/min at 40 °C on two polystyrene gel columns; both Shodex KF-805L, that were connected to a JASCO PU-980 precision pump and a JASCO RI-930 detector. The molecular weight was calibrated against eight standard polystyrene samples (M_n = 526–900,000). The monomer conversions were determined from the concentration of the residual monomer measured by gas chromatography, using toluene as the internal standard.

Results and Discussion

1. Living Polymerization of Styrene with R-Cl/FeCl$_n$/PnBu$_3$: Effect of Higher Oxidation State FeCl$_3$

The author first investigated the possibility of the living radical polymerization of styrene with a lower oxidation state iron chloride, $FeCl_2$, in conjunction with a chloride initiator in the presence of the P*n*Bu$_3$ ligand and then examined the effects of a higher oxidation state $FeCl_3$ on the polymerization. Throughout this study, both iron salts were of the highly purified and anhydrous form (>99.99%), which are commercially available. They were used as received and handled in a glove box under a moisture- and oxygen-free argon atmosphere.

The divalent iron chloride ($FeCl_2$) coupled with a chloride initiator [$Me_2C(CO_2Me)CH_2C(CO_2Me)(Me)Cl$ (**1**)] induced the polymerization of styrene in the presence of P*n*Bu$_3$ in toluene at 100 °C to give the polymers with controlled molecular weights, which increased with the monomer conversion (Figure 1). The MWDs were narrow throughout the polymerization (M_w/M_n ~ 1.2) (Figure 2). These results suggest that the $FeCl_2$/P*n*Bu$_3$ initiating system induced the living polymerization of styrene via activation of the C–Cl bond, which is much less common than the activation of a weaker C–Br bond for the metal-catalyzed living

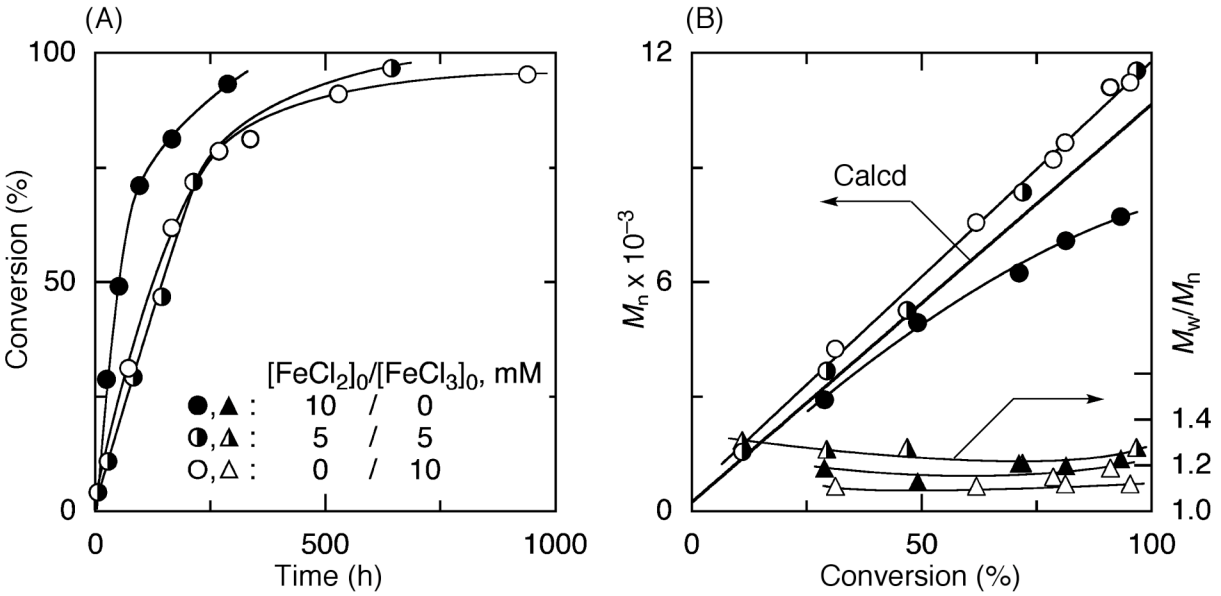

Figure 1. Time-conversion, M_n, and M_w/M_n curves for the polymerization of styrene with **1**/$FeCl_n$/P*n*Bu_3 in toluene at 100 °C: $[styrene]_0 = 4.0$ M; $[\mathbf{1}]_0 = 40$ mM; $[FeCl_2]_0 = 10$ mM (●, ▲), $[FeCl_2]_0 = [FeCl_3]_0 = 5.0$ mM (◑, ◭), or $[FeCl_3]_0 = 10$ mM (○, △); $[P\textit{n}Bu_3]_0 = 20$ mM. The diagonal bold line indicates the calculated M_n assuming the formation of one living polymer per **1** molecule.

radical polymerization or atom transfer radical polymerization.[3,4] The use of the C–Cl bond is preferable in terms of stability because it is less susceptible to side reactions.[3]

The effects of $FeCl_3$ on the living polymerization of styrene with R–Cl/$FeCl_2$/P*n*Bu_3 were then investigated. Styrene was thus polymerized by varying the $[FeCl_2]_0/[FeCl_3]_0$ ratio, while the concentrations of the total iron and the phosphine ligand were fixed ($[FeCl_2]_0 + [FeCl_3]_0 = 10$ mM; $[P\textit{n}Bu_3]_0 = 20$ mM), in conjunction with **1** in toluene at 100 °C. Contrary to our expectation and general belief that a higher oxidation state metal species should inhibit or retard the polymerization as previously reported with the Cu(I)/Cu(II) counterparts,[4] the polymerization smoothly proceeded even with the use of an equimolar amount of $FeCl_3$ to $FeCl_2$, in which the rate was about half that without $FeCl_3$ [Figure 1(A)].

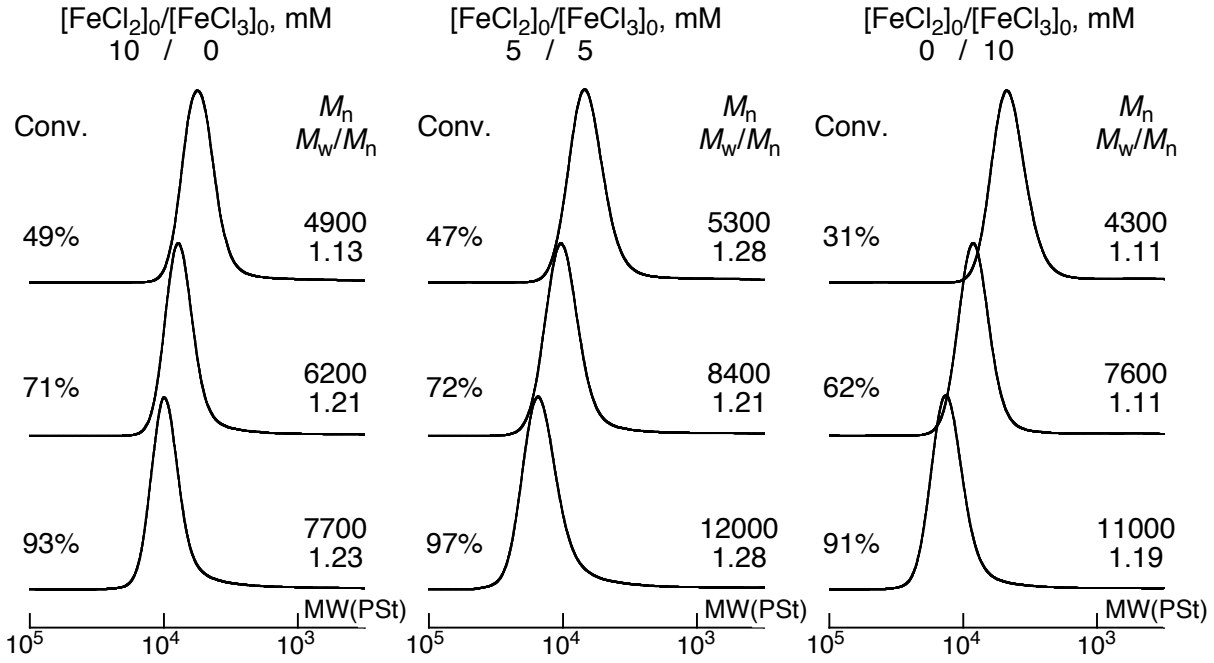

Figure 2. SEC curves of polystyrene obtained in the same experiments as for Figure 1.

Furthermore, only the use of $FeCl_3$ without $FeCl_2$ induced the polymerization at almost the same rate. The number-average molecular weights (M_n) of the polymers obtained with both $FeCl_2/FeCl_3$ and $FeCl_3$ alone increased in direct proportion to the monomer conversion and agreed well with the calculated values on the assumption that one initiator molecule generates one living polymer chain [Figure 1(B)]. The MWDs were also narrow for both systems. Especially, among the three systems, $FeCl_3$ afforded the narrowest MWDs throughout the polymerization ($M_w/M_n = 1.1$).

There have been no reports on the styrene living radical polymerization using Fe(III) species even for the system containing radical initiators. There was an attempt with $FeBr_3$ and AIBN in the presence of ammonium salts, in which the control failed presumably because of the occurrence of the cationic process by the Lewis acidic $FeBr_3$.[20] Furthermore, the polymers obtained after the treatment of the reaction solution using acidic water became apparently colorless, which suggests that these simple ironbased catalysts are easily removable, in addition to the inherently less hazardous nature of the iron atom. Thus, the iron(III) complexes with phosphine

ligands can induce the living radical polymerization of styrene under the appropriate conditions to give the polymers with controlled molecular weights.

The terminal structure of the polystyrene obtained with **1**/$FeCl_3$/P*n*Bu_3 in toluene at 100 °C was examined by ^{1}H NMR spectroscopy. Figure 3 shows the ^{1}H NMR spectrum of the product polymers after removing the catalyst with dilute hydrochloric acid solution. The polymer gave the characteristic signals of polystyrene; that is, phenyl groups (*e*) and main-chain aliphatic protons (*c* and *d*). In addition to these large absorptions, small signals due to the end groups appeared. They are the CH_3– (*α*; 0.6–1.1 ppm) and CH_3O– group (β; 2.8–3.7 ppm) at the α-end derived from the MMA dimer as an initiator, in which the complicated pattern of the signals is due

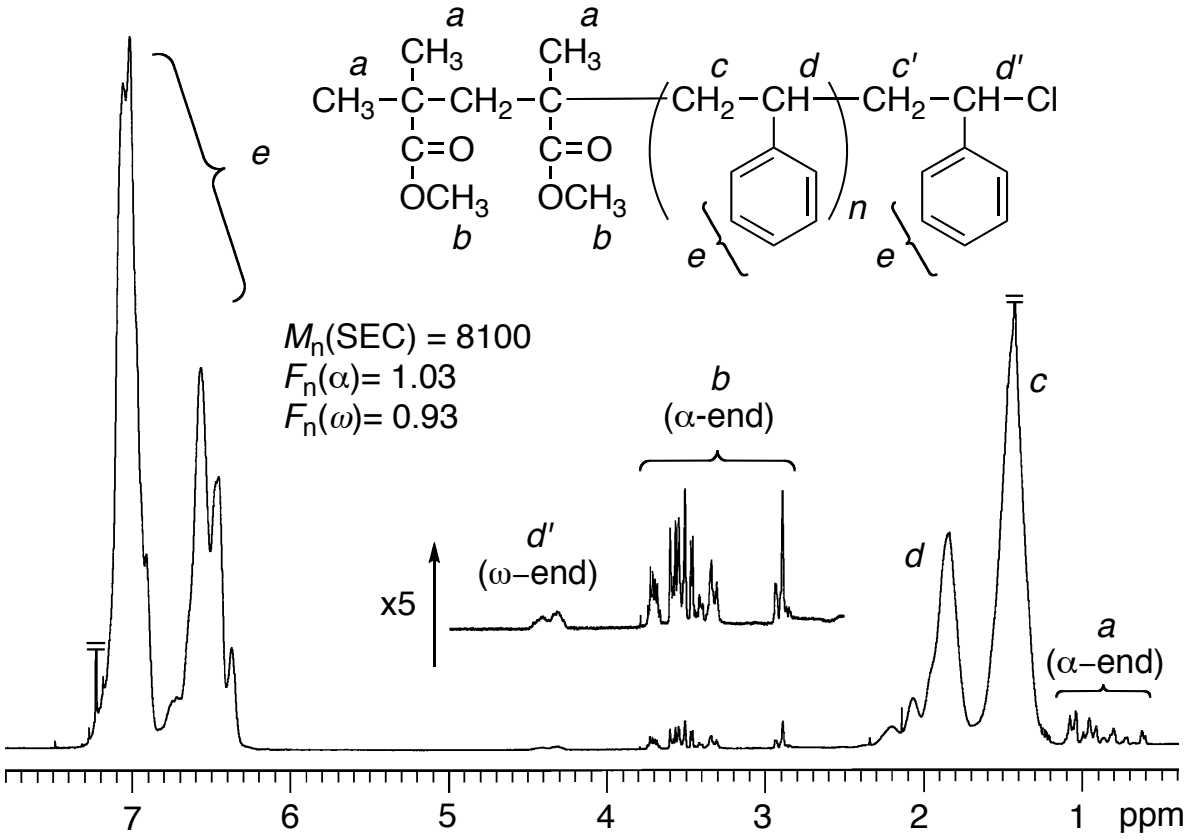

Figure 3. ^{1}H NMR spectrum ($CDCl_3$, 55 °C) of polystyrene (M_n = 8100, M_w/M_n = 1.12) obtained with **1**/$FeCl_3$/P*n*Bu_3 (40/10/20 mM, $[styrene]_0$ = 4.0 M) in toluene at 100 °C.

to the stereoisomer in the initiator, and the –CH–Cl group (*d'*; 4.3 ppm) at the ω-end attributed to the chlorine atom at the growing terminal. The functionalities of the α-end (*β*: F_n = 0.96) and of the ω-end (*d'*: F_n = 0.94) were almost unity, indicating that one polymer was generated from one initiator in a controlled manner. The reaction most probably did not involve the cationic pathway based on the C–Cl bondactivation by the Lewis acidic $FeCl_3$ because there were no peaks of the olefin or indane ring in the spectrum, which might have appeared because of the low stability of the styryl cation at such a high temperature.

2. Living Radical Copolymerization of Styrene and (Meth)acrylic Monomers with R-Cl/FeCl$_3$/P*n*Bu$_3$

The iron(III) system was then applied to the copolymerization of styrene and other monomers, such as MMA, MA, and BA. For the copolymerization of styrene and MMA, both monomers were polymerized at almost the same rate, similar to the conventional radical copolymerization of the two monomers, and were almost quantitatively consumed in 40 h [Figure 4(A)]. The copolymerization was much faster than styrene homopolymerization. Styrene was also copolymerized with MA and BA by the **1**/$FeCl_3$/P*n*Bu_3 system. Independent of the comonomer structures, the obtained polymers had narrow MWDs (M_w/M_n ~ 1.3) [Figure 4(B)], and the M_n values of the copolymers increased in direct proportion to the monomer conversions and were close to the calculated ones. These results also indicated that the R–Cl/$FeCl_3$/P*n*Bu_3 initiating system induced the living radical polymerization and copolymerization despite the use of the higher oxidation state iron catalyst.

The working mechanism of $FeCl_3$ has not been clarified for the iron-catalyzed living radical polymerization. Although the Fe(III) species may work as an activator for the C–Cl bond cleavage, it can be changed into the Fe(II) species in the presence of phosphine at higher temperatures.[50,51] According to the literature, $FeCl_3(PR_3)$ (R = Ph, tBu, Cy) decomposed into possibly Fe(II) species at ambient temperature, as suggested by some identified decomposed

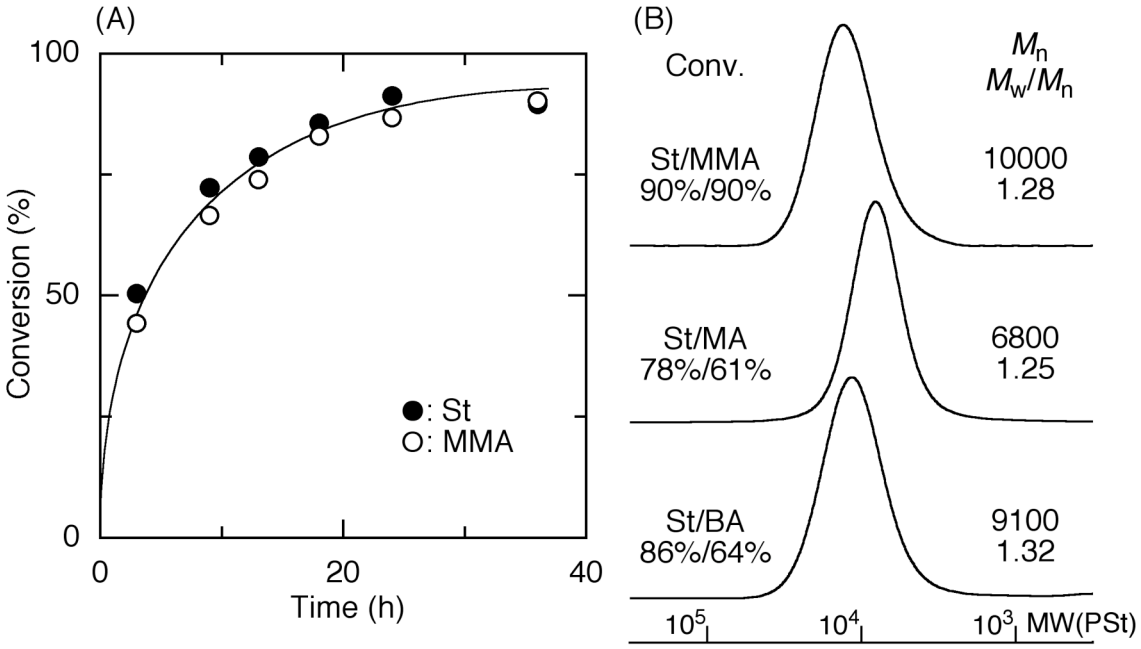

Figure 4. Time-conversion curve for the random copolymerization of styrene (●) and MMA (○) (A) and the molecular weight distribution curves for styrene-methyl methacrylate (MMA), styrene-methyl acrylate (MA), and styrene-butyl acrylate (BA) random copolymerization (B) with **1**/$FeCl_3$/P*n*Bu_3 in toluene at 100 °C: $[styrene]_0 = [comonomer]_0 = 2.0$ M; $[\mathbf{1}]_0 = 40$ mM; $[FeCl_3]_0 = 10$ mM; $[P\textit{n}Bu_3]_0 = 20$ mM.

byproducts.[50] Determining the catalytic mechanism and the applicability of the $FeCl_3$-based system are now under way.

Conclusion

This chapter reveals that the R–Cl/$FeCl_3$/P*n*Bu_3 system is effective for the living radical polymerizations and is promising in terms of industrial applications because of the use of a higher oxidation stable and environmentally benign iron complex with a simple ligand.

References and Notes

1. Moad, G.; Solomon, D. H. *The Chemistry of Radical Polymerization, 2nd ed.*; Elsevier: Oxford, UK, 2006.
2. Braunecker, W. A.; Matyjaszewski, K. *Prog. Polym. Sci.* **2007**, *32*, 93–146.
3. (a) Kamigaito, M.; Ando, T.; Sawamoto, M. *Chem. Rev.* **2001**, *101*, 3689–3745. (b) Kamigaito, M.; Ando, T.; Sawamoto, M. *Chem. Rec.* **2004**, *4*, 159– 175.
4. (a) Matyjaszewski, K.; Xia, J. *Chem. Rev.* **2001**, *101*, 2921–2990. (b) Tsarevsky, N. V.; Matyjaszewski, K. *Chem. Rev.* **2007**, *107*, 2270–2299.
5. Poli, R. *Angew. Chem. Int. Ed.* **2006**, *45*, 5058–5070.
6. (a) Hawker, C. J.; Bosman, A. W.; Harth, E. *Chem. Rev.* **2001**, *101*, 3661–3688. (b) Studer, A.; Schulte, T. *Chem. Rec.* **2005**, *5*, 27–35.
7. Moad, G.; Rizzardo, E.; Thang, S. H. *Aust. J. Chem*. **2005**, *58*, 379–410.
8. Kato, M.; Kamigaito, M.; Sawamoto, M.; Higashimura, T. *Macromolecules* **1995**, *28*, 1271–1273.
9. Wang, J.-S.; Matyjaszewski, K. *J. Am. Chem. Soc.* **1995**, *117*, 5614–5615.
10. Percec, V.; Barboiu, B. *Macromolecules* **1995**, *28*, 7970–7972.
11. Haddleton, D. M.; Jasieczek, C. B.; Hannon, M. J.; Shooter, A. J. *Macromolecules* **1997**, *30*, 2190–2193.
12. Granel, C.; Dubois, Ph.; Jérôme, R.; Teyssié, Ph. *Macromolecules* **1996**, *29*, 8576–8582.
13. Uegaki, H.; Kotani, Y.; Kamigaito, M.; Sawamoto, M. *Macromolecules* **1997**, *30*, 2249–2253.
14. Ando, T.; Kamigaito, M.; Sawamoto, M. *Macromolecules* **1997**, *30*, 4507–4510.
15. Matyjaszewksi, K.; Wei, M.; Xia, J.; McDermott, N. E. *Macromolecules* **1997**, *30*, 8161–8164.
16. Uchiike, C.; Terashima, T.; Ouchi, M.; Ando, T.; Kamigaito, M.; Sawamoto, M. *Macromolecules* **2007**, *40*, 8658–8662.

17. (a) Kotani, Y.; Kamigaito, M.; Sawamoto, M. *Macromolecules* **1999**, *32*, 6877–6880. (b) Kotani, Y.; Kamigaito, M.; Sawamoto, M. *Macromolecules* **2000**, *33*, 3543–3549. (c) Kotani, Y.; Kamigaito, M.; Sawamoto, M. *Macromolecules* **2000**, *33*, 6746–6751. (d) Onishi, I.; Baek, K.-Y.; Kotani, Y.; Kamigaito, M.; Sawamoto, M. *J. Polym. Sci., Part A: Polym. Chem.* **2002**, *40*, 2033–2043. (e) Fuji, Y.; Ando, T.; Kamigaito, M.; Sawamoto, M. *Macromolecules* **2002**, *35*, 2949–2954.
18. (a) Kamigaito, M.; Onishi, I.; Kimura, S.; Kotani, Y.; Sawamoto, M. *Chem. Commun.* **2002**, 2694–2695. (b) Wakioka, M.; Baek, K.-Y.; Ando, T.; Kamigaito, M.; Sawamoto, M. *Macromolecules* **2002**, *35*, 330–333. (c) Sugiyama, Y.; Satoh, K.; Kamigaito, M.; Okamoto, Y. *J. Polym. Sci., Part A: Polym. Chem.* **2006**, *44*, 2086–2096.
19. (a) Göbelt, B.; Matyjaszewski, K. *Macromol. Chem. Phys.* **2000**, *201*, 1619–1624. (b) Sarbu, T.; Matyjaszewski, K. *Macromol. Chem. Phys.* **2001**, *202*, 3379–3391.
20. Teodorescu, M.; Gaynor, S. G.; Matyjaszewski, K. *Macromolecules* **2000**, *33*, 2335–2339.
21. Louie, J.; Grubbs, R. H. *Chem. Commun.* **2000**, 1479–1480.
22. (a) Gibson, V. C.; O' Reilly, R. K.; Reed, W.; Wass, D. F.; White, A. J. P.; Williams, D. J. *Chem. Commun.* **2002**, 1850–1851. (b) Gibson, V. C.; O' Reilly, R. K.; Wass, D. F.; White, A. J. P.; Williams, D. J. *Macromolecules* **2003**, *36*, 2591–2593. (c) Gibson, V. C.; O'Reilly, R. K.; Wass, D. F.; White, A. J. P.; Williams, D. J. *Dalton. Trans.* **2003**, 2824–2830. (d) O'Reilly, R. K.; Gibson, V. C.; Wass, D. F.; White, A. J. P.; Williams, D. J. *Poyhedron* **2004**, *23*, 2921–2928. (e) Shaver, M. P.; Allan, L. E. N.; Rzepa, H. S.; Gibson, V. C. *Angew. Chem. Int. Ed.* **2006**, *45*, 1241–1244. (f) O'Reilly, R. K.; Shaver, M. P.; Gibson, V. C.; White, A. J. P.; Williams, D. J. *Macromoleucles* **2007**, *40*, 7441–7452. (g) Shaver, M. P.; Allan, L. E. N.; Gibson, V. C. *Organometallics* **2007**, *26*, 4725–4730. (h) Allan, L. E. N.; Shaver, M. P.; White, A. J. P.; Gibson, V. C. *Inorg. Chem.* **2007**, *46*, 8963–8970.
23. O' Reilly, R. K.; Gibson, V. C.; White, A. J. P.; Williams, D. J. *J. Am. Chem. Soc.* **2003**, *125*, 8450–8451.

24. (a) Zhang, H.; Schubert, U. S. *Chem. Commun.* **2004**, 858–859. (b) Zhang, H.; Schubert, U. S. *J. Polym. Sci., Part A: Polym. Chem.* **2004**, *42*, 4882–4894.

25. Ferro, R.; Milione, S.; Bertolasi, V.; Capacchione, C.; Grassi, A. *Macromolecules* **2007**, *40*, 8544–8546.

26. Niibayashi, S.; Hayakawa, H.; Jin, R.-H.; Nagashima, H. *Chem. Commun.* **2007**, 1855–1857.

27. Andou, Y.; Yasutake, M.; Jeong, J.-M.; Nishida, H.; Endo, T. *Macromol. Chem. Phys.* **2005**, *206*, 1788–1783.

28. Ibrahim, K.; Yliheikkilä, K.; Abu-Surrah, A.; Löfgren, B.; Lappalainen, K.; Leskelä, M.; Repo, T.; Seppälä, J. *Eur. Polym. J.* **2004**, *40*, 1095–1104.

29. (a) Chen, J.; Chu, J.; Zhang, K. *Polymer* **2004**, *45*, 151–155. (b) Cao, J.; Chen, J.; Zhang, K.; Shen, Q.; Zhang, Y. *Appl. Cat. A: General* **2006**, *311*, 76–78.

30. Wang, G.; Zhu, X.; Zhu, J.; Cheng, Z. *J. Polym. Sci., Part A: Polym. Chem.* **2006**, *44*, 483–489.

31. (a) Ibrahim, K.; Löfgren, B.; Seppälä, J. *Eur. Polym. J*. **2003**, *39*, 939–944. (b) Ibrahim, K.; Starck, P.; Löfgren, B.; Seppälä, J. *J. Polym. Sci.: Part A: Polym. Chem.* **2005**, *43*, 5049–5061.

32. (a) Xue, Z.; Lee, B. W.; Noh, S. K.; Lyoo, W. S. *Polymer* **2007**, *48*, 4704–4714. (b) Xue, Z.; Noh, S. K.; Lyoo, W. S.; *J. Polym. Sci., Part A: Polym. Chem.* **2008**, *46*, 2922–2935.

33. (a) Zhu, S.; Yan, D. *Macromol. Rapid Commun.* **2000**, *21*, 1209–1213. (b) Zhu, S.; Yan, D. *Macromolecules* **2000**, *33*, 8233–8238. (c) Zhu, S.; Yan, D. *J. Polym. Sci., Part A: Polym. Chem.* **2000**, 38, 4308–4314. (d) Zhu, S.; Yan, D.; Zhang, G. *Polym. Bull.* **2001**, 45, 457–464. (e) Hou, C.; Ying, L.; Wang, C. *J. Appl. Polym. Sci.* **2006**, *99*, 1050–1054.

34. Wang, J.-S.; Matyjaszewski, K. *Macromolecules* **1995**, *28*, 7572–7573.

35. Moineau, G.; Dubois, Ph.; Jérôme, R; Senninger, T.; Teyssié, Ph. *Macromolecules* **1998**, *31*, 545–547.

36. Min, K.; Gao, H.; Matyjaszewski, K. *J. Am. Chem. Soc.* **2005**, *127*, 3825–3830.

37. Jakubowski, W.; Matyjaszewski, K. *Angew. Chem. Int. Ed.* **2006**, *45*, 4482–4486.

38. Matyjaszewski, K.; Jakubowski, W.; Min, K.; Tang, W.; Huang, J., Braunecker, W. A.; Tsarevsky, N. V.; *Proc. Natl. Acad. Sci. U.S.A.* **2006**, *42*, 15309–15314.

39. Percec, V.; Guliashvill, T.; Ladislaw, J. S.; Wistrand, A.; Stjerndahl, A.; Sienkowska, M. J.; Monteiro, M. J.; Sahoo, S. *J. Am. Chem. Soc.* **2006**, *128*, 14156–14165.

40. (a) Cheng, Z.; Zhu, X.; Zhang, L.; Zhou, N.; Xue, X. *Polym. Bull.* **2003**, *49*, 363–369. (b) Hou, C.; Qu, R.; Ji, C.; Wang, C.; Wang, C. *Polym. Int.* **2006**, *55*, 326–329.

41. (a) Saikia, P. J.; Goswami, A.; Baruah, S. D. *J. Appl. Polym. Sci.* **2002**, *85*, 1236–1245. (b) Saikia, P. J.; Goswami, A.; Baruah, S. D. *J. Appl. Polym. Sci.* **2002**, 86, 386–394. (c) Saikia, P. J.; Dass, N. N.; Baruah, S. D. *J. Appl. Polym. Sci.* **2005**, *97*, 2147–2154.

42. (a) Wang, G.; Zhu, X.; Cheng, Z.; Zhu, J. *Eur. Polym. J.* **2003**, *39*, 2161–2165. (b) Wang, G.; Zhu, X.; Cheng, Z.; Zhu, J. *J. Polym. Sci., Part A: Polym. Chem.* **2006**, *44*, 2912–2921. (c) Hou, C.; Qu, R.; Liu, J., Guo, Z.; Wang, C.; Ji, C.; Sun, C.; Wang. C. *Polymer* **2006**, *47*, 1505–1510. (d) Hou, C.; Ji, C.; Qu, R.; Wang, C.; Sun, C.; Zhou, W.; Yu, M. *J. Appl. Polym. Sci.* **2007**, *105*, 1575–1580.

43. (a) Chen, X.-P.; Qiu, K.-Y. *Chem. Commun.* **2000**, 1403–1404. (b) Qin, S.-H.; Qin, D.-Q.; Qiu, K.-Y. *New J. Chem.* **2001**, *25*, 893–895. (c) Qin, D.-Q.; Qin, S.-H.; Qiu, K.-Y. *J. Polym. Sci., Part A: Polym. Chem.* **2001**, *39*, 3464–3473.

44. Luo, R.; Sen, A. *Macromolecules* **2008**, *41*, 4514–4518.

45. (a) Bolm, C.; Legros, J.; Paih, J. L.; Zani, L. *Chem. Rev.* **2004**, *104*, 6217–6254. (b) Pearson, A. J. *Iron Compounds in Organic Synthesis*; Academic Press, London, U.K., 1994.

46. Recently $FeCl_3$-catalyzed living cationic polymerization of vinyl ether via the heterolytic activation of the C–X bond was reported, see: Kanazawa, A.; Hirabaru, Y.; Kanaoka, S.; Aoshima, S. *J. Polym. Sci., Part A: Polym. Chem.* **2006**, *44*, 5795–5800.

47. There are reports that iron(III)salts induce the oxidation of phosphine into phosphine oxide by O_2 under the catalytic effect of the iron compounds, suggesting the iron(III) salts are

stable to air: (a) Ondrejkovicová , I.; Vancová , V.; Ondrejovic, G. Czech *Chem. Commum.* 1983, 48, 254–257. (b) Dunbar, K. RK. R.; Quillevéré, A. *Polyhedron* **1993**, *12*, 807–819.

48. Aoshima, H.; Satoh, K.; Kamigaito, M. *Polym. Prepr. Jpn*. **2008**, *57*, 433.
49. Ando, T.; Kamigaito, M.; Sawamoto, M. *Macromolecules* **2000**, *33*, 2819–2824.
50. (a) Walker, J. D.; Poli, R. *Inorg. Chem.* **1989**, *28*, 1793–1801. (b) Walker, J. D.; Poli. R. *Inrog. Chem*. **1990**, *29*, 756–761.
51. Renkema, K. B.; Ogasawara, M.; Streib, W. B.; Huffman, J. C.; Caulton, K. G. *Inorg. Chim. Acta* **1999**, *317*, 226–230.

Chapter 2

A Simple Combination of Higher Oxidation State FeX_3 and Phosphine or Amine Ligand for Living Radical Polymerization of Styrene, Methacrylate, and Acrylate

Abstract

A higher-oxidation-state iron halide [FeX_3 (X = Cl, Br)] was employed in conjunction with a series of ligands, mainly monodentate phosphines and amines, to effect the living radical polymerization of various vinyl monomers such as styrene, methyl methacrylate (MMA), and methyl acrylate (MA). Almost all combinations examined could enable polymerizations in the absence of exogenous reducing agents. However, appropriate combinations of FeX_3 and ligands gave rise to polymers in a living manner, with controlled molecular weights and narrow molecular weight distributions (M_w/M_n = 1.1–1.2). Ligand combinations included $FeCl_3$ with P*n*Bu_3, P*t*Bu_3, or N*n*Bu_3 (for styrene); $FeCl_3$ with P*t*Bu_3 or N*n*Bu_3 (for MMA); and $FeBr_3$ with PPh_3 (for MA). Model reactions and spectroscopic analysis suggest that $FeCl_3$ most likely disproportionates into Fe(III)Cl_4^- anion and Fe(III)Cl_2^+ cation in the presence of Lewis base ligands (PR_3 and NR_3). The latter cationic species, coordinated with the ligand [Fe(III)$Cl_2(PR_3)^+$ or Fe(II)$Cl_2(PR_3)\cdot^+$], acts as the active catalyst. Assistance from the electron-rich ligand allows the catalyst to induce metal-catalyzed living radical polymerization. The Fe(III)-based catalyst could also be easily and almost quantitatively removed from the polymer product simply by washing with aqueous acid to minimize the amount of iron contamination (< 5 ppm).

Introduction

In the past two decades, controlled/living radical polymerization has undergone significant development to permit straightforward syntheses of polymers with well-controlled molecular weights. In addition, this technique has enabled the formation of intricate structures such as block, star, and graft polymers.[1–6] Transition metal-catalyzed living radical polymerization, or atom transfer radical polymerization (ATRP), is one of the most widely employed of these methods, due to the variety of controllable vinyl monomers and the accessibility of catalysts and initiators.[3–5] The polymerization relies on the reversible activation of covalent carbon–halogen bonds in the growing radical species via one-electron redox reaction at the metal center. A variety of metal catalysts are currently employed, including Ru(II),[7] Fe(II),[8–28] Cu(I),[29–31] Ni(II),[32,33] and Mn(0),[34] which are fundamentally in a lower oxidation state and thus can donate one electron to the dormant carbon–halogen covalent bond for homolytic cleavage. Among the various metals, iron has great potential as a catalyst due to its properties. Iron is non-toxic, environmentally benign, abundant, and cost-effective,[35] and many Fe-based catalysts have been designed for living radical polymerization. These catalysts typically consist of lower-oxidation-state species, such as Fe(II) halide (FeX_2), used in conjunction with a wide range of ligands. Such ligands include phosphines, amines, imines, pyridines, carboxylic acids, and onium salts.[8–28] However, lower oxidation state Fe(II) halides are, in principle, sensitive to air, which necessitates careful handling of the metal species during catalyst preparation.

By contrast, Fe(III) trihalides (FeX_3), which are stable to air or oxygen and easy to handle, are inactive but can be reduced to the active Fe(II) state. Addition of a radical initiator or reducing reagent allows these Fe(III) trihalides to be employed in living radical polymerizations similar to the so-called reverse ATRP, AGET, or ARGET.[36–42] It is widely believed that the higher-oxidation-state Fe(III) species are radical inhibitors and would not be able to promote radical polymerization without the addition of exogenous reducing agents or radical initiators. However, the author recently observed that $FeCl_3$ can induce the living radical polymerization of

styrene in combination with an appropriate ligand, such as tributylphosphine as described in Chapter 1.[43] Similar higher oxidation state metal-based systems have also been reported with Fe(III),[44,45] Cu(II),[46–48] and Ru(III).[49] Plausible mechanisms and catalytic pathways remain under discussion; it is unclear if the higher oxidation state metal species is reduced by the monomer or by the ligand to generate active lower oxidation state counterparts or if the higher oxidation state metal is active in its own right.

In this chapter, the author describes investigations on the living radical polymerization of various monomers with FeX_3 (X = Cl, Br) in the presence of a series of phosphine and amine ligands and subsequent removal of the catalysts (Scheme 1). The Fe(III)-based system induced the living radical polymerizations of styrene, methacrylate, and acrylate when an appropriate ligand and initiator were chosen. A detailed mechanism of FeX_3-mediated polymerization is also discussed based on model reactions and spectroscopic analysis of the reaction mixtures.

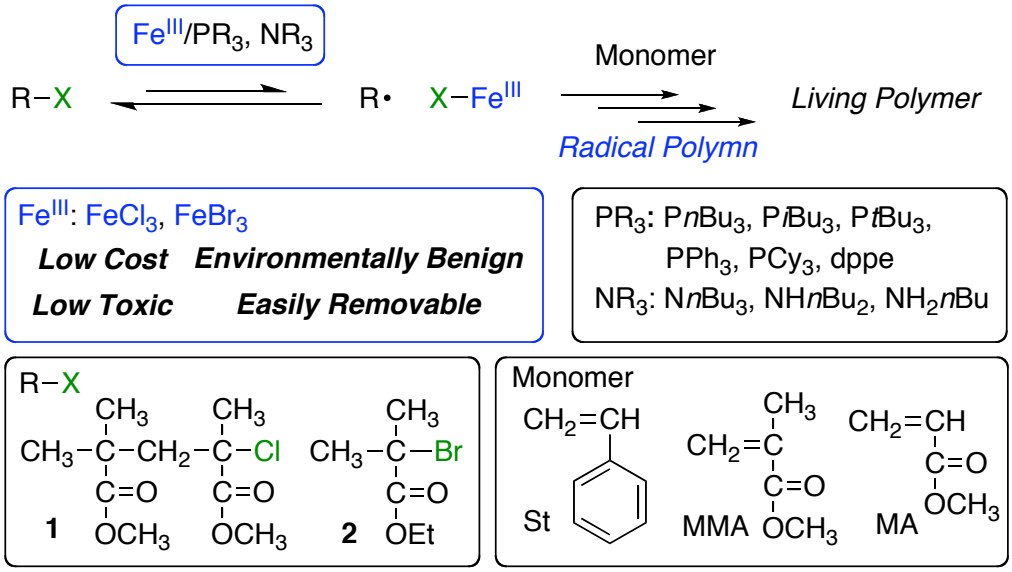

Scheme 1. Living Radical Polymerization with Fe(III)/Phoshphine and Amine Ligands

Experimental Section

Materials

Styrene (KISHIDA, 99.5%), methyl methacrylate (MMA; TCI, >99.8%), and methyl acrylate (MA; TCI, >99%) were distilled over calcium hydride under reduced pressure before use. $FeCl_3$ (Aldrich, >99.99%), $FeBr_3$ (Aldrich, >98%), PPh_3 (Aldrich, 99%), PCy_3 (Aldrich), 1,2-bis(diphenylphosphino)ethane (KANTO, >98%), and nBu$_4$NCl (Furuka, >97%) were used as received and handled in a glove-box (VAC Nexus) under a moisture- and oxygen-free argon atmosphere (O_2 < 1 ppm). PnBu$_3$ (KANTO, > 98%), PiBu$_3$ (Aldrich, 95%), and PtBu$_3$ (Aldrich, 98%) were used as received. NnBu$_3$ (Wako, >98%), NHnBu$_2$ (KISHIDA, 99%), NH$_2$$n$Bu (KISHIDA, 99%), *N,N,N',N'',N''*-pentamethyldiethylenetriamine (PMDETA; TCI, >98%), EMA–Br (**2**) [Me$_2$C(CO$_2$Et)Br] (TCI, >98%), and ethyl acetate (KANTO; >99%) were distilled from calcium hydride before use. (MMA)$_2$–Cl (**1**) [Me$_2$C(CO$_2$Me)CH$_2$C-(CO$_2$Me)(Me)Cl] was prepared according to the literature.[50] α,α-Azobis(isobutyronitrile) (AIBN; Kishida, >90%) was purified by recrystallization from methanol. Toluene was distilled over sodium benzophenone ketyl and bubbled with dry nitrogen over 15 min just before use.

Polymerization

Polymerization was carried out under dry nitrogen in baked glass tubes equipped with a three-way stopcock. A typical example for the polymerization of MMA with (MMA)$_2$–Cl/$FeCl_3$/PtBu$_3$ system is given below. Toluene (8.65 mL), a stock solution (0.30 mL) of PtBu$_3$ (0.12 mmol, 400 mM in toluene), MMA (23.9 mmol, 2.56 mL), and a stock solution (0.45 mL) of (MMA)$_2$–Cl (0.239 mmol, 530 mM in toluene) were added into $FeCl_3$ (19.4 mg, 0.12 mmol) sequentially in this order at room temperature under dry nitrogen. Immediately after mixing, the solution was evenly charged in nine glass tubes, and the tubes were sealed by flame under a nitrogen atmosphere. The tubes were immersed in thermostatic oil bath at 100 °C. In predetermined intervals, the polymerization was terminated by cooling the reaction mixtures to

–78 °C. Monomer conversion was determined from the concentration of residual monomer measured by gas chromatography with toluene as an internal standard (24 h, 90% conversion). The quenched reaction mixture was diluted with toluene (30 mL), washed with dilute hydrochloric acid solution and water to remove complex residues, evaporated to dryness under reduced pressure, and vacuum-dried to give the product polymers (0.20 g; M_n = 9600, M_w/M_n = 1.24).

Measurements

^{1}H NMR spectrum was recorded on a JEOL ECS-400 spectrometer (400 MHz). The number average molecular weights (M_n) and molecular weight distributions (MWDs: M_w/M_n) of the polymers were measured by size exclusion chromatography (SEC) using THF at a flow rate 1.0 mL/min. at 40 °C on two polystyrene gel columns; both Shodex KF-805L, that were connected to a JASCO PU-980 precision pump and a JASCO RI-930 detector. The molecular weight was calibrated against eight standard poly(MMA) samples (M_n = 202–1950,000) for poly(MMA) and poly(MA) and polystyrene samples (M_n = 526–900,000) for polystyrene. The monomer conversions were determined from the concentration of the residual monomer measured by gas chromatography using toluene as the internal standard. UV–vis absorption spectra were recorded by Jasco V-550 spectrophotometer. The metal residue content in polymer was analyzed by inductively coupled plasma mass spectrometry (ICP-MS) on Thermo Scientific ELEMENT2.

Results and Discussion

1. Living Radical Polymerization of Styrene with $FeCl_3$/Ligand.

As described in chapter 1, $FeCl_3$ is effective for the living radical polymerization of styrene with **1** in the presence of P*n*Bu_3 as the ligand, in which **1** acts as an initiator to form a polymer chain.[43] In this chapter, a series of phosphines and amines (P*n*Bu_3, P*i*Bu_3, P*t*Bu_3, PPh_3, PCy_3, NH_2*n*Bu, NH*n*Bu_2, N*n*Bu_3, and PMDETA) were first employed as ligands for $FeCl_3$ in the

Table 1. Living Radical Polymerization of styrene with $FeCl_3$/ligand [a]

entry	ligand	time, h	conv.[b], %	M_n[c]	M_n(calcd)[d]	M_w/M_n[c]
1	P*n*Bu$_3$	581	90	8700	9600	1.12
2	P*i*Bu$_3$	1120	44	4500	4800	1.22
3	P*t*Bu$_3$	985	94	10000	10000	1.11
4	PPh_3	1098	75	3800	8100	1.57
5	dppe	865	60	5300	6500	1.16
6	PCy_3	865	91	10400	9700	1.11
7	N*n*Bu$_3$	2970	87	10300	9300	1.11
8	NH*n*Bu$_2$	1630	74	7000	7900	1.26
9	NH_2*n*Bu	2450	19	1900	2200	1.46
10	PMDETA	715	92	27400	9800	2.46

[a] $[\text{styrene}]_0$ = 4.0 M, $[\mathbf{1}]_0$ = 40 mM; $[FeCl_3]_0$ = 10 mM, $[\text{ligand}]_0$ = 20 mM in toluene at 100 °C. [b] Determined by gas chromatography. [c] The number average molecular weight (M_n) and molecular weight distribution (M_w/M_n) were determined by size-exclusion chromatography (SEC). [d] $M_n(\text{calcd}) = \text{MW(styrene)} \times [M]_0/[\mathbf{1}]_0 \times \text{Conv.} + \text{MW}(\mathbf{1})$.

radical polymerization of styrene with **1** in toluene at 100 °C. Table 1 summarizes the radical polymerization of styrene with various ligands in the $FeCl_3$ system. Styrene polymerization reactions proceeded under all conditions, although the rate of monomer consumption was greater with phosphines than with butylamines (Figure 1). Alkylphosphine and butylamine ligands for $FeCl_3$ afforded polystyrene with particularly well-controlled number averages of molecular weight (M_n) and narrow molecular weight distributions (MWDs).

Figure 2 shows the M_n, M_w/M_n, and SEC curves of polystyrene obtained using **1** as the initiator and $FeCl_3$ as the metal in the presence of P*n*Bu$_3$, P*t*Bu$_3$, PPh_3, and N*n*Bu$_3$ in toluene at 100 °C (entries 1, 3, 4, and 7). With the exception of PPh_3, the M_n values increased in direct proportion to monomer conversion and were in good agreement with the values calculated based on the assumption that one chloride initiator molecule generates one living polymer chain. The MWD values were narrow throughout the polymerization. By contrast, the $FeCl_3/PPh_3$ system gave polymers with values of M_n that were lower than the calculated values. The MWD value

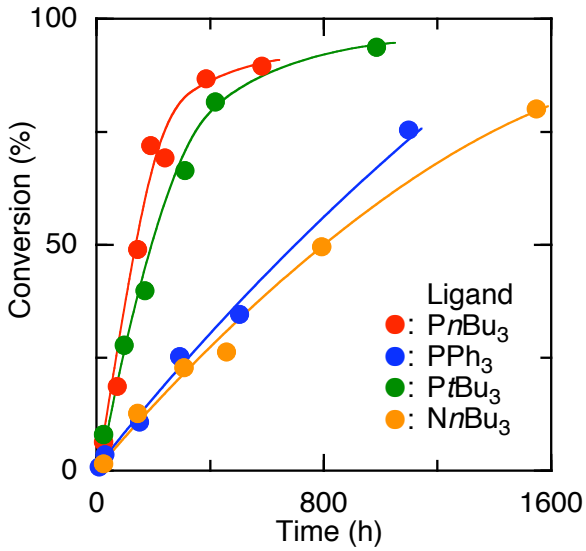

Figure 1. Time-conversion curves of living radical polymerization of styrene with **1**/FeCl$_3$/ligand system: [styrene]$_0$ = 4.0 M, [**1**]$_0$ = 40 mM, [FeCl$_3$]$_0$ = 10 mM, [ligand]$_0$ = 20 mM in toluene at 100 °C.

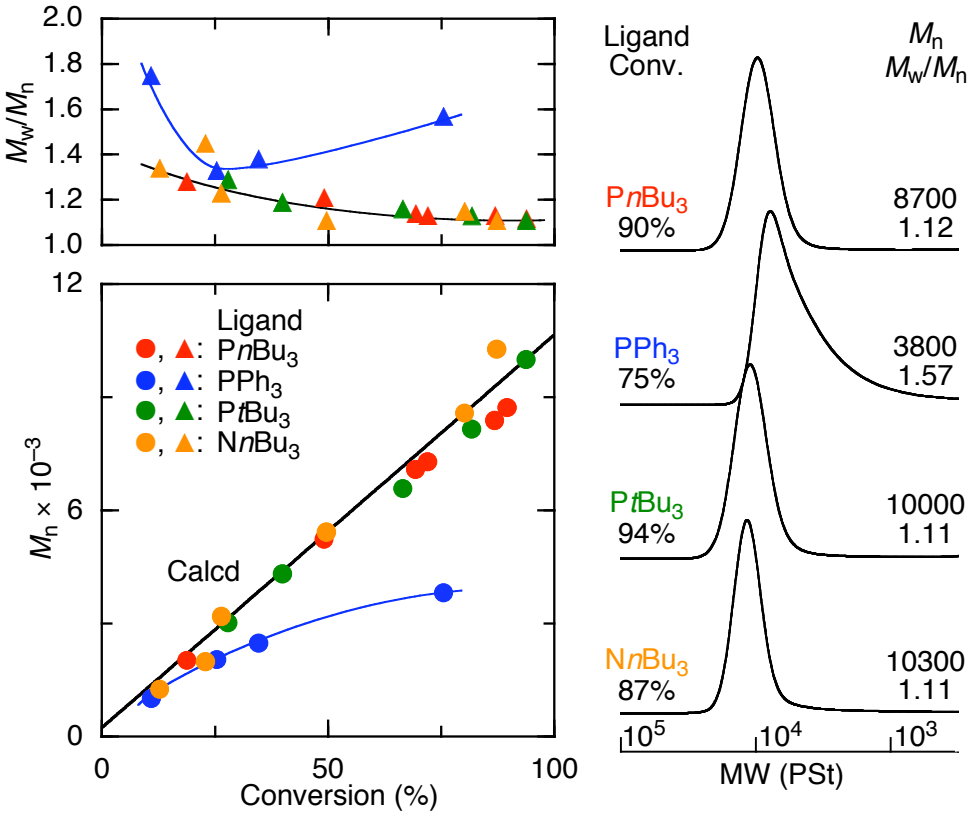

Figure 2. M_n, M_w/M_n, and SEC curves for the polymerization of styrene with **1**/FeCl$_3$/ligand system: [styrene]$_0$ = 4.0 M, [**1**]$_0$ = 40 mM, [FeCl$_3$]$_0$ = 10 mM, [ligand]$_0$ = 20 mM in toluene at 100 °C.

also became broader as the polymerization proceeded, indicating chain-transfer reactions most likely originating from β-proton elimination at the terminal carbon–chlorine bond via a cationic mechanism. This was induced by the Lewis acidic $FeCl_3$ in the presence of PPh_3, which is a weaker Lewis base than the other alkylphosphines.

2. Living Radical Polymerization of Methyl Methacrylate with $FeCl_3$/Ligand.

The polymerization of MMA was also examined using **1** as an initiator and $FeCl_3$ as the metal in the presence of various ligands in toluene at 100 °C (Table 2). As was observed in the styrene polymerizations, MMA was smoothly consumed regardless of ligand choice. Ligand concentration did affect the polymerization such that the polymerization was more controllable at relatively low concentrations (10 mM, equimolar to $FeCl_3$). This control resulted in narrower MWDs through a slower polymerization reaction (entries 1 vs. 2, 4 vs. 5, and 9 vs. 10). The

Table 2. Living Radical Polymerization of MMA with $FeCl_3$/Ligand [a]

entry	Ligand	$[ligand]_0$, mM	time, h	conv.[b], %	M_n[c]	M_n(calcd)[d]	M_w/M_n[c]
1	P*n*Bu$_3$	20	13	91	8600	9400	1.60
2	P*n*Bu$_3$	10	36	90	7500	9300	1.36
3	P*i*Bu$_3$	10	45	91	7200	9400	1.44
4	P*t*Bu$_3$	20	10	90	9100	9100	1.45
5	P*t*Bu$_3$	10	24	90	9200	9300	1.24
6	PPh_3	10	130	92	7600	9500	1.47
7	dppe	10	24	92	8200	9500	1.37
8	PCy_3	10	36	92	8300	9500	1.43
9	N*n*Bu$_3$	20	76	91	9700	9400	1.26
10	N*n*Bu$_3$	10	720	93	9500	9600	1.18
11	NH*n*Bu$_2$	20	683	90	9200	9200	1.31
12	NH_2*n*Bu	20	2510	88	8700	9100	1.36
13	PMDETA	10	128	90	44800	9300	2.92

[a] $[MMA]_0$ = 2.0 M; $[\mathbf{1}]_0$ = 20 mM; $[FeCl_3]_0$ = 10 mM; $[ligand]_0$ = 10 or 20 mM in toluene at 100 °C. [b] Determined by gas chromatography. [c] The M_n and M_w/M_n were determined by SEC. [d] $M_n(calcd) = MW(MMA) \times [M]_0/[\mathbf{1}]_0 \times Conv. + MW(\mathbf{1})$.

effects of ligands will be discussed in more detail, as will our working hypothesis regarding the mechanism (*vide infra*). In most cases, the M_n values of the resulting PMMA were close to the calculated values, with relatively narrow MWD values (M_w/M_n ~ 1.5).

Figure 3 shows the plot of conversion vs. time for MMA polymerization. SEC curves of the polymers obtained with $FeCl_3$ in the presence of the same ligands used in the previous styrene polymerization are also shown in Figure 3 (entries 2, 5, 6, and 10). Polymerization reactions with $FeCl_3$ and P*t*Bu$_3$, P*n*Bu$_3$, or PPh$_3$ proceeded faster than those with $FeCl_3$ and N*n*Bu$_3$. This result is similar to that for the polymerization of styrene, in which M_n increased linearly with MMA conversion (Figure 4). In reactions using P*t*Bu$_3$ or N*n*Bu$_3$, the M_n values were closer to the calculated values, and the MWDs were narrower (M_w/M_n ~ 1.2).

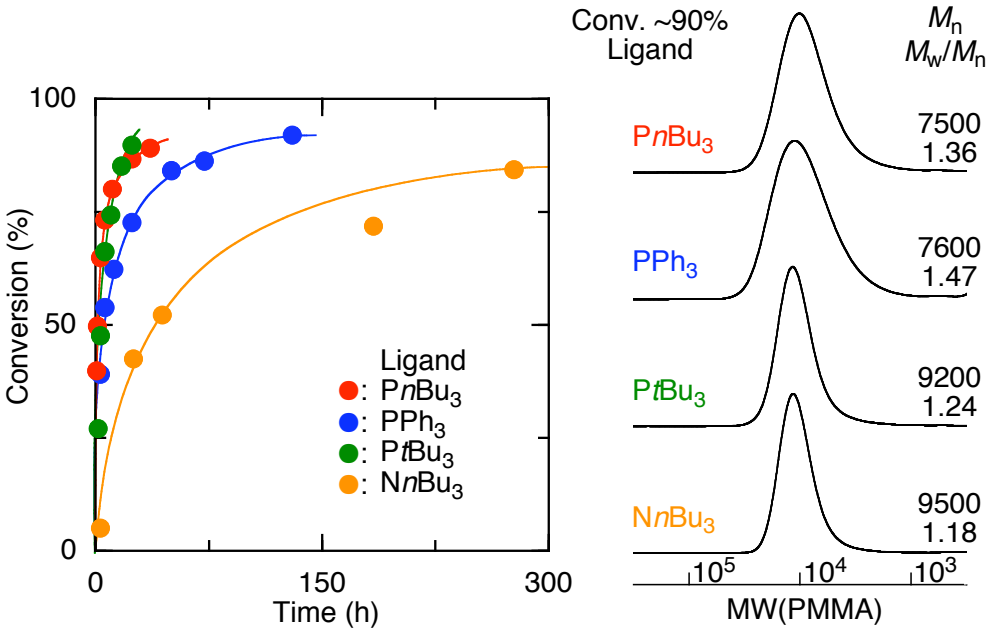

Figure 3. Time-conversion and SEC curves for the polymerization of MMA with **1**/$FeCl_3$/ligand system: $[MMA]_0$ = 2.0 M, $[\mathbf{1}]_0$ = 20 mM, $[FeCl_3]_0$ = 10 mM, $[ligand]_0$ = 10 mM in toluene at 100 °C.

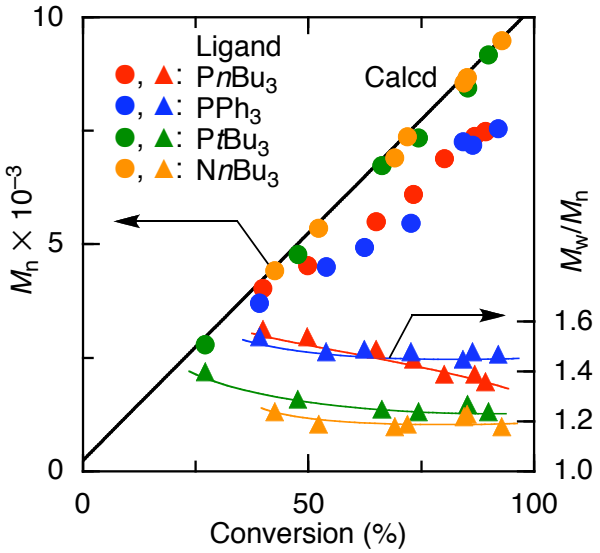

Figure 4. M_n and M_w/M_n of PMMA obtained in the living radical polymerization of MMA with $FeCl_3$/ligand: $[MMA]_0 = 2.0$ M, $[\mathbf{1}]_0 = 20$ mM, $[FeCl_3]_0 = 10$ mM, $[ligand]_0 = 20$ mM in toluene at 100 °C.

The terminal structures of the polystyrene and PMMA obtained under these conditions were examined by ^{1}H NMR spectroscopy. Figure 5 shows the ^{1}H NMR spectra of polystyrene and PMMA obtained from the reaction mixture of **1**, $FeCl_3$, and P*t*Bu$_3$ in toluene at 100 °C. In addition to the large absorptions (*a*, *b*, and *c*) corresponding to the repeating units of styrene and MMA, small signals were observed that correspond to the ω-end groups adjacent to the chlorine atom, including the –CH(Ph)–Cl (*b'*, 4.4 ppm) group (A) and the –OCH_3 (*c'*, 3.8 ppm) group (B). In addition, the spectrum of polystyrene (A) exhibited the characteristic peaks of α–CH_3 (0.6–1.1 ppm) and –OCH_3 (2.8–3.7 ppm) groups at the α-end derived from the MMA dimer (**1**) as an initiator. The M_n values obtained from the peak intensity ratio between the main chain and end-terminal signals of polystyrene were both 8400 (*d*; α-end and *b'*; ω-end). The value for PMMA was 8100 (*c'*; ω-end); these values are in agreement with those obtained by SEC [M_n(SEC) = 8200 and 7700, respectively]. The end functionalities of both polymers were thus calculated to be nearly unity, indicating that one polymer chain was generated from one initiator, as would be expected from conventional Fe(II)-catalyzed living radical polymerizations.

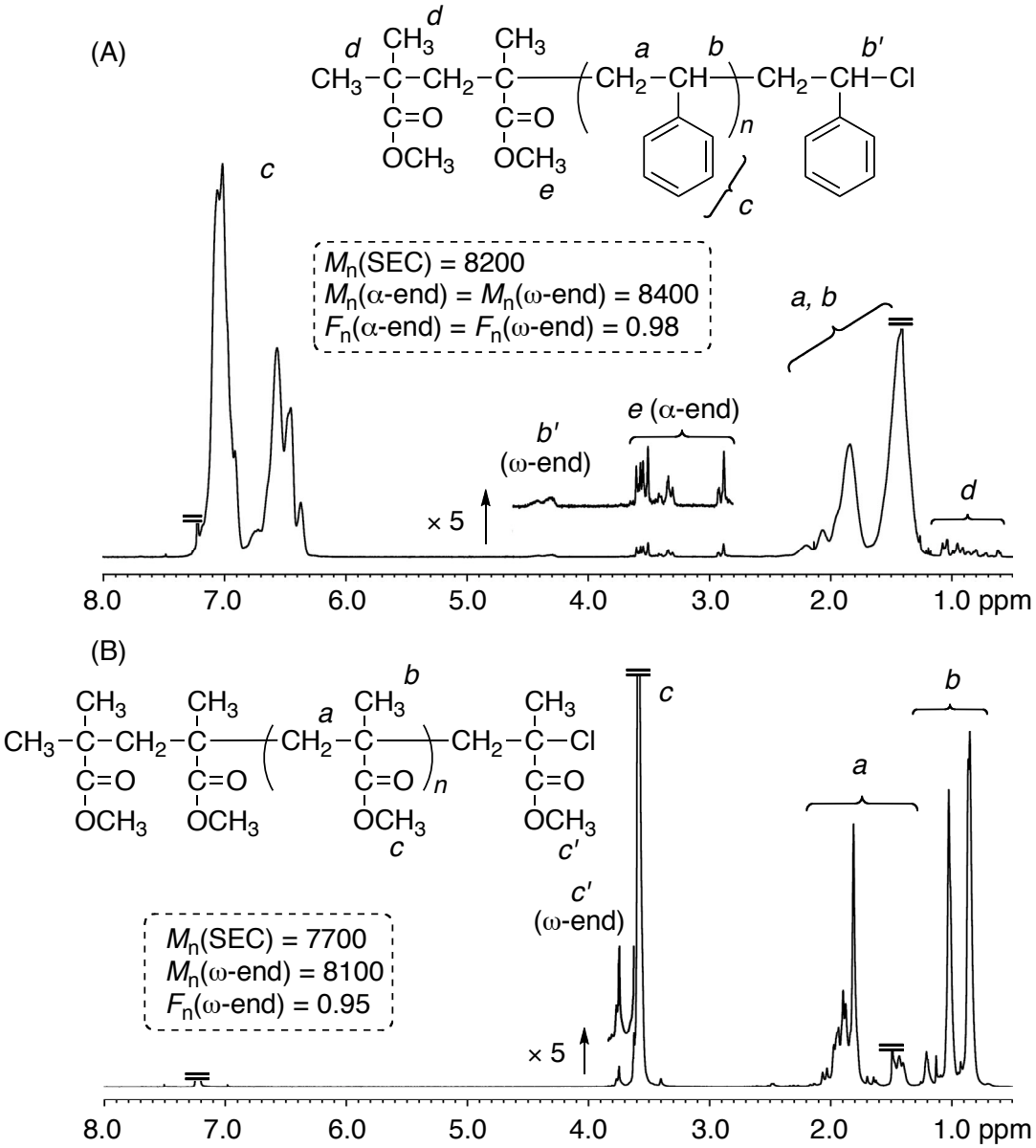

Figure 5. ^{1}H NMR spectra ($CDCl_3$, 55 °C) of polystyrene and PMMA obtained with **1**/$FeCl_3$/P*t*Bu_3 in toluene at 100 °C.

To investigate the living nature of the MMA polymerization with the **1**/$FeCl_3$/P*t*Bu_3 system, a fresh feed of MMA was added directly to the reaction mixture just before the initial charge of monomer was fully polymerized (conversion ~ 90%). Figure 6 shows the M_n, M_w/M_n, and SEC curves of the polymers. The additional portion of MMA was polymerized smoothly, and the peaks of the SEC curves shifted to high molecular weights while retaining relatively

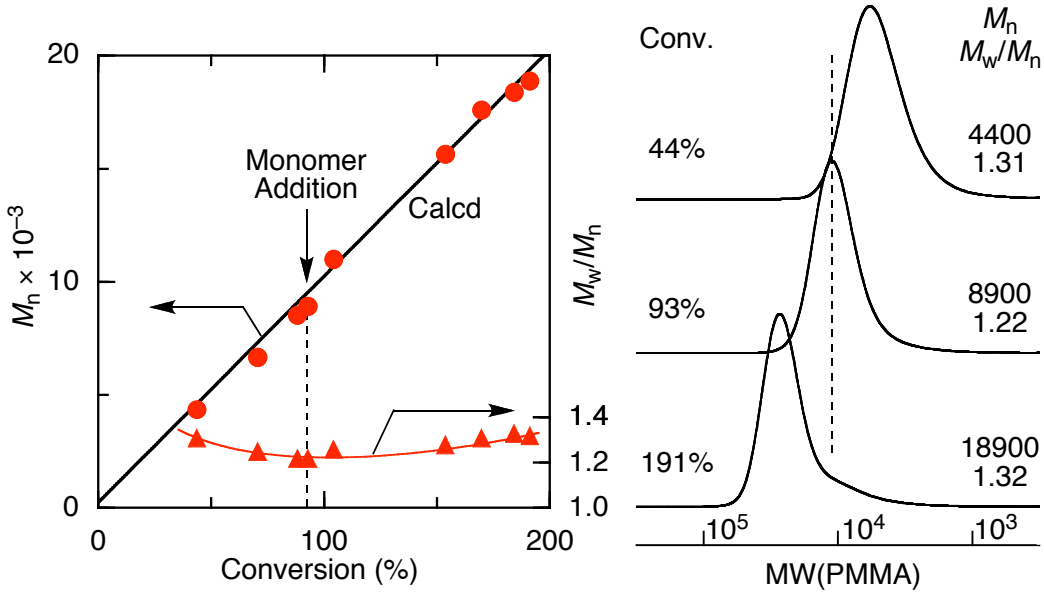

Figure 6. M_n, M_w/M_n, and SEC curves of PMMA obtained in a monomer-addition experiment in the polymerization with **1**/$FeCl_3$/P*t*Bu_3 system: $[MMA]_0 = [MMA]_{add} = 2.0$ M, $[\mathbf{1}]_0 = 20$ mM, $[FeCl_3]_0 = 10$ mM, $[P tBu_3]_0 = 10$ mM in toluene at 80 °C.

narrow molecular weight distributions ($M_w/M_n \sim 1.3$). The values of M_n increased in direct proportion to monomer conversion and were in good agreement with the theoretical values. These results indicate that the growing chains in the $FeCl_3$/P*t*Bu_3 system have a long-lived nature.

The removal of iron catalysts from the PMMA obtained using $FeCl_3$ with P*t*Bu_3 or $FeCl_3$ with N*n*Bu_3 was also investigated (see entries 5 and 9 in Table 2 for the polymerization conditions). The polymerization solution was diluted with toluene and washed three times each with dilute hydrochloric acid and distilled water to give an apparently colorless solution. Inductively coupled plasma mass spectrometry (ICP-MS) analysis of the polymers obtained under both conditions revealed that the Fe content was 4.0 ppm (for P*t*Bu_3) and 3.6 ppm (for N*n*Bu_3). These concentrations indicate almost quantitative removal of the residual iron catalyst compared with the initial catalyst concentrations (3090 ppm for P*t*Bu_3 and 3010 ppm for N*n*Bu_3). Thus, Fe(III)-based catalysts can be removed easily from the resultant polymer, as previously reported for Fe(II)-based systems.[10b,11b,22]

3. Synthesis of MMA-*b*-Styrene Block Copolymer

Based on the successful living radical polymerization of MMA and styrene, the synthesis of the corresponding block copolymers was investigated with the $FeCl_3$-based system (Figure 7). Chlorine-terminated PMMA was first synthesized with the **1**/$FeCl_3$/P*t*Bu$_3$ system in toluene at 100 °C. Using PMMA as the macroinitiator, block polymerization of styrene was then conducted with $FeCl_3$/P*n*Bu$_3$ in toluene at 100 °C. The second-stage polymerization of styrene also proceeded smoothly. The peaks of the SEC curves of the resulting copolymer shifted to the high molecular weight region while retaining relatively narrow molecular weight distributions (M_w/M_n ~ 1.3). ^{1}H NMR analysis of the copolymer revealed the monomer compositions to be in good agreement with those calculated from the initial feed ratio and monomer conversion. The ω-end signal of polystyrene appeared after the block copolymerization and not at the PMMA–Cl terminus (Figure 8). These results indicate that the $FeCl_3$/ligand system was also effective for the synthesis of PMMA-*block*-polystyrene.

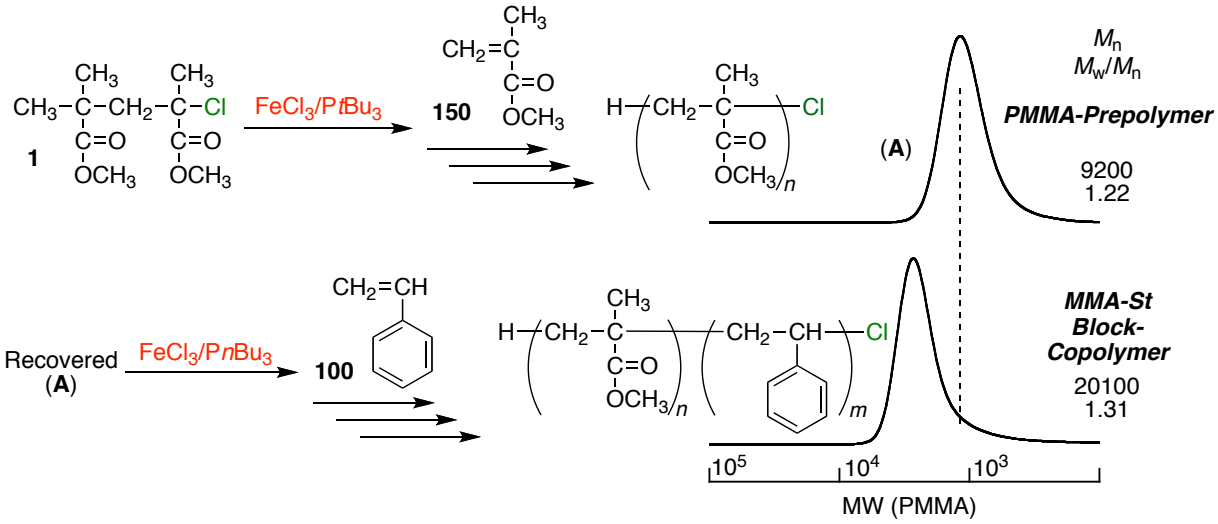

Figure 7. SEC curves of PMMA and PMMA-*block*-poly(styrene): (A) was synthesized with **1**/$FeCl_3$/P*t*Bu$_3$ (20/10/10 mM) in toluene at 80 °C (MMA Conversion = 63%). Styrene was polymerized with (A)/$FeCl_3$/P*n*Bu$_3$ (40/10/20 mM) in toluene at 100 °C: $[styrene]_0$ = 4.0 M.

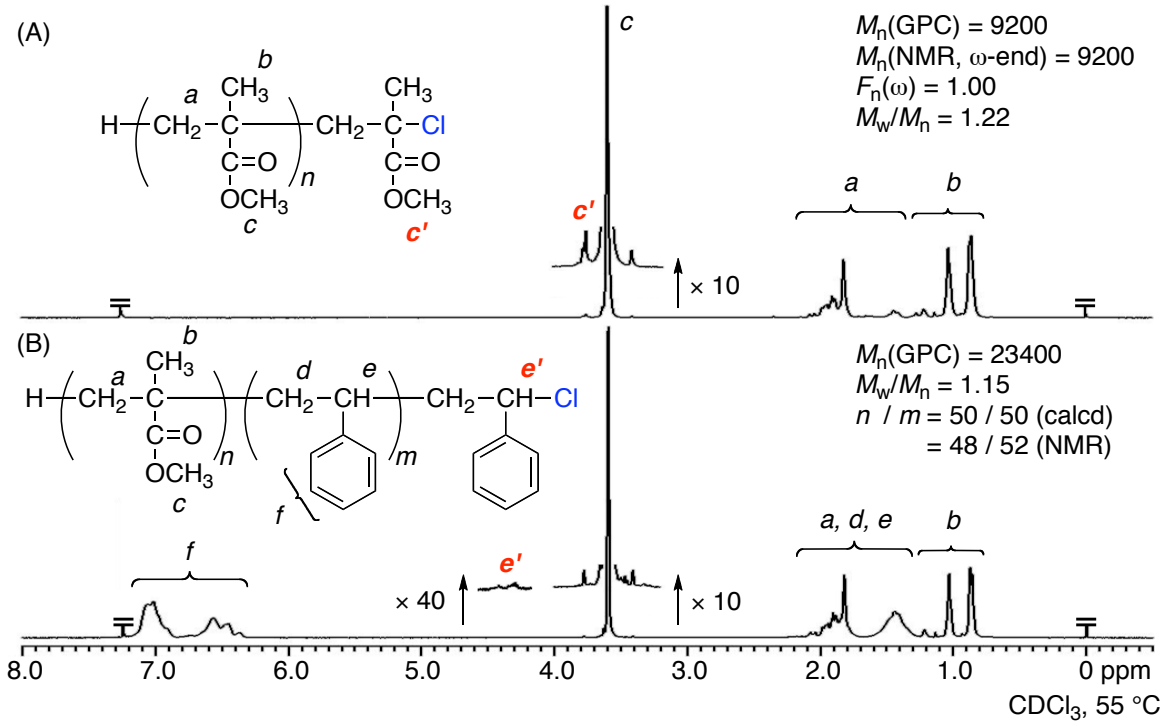

Figure 8. ^{1}H NMR spectra ($CDCl_3$, 55 °C) of PMMA-Cl (A) and PMMA-*b*-polystyrene block copolymer (B): (A) was synthesized with **1**/$FeCl_3$/P*t*Bu_3 (20/10/10 mM) in toluene at 80 °C (MMA Conversion = 63%). Styrene was polymerized with (A)/$FeCl_3$/P*n*Bu_3 (40/10/20 mM) in toluene at 100 °C: $[styrene]_0$ = 4.0 M.

4. Living Radical Polymerization of methyl acrylate with FeX_3/ligand system.

We further applied the **1**/$FeCl_3$/ligand system to the radical polymerization of methyl acrylate (MA) in toluene at 100 °C. In contrast to the polymerizations of styrene and MMA, $FeCl_3$/N*n*Bu_3 did not induce any polymerization (entry 8), while $FeCl_3$/P*n*Bu_3 and $FeCl_3$/P*t*Bu_3 produced poly(MA) with uncontrolled M_n and broad MWDs throughout the reaction. With PPh_3 as the ligand, however, the M_n values of the polymers produced were closer to theoretical values. The MWD values were also narrower, although consumption of MA leveled off at approximately 50% (entry 4 and Figure 9). In addition, decreasing the concentration of ligand (20 mM to 10 mM) slightly improved the controllability of the polymerization to result in narrower MWDs (entry 5).

Table 3. Living Radical Polymerization of MA with $FeCl_3$/ligand [a]

entry	ligand	[ligand]$_0$, mM	time, h	conv.[b], %	M_n[c]	M_n(calcd)[d]	M_w/M_n[c]
1	P*n*Bu$_3$	20	204	70	6000	6300	2.59
2	P*i*Bu$_3$	20	350	92	5700	8200	2.70
3	P*t*Bu$_3$	20	50	86	5300	7600	3.49
4	PPh_3	20	159	53	4600	4800	1.94
5	PPh_3	10	510	70	4600	6300	1.73
6	dppe	20	290	93	4700	8200	2.95
7	PCy_3	20	250	92	5300	8200	4.40
8	N*n*Bu$_3$	20	708	5	-	-	-

[a] $[MA]_0$ = 2.0 M, $[\mathbf{1}]_0$ = 20 mM, $[FeCl_3]_0$ = 10 mM, $[ligand]_0$ = 20 mM in toluene at 100 °C. [b] Determined by gas chromatography. [c] M_n and M_w/M_n were determined by SEC. [d] M_n(calcd) = MW(MA) × $[M]_0/[\mathbf{1}]_0$ × Conv. + MW(**1**).

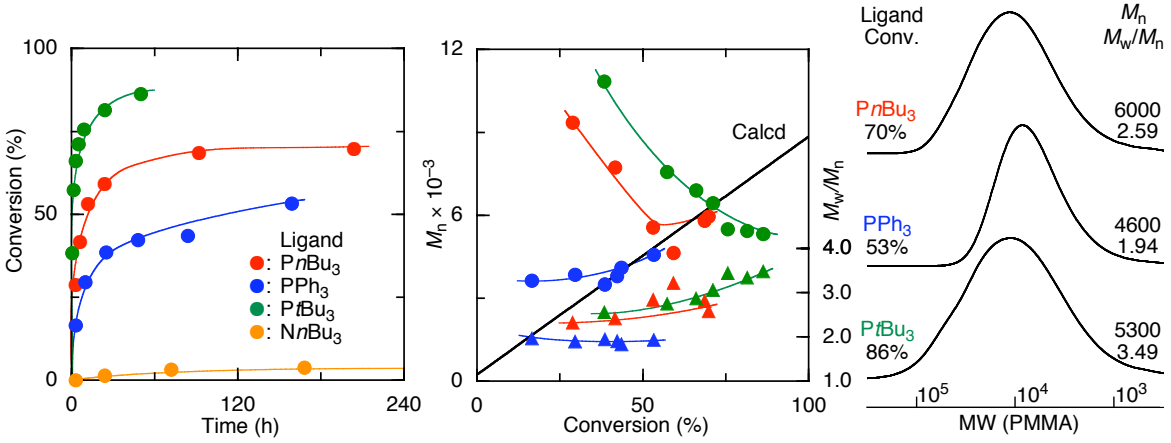

Figure 9. Time-conversion, M_n, M_w/M_n, and SEC curves of living radical polymerization of MA with $FeCl_3$/ligand: $[MA]_0$ = 2.0 M, $[\mathbf{1}]_0$ = 20 mM, $[FeCl_3]_0$ = 10 mM, $[ligand]_0$ = 20 mM in toluene at 100 °C.

To improve the controllability of the MA polymerization, the concentrations of monomer and catalyst were increased in the system consisting of FeX_3 (X = Cl, Br), PPh_3, and the corresponding halide initiator (Figure 10). Under bulk conditions, the **1**/$FeCl_3$/PPh_3 system induced the quantitative polymerization of MA. This process gave a controlled polymer in which M_n values increased with monomer conversion and were close to the calculated values, albeit with slightly broadened MWDs. The use of bromide for both iron halide ($FeBr_3$) and the initiator (**2**) further improved the MA polymerization to result in much narrower MWDs (M_w/M_n = 1.15).

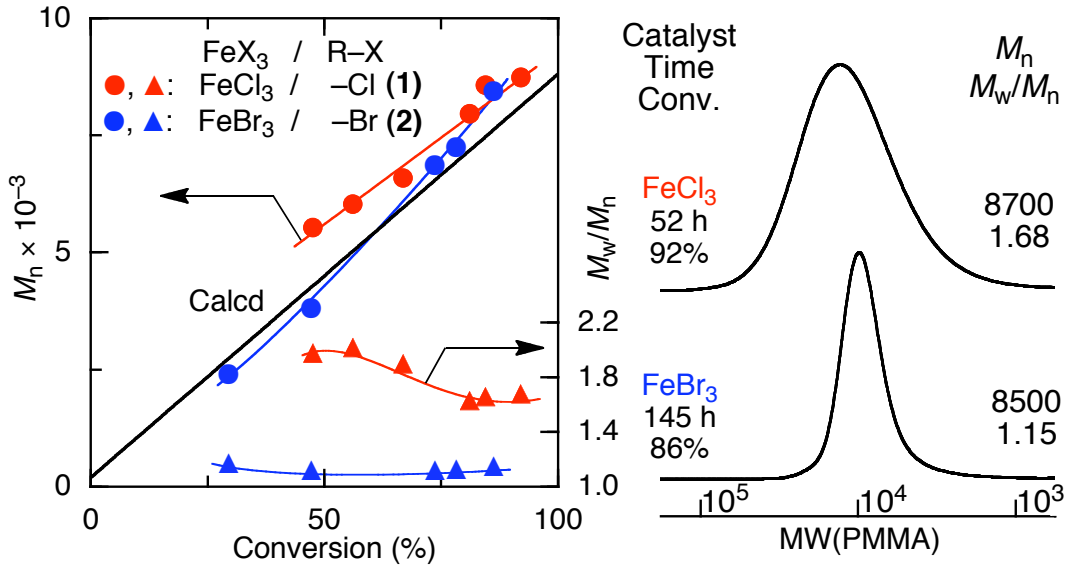

Figure 10. M_n, M_w/M_n, and SEC curves for the polymerization of MA with R–X/FeX_3/ligand system: $[MA]_0$ = bulk, $[MA]_0/[initiator]_0$ = 100, $[FeX_3]_0$ = 40 mM, $[PPh_3]_0$ = 40 mM in bulk at 100 °C.

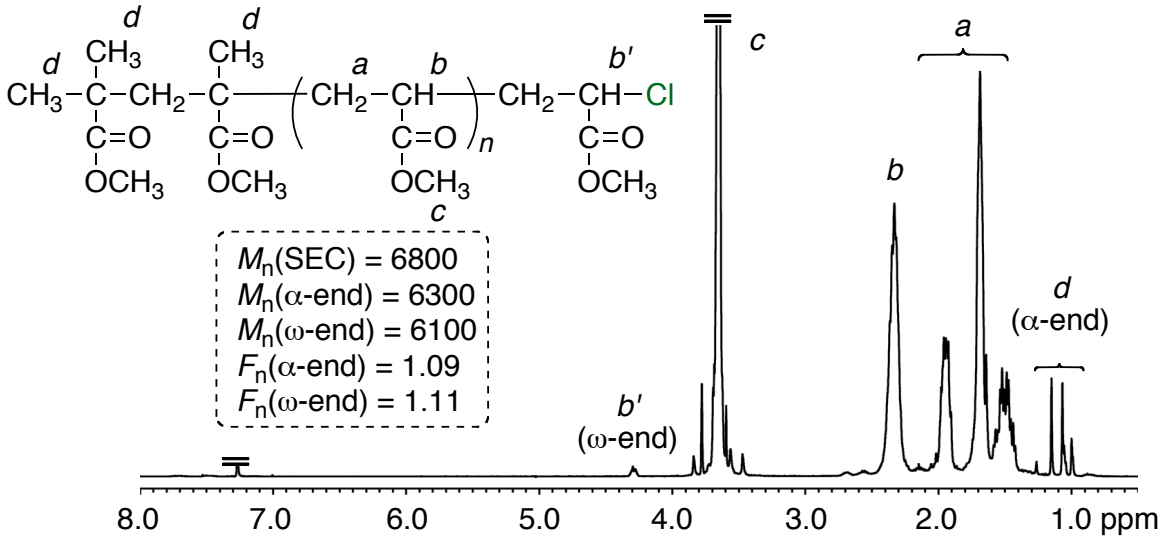

Figure 11. ^1H NMR spectra ($CDCl_3$, 55 °C) of poly(MA) obtained with **1**/$FeCl_3$/PPh_3 in toluene at 100 °C.

The ^{1}H NMR spectra of poly(MA) obtained with **1**/$FeCl_3$/PPh_3 also revealed small signals that could be assigned to an α-CH_3– group at the α-end and to a CH_2–$CH(CO_2CH_3)$–Cl group at the ω-end, in addition to the characteristic peaks of the MA unit (*a*, *b*, and *c*) (Figure 11). The functionalities were close to unity for both the α- and ω-end terminals [*d*; F_n(α-end) = 1.09, *b'*; F_n(ω-end) = 1.11]. The Fe(III)-based system, coupled with a judicious choice of ligands and halogen atoms, thus proved to be a versatile catalyst for living radical polymerization that is applicable to a wide range of monomers..

5. Polymerization Mechanism

How the higher oxidation state iron species, FeX_3, becomes active in the presence of phosphine and amine ligands and induces living radical polymerization has been unclear. The author investigated several model reactions as well as polymerizations under different conditions and analyzed them spectroscopically to clarify the mechanism.

(a) $FeCl_3$ as Inhibitor of Radical Polymerization of MMA

To confirm the ability of $FeCl_3$ to inhibit radical polymerization, the effect of $FeCl_3$ on MMA polymerization using AIBN as a radical initiator was first examined (Figure 12). When the free radical polymerization was first performed without $FeCl_3$ in toluene at 60 °C, the reaction reached almost quantitative conversion, 91%, in 48 h. In a subsequent experiment, $FeCl_3$ was added to the polymerization mixture when the conversion had reached 53% after 12 h. No further conversion was observed after the addition, and the polymerization clearly failed to proceed even after 80 h (blue circles). The molecular weights of the polymers that were produced were also unaltered after the addition. Thus, our results confirm that $FeCl_3$ alone in the absence of ligand actually serves as an inhibitor of radical polymerization.[51]

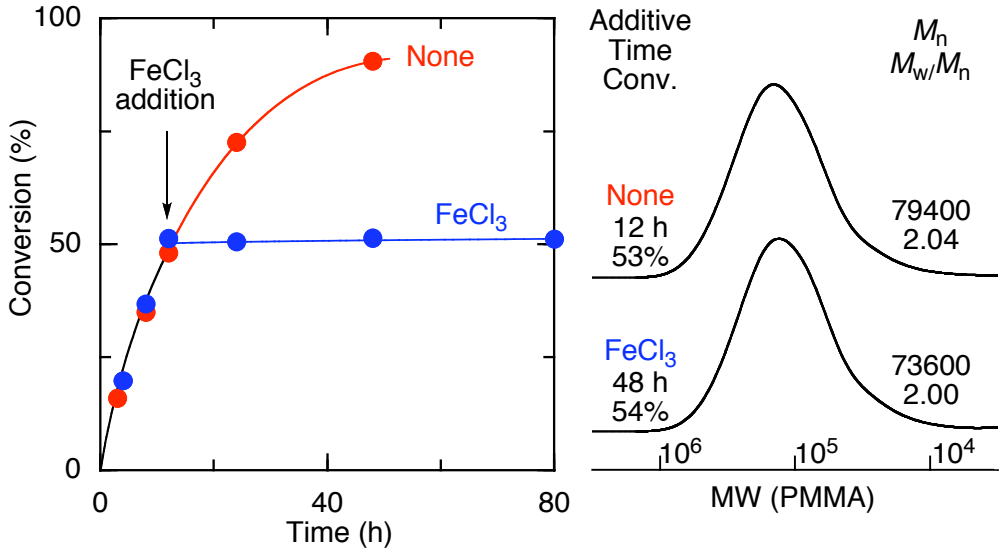

Figure 12. Effect of $FeCl_3$ on the MMA radical polymerization using AIBN: $[MMA]_0$ = 2.0 M, $[AIBN]_0$ = 20 mM, $[FeCl_3]_{add}$ = 10 mM in toluene at 60 °C.

(b) Model Reaction 1: Formation of Radical Species from C–X Bond with FeX_3/PR_3

Model reactions between **1** and $FeCl_3$ in the presence of P*n*Bu_3 without monomer were investigated to confirm the formation of radical species. This experiment also provided an opportunity to examine the possibility of irreversible reduction of $FeCl_3$ by the monomer, as has been suggested in other systems.[44,46,48,49] Figure 13 shows the ^{1}H NMR spectra of **1** alone (A), the products obtained from **1** and $FeCl_3$ with P*n*Bu_3 in toluene at 100 °C (B), and those obtained from **1**/$FeCl_2$/P*n*Bu_3 under similar conditions (C) as a control experiment for the normal lower-oxidation-state metal-catalyzed living radical polymerization. In Figure 13A, the characteristic peaks of the α-CH_3 (*a* and *b*, 1.1 and 1.7 ppm), –CH_2– (*c*, 2.6 ppm), and –OCH_3 groups (*d* and *e*, 3.6 and 3.7 ppm) can be observed. The products obtained with both iron halides in the presence of P*n*Bu_3 exhibit nearly identical spectra, irrespective of the oxidation state of the iron halides (Figures 13B and C). In addition to the peaks of **1** and possible coupling products, new signals corresponding to C=CH_2 (*f*, 5.5 and 6.2 ppm) and C–H (*g*, 2.5 ppm) groups appeared, suggesting disproportionation of the radical species derived from **1** in both cases. This

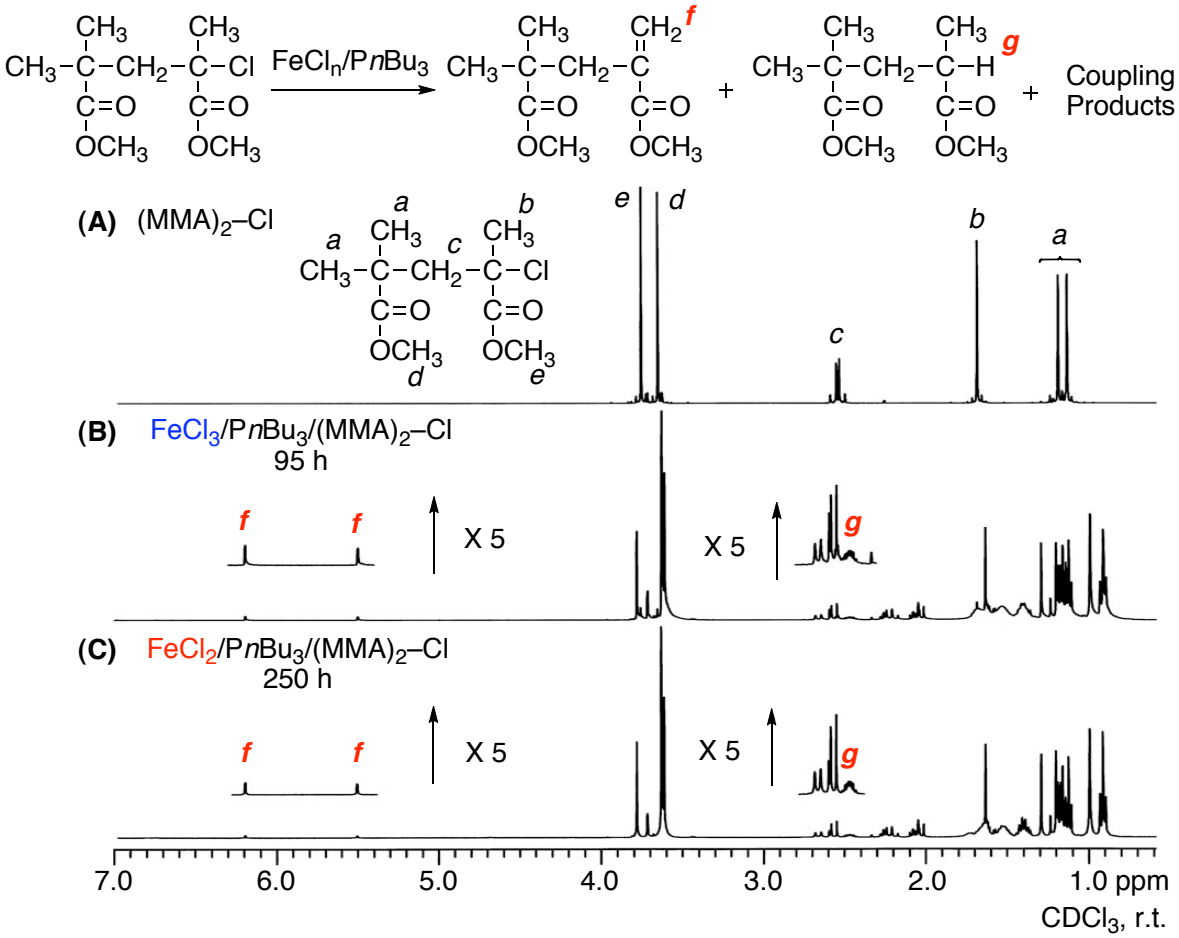

Figure 13. ^{1}H NMR spectra of **1** (A) and products obtained in the model reaction between **1** and FeCl$_n$/PnBu$_3$ (n = 3, 2) (B and C): [**1**]$_0$ = 100 mM, [FeCl$_n$]$_0$ = 100 mM, [PnBu$_3$]$_0$ = 200 mM in toluene at 100 °C.

indicates that the higher-oxidation-state FeCl$_3$ can activate the carbon-halogen bond in the presence of a ligand to generate radical species. This is true even in the absence of a monomer, as is the case for the lower oxidation state FeCl$_2$.

(c) Model Reaction 2: Formation of FeX_4^- from FeX_3/PR_3

Additional insight was gained from UV-Vis absorption studies. Model reactions between FeCl$_3$ and phosphine ligands were analyzed by UV-Vis spectroscopy to evaluate the state of FeCl$_3$ in the presence of the ligand. Figure 14 shows the spectra of FeCl$_3$ in the absence and

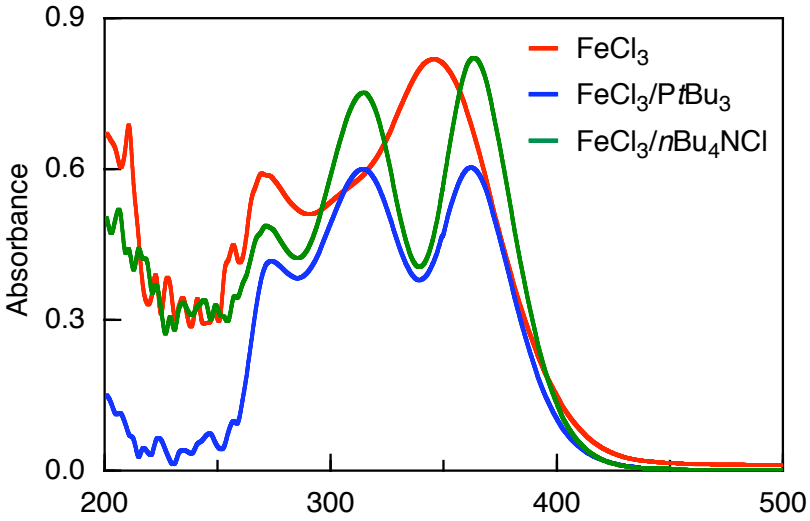

Figure 14. UV-vis spectra of $FeCl_3$ in absence and presence of additives; $[FeCl_3]_0$ = 0.1 mM, $[P\textit{t}Bu_3]_0$ = 0.05 mM, $[\textit{n}Bu_4NCl]_0$ = 0.1 mM in EtOAc at 25 °C.

presence of the ligand in ethyl acetate at 25 °C. In the absence of the ligand, $FeCl_3$ exhibited an absorption peak at 350 nm (red line). Upon the addition of $P\textit{t}Bu_3$ (0.5 equivalents to $FeCl_3$), the absorption peak of $FeCl_3$ alone disappeared, and two new peaks appeared at 310 and 360 nm (blue line). These two peaks are quite similar to those observed for the Fe(III) anion $[Fe(III)Cl_4^-]$,[52] which formed in the equimolar mixture of $FeCl_3$ and $\textit{n}Bu_4NCl$ (green line).

Furthermore, these two peaks were consistently observed in mixtures of $FeCl_3$ and $P\textit{n}Bu_3$ with $[FeCl_3]_0/[P\textit{n}Bu_3]_0$ ratios varying from 10/20 to 10/4 (Figure 15). When the concentration of $P\textit{n}Bu_3$ was appreciably less than half that of $FeCl_3$, e.g., $[FeCl_3]_0/[P\textit{n}Bu_3]_0$ = 10/4, the spectrum appeared to change, and the absorption at approximately 350 nm became more intense. These results indicate that $FeCl_3$ generates $Fe(III)Cl_4^-$ in the presence of $P\textit{n}Bu_3$ and that the concentration of $Fe(III)Cl_4^-$ is minimally altered in the presence of at least 0.5 equivalents of $P\textit{n}Bu_3$. Thus, it seems likely that $FeCl_3$ disproportionates into the Fe(III) anion $[Fe(III)Cl_4^-]$ and Fe(III) cation $[Fe(III)Cl_2^+]$ in the presence of 0.5 equivalents of $P\textit{n}Bu_3$.

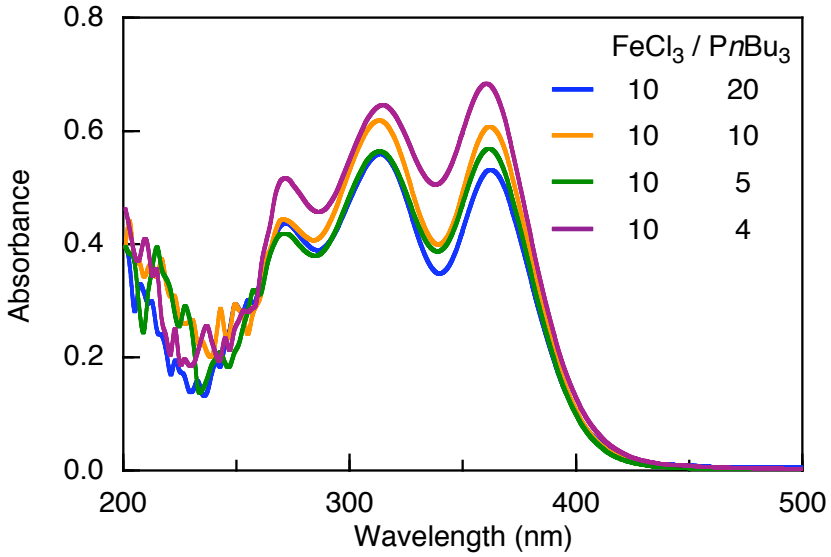

Figure 15. UV–Vis spectra of $FeCl_3$ in the presence of P*n*Bu$_3$: $[FeCl_3]_0$ = 0.1 mM, $[PnBu_3]_0$ = 0.04 – 0.2 mM in EtOAc at 25 °C.

(d) Effects of $[FeCl_3]_0/[PtBu_3]_0$ on Living Radical Polymerization of MMA

To clarify the effects of the ratio of $FeCl_3$ and P*t*Bu$_3$ on living radical polymerization, MMA was polymerized at various ratios of $[FeCl_3]_0/[PtBu_3]_0$; $[PtBu_3]_0$ was varied from 4.0 to 40 mM, and $[FeCl_3]_0$ was fixed at 10 mM (Figure 16). Polymerization of MMA proceeded smoothly at ratios of $[FeCl_3]_0/[PtBu_3]_0$ between 10/40 and 10/5, although the rate of polymerization was reduced at lower $[PtBu_3]_0$. All of the polymers produced possessed controlled molecular weights close to the calculated values and narrow MWDs, irrespective of metal and ligand concentrations. No polymerization occurred even after 300 h when the concentration of P*t*Bu$_3$ was less than half that of $FeCl_3$ ($[FeCl_3]_0/[PtBu_3]_0$ = 10/4). The abrupt change around $[FeCl_3]_0/[PtBu_3]_0$ = 2/1 is in close agreement with the corresponding observation by UV-Vis spectroscopy, suggesting that the disproportionation of $FeCl_3$ into Fe(III)Cl_4^- and Fe(III)Cl_2^+ in the presence of the phosphine ligand is crucial to inducing the living radical polymerization.

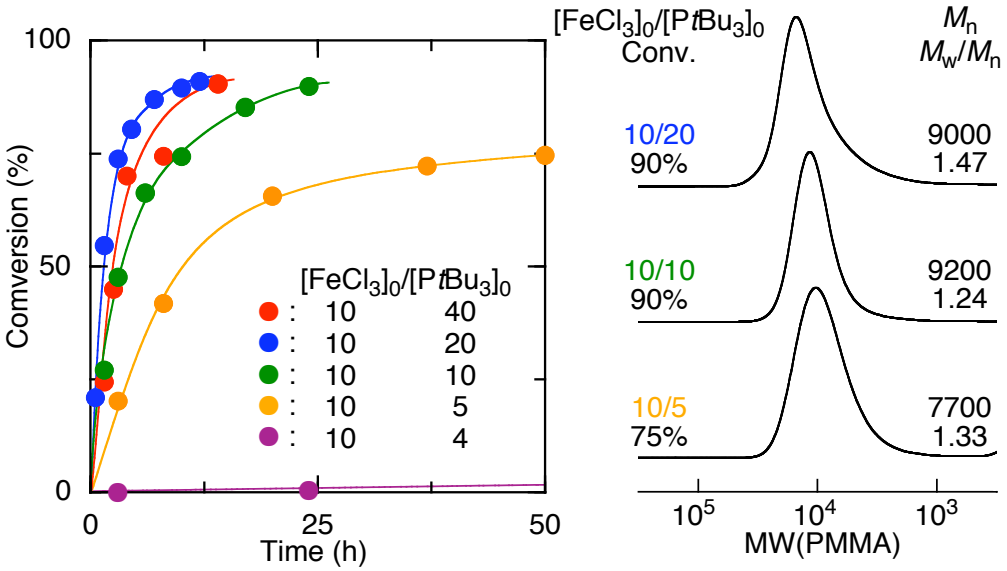

Figure 16. Living radical polymerization of MMA with various ratio of $FeCl_3$/P*t*Bu$_3$: $[MMA]_0$ = 2.0 M, $[\mathbf{1}]_0$ = 20 mM, $[FeCl_3]_0$ = 10 mM, $[ligand]_0$ = 40 – 4 mM in toluene at 100 °C.

(e) Proposed Mechanism

The proposed mechanism for the living radical polymerization with $FeCl_3/PR_3$ is depicted in Scheme 2. In the presence of a phosphine or amine ligand, $FeCl_3$ disproportionates into an anionic Fe(III) [Fe(III)Cl_4^-] and a cationic Fe(III) [Fe(III)Cl_2^+], where the Lewis base ligand coordinates to the latter cationic species to give Fe(III)$Cl_2(PR_3)^+$. Although the PR_3-coordinated cationic Fe(III) species may be transformed into the Fe(II) species [Fe(II)$Cl_2(PR_3)^{\cdot+}$] via reduction of Fe(III) by PR_3, the cationic Fe species [Fe(III)$Cl_2(PR_3)^+$ or Fe(II)$Cl_2(PR_3)^{\cdot+}$] could be an active catalyst and could activate the carbon–halogen bond by donating one electron from PR_3 or Fe(II) to generate a radical species. The resulting carbon radical species is deactivated by the Fe(III) species to regenerate the carbon–halogen terminal to enable living radical polymerization. Although attempts to isolate the active catalyst were unsuccessful, the Lewis basic phosphine or amine ligand most likely plays an important role in the catalytic cycle by donating an electron (either directly or indirectly) to the dormant carbon–halogen bond via its interaction with the Fe species.

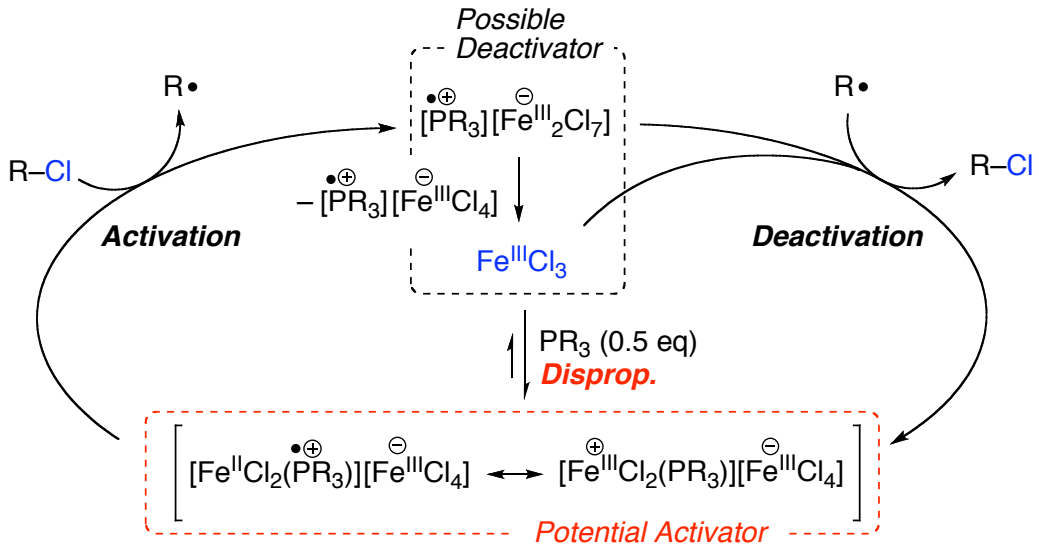

Scheme 2. Postulated Mechanism for Reversible Activation of C–Cl Bond with $FeCl_3/PR_3$.

Conclusion

In conclusion, the higher-oxidation-state Fe(III) halides were effective for living radical polymerization of various monomers, including styrene, methacrylate, and acrylate, in the presence of phosphine and amine ligands. It is proposed that $FeCl_3$ disproportionates into the Fe(III) anion [Fe(III)Cl_4^-] and Fe(III) cation [Fe(III)Cl_2^+] via interaction with the Lewis basic ligand and that this cation is the active catalyst for living radical polymerization. This system is promising in terms of industrial applications because of the easily removed, stable, abundant, and environmentally benign combination of an Fe(III) species and a simple ligand.

References

1. Moad, G.; Solomon, D. H. *The Chemistry of Radical Polymerization, 2nd ed.*; Elsevier: Oxford, UK, 2006.
2. Hawker, C. J.; Bosman, A. W.; Harth, E. *Chem. Rev*. **2001**, *101*, 3661–3688.
3. (a) Kamigaito, M.; Ando, T.; Sawamoto, M. *Chem. Rev*. **2001**, *101*, 3689–3745. (b) Kamigaito, M.; Ando, T.; Sawamoto, M. *Chem. Rec*. **2004**, *4*, 159–175. (c) Ouchi, M.; Terashima, T.; Sawamoto, M. *Acc. Chem. Res*. **2008**, *41*, 1120–1132. (d) Ouchi, M.; Terashima, T.; Sawamoto, M. *Chem. Rec*. **2009**, *109*, 4963–5050. (e) Kamigaito, M. *Polym. J.* **2010**, *43*, 105–120.
4. (a) Matyjaszewski, K.; Xia, J. *Chem. Rev*. **2001**, *101*, 2921–2990. (b) Tsarevsky, N. V.; Matyjaszewski, K. *Chem. Rev*. **2007**, *107*, 2270–2299. (c) Braunecker, W. A.; Matyjaszewski, K. *Prog. Polym. Sci*. **2007**, *32*, 93–146. (d) di Lena, F.; Matyjaszewski, K. *Prog. Polym. Sci*. **2010**, *35*, 959–1021. (e) Matyjaszewski, K. *Macromolecules* **2012**, *45*, 4015–4039.
5. Rosen, B. M.; Percec, V. *Chem. Rev*. **2009**, *109*, 5069–5119.
6. Moad, G.; Rizzardo, E.; Thang, S. H. *Aust. J. Chem.* **2005**, *58*, 379–410.
7. Kato, M.; Kamigaito, M.; Sawamoto, M.; Higashimura, T. *Macromolecules* **1995**, *28*, 1721–1723.
8. Ando, T.; Kamigaito, M.; Sawamoto, M. *Macromolecules* **1997**, *30,* 4507–4510.
9. Matyjaszewski, K.; Wei, M. Xia, J.; McDermott, N. E. *Macromolecules* **1997**, *30*, 8161–8164.
10. (a) Uchiike, C.; Terashima, T.; Ouchi, M.; Ando, T.; Kamigaito, M.; Sawamoto, M. *Macromolecules* **2007**, *40*, 8658–8662. (b) Uchiike, C.; Ouchi, M.; Ando, T.; Kamigaito, M.; Sawamoto, M. *J. Polym. Sci., Part A: Polym. Chem.* **2008**, *46*, 483–489.
11. (a) Kotani, Y.; Kamigaito, M.; Sawamoto, M. *Macromolecules* **1999**, *32*, 6877–6880. (b) Ishio, M.; Terashima, T.; Ouchi, M.; Sawamoto, M. *Macromolecules* **2010**, *43*, 920–926.
12. Kamigaito, M.; Onishi, I.; Kimura, S.; Kotani, Y.; Sawamoto, M. *Chem. Commun.* **2002**,

2694–2695.

13. Göbelt, B.; Matyjaszewski, K. *Macromol. Chem. Phys.* **2000**, *201*, 1619–1624.
14. Teodorescu, M.; Gaynor, S. G.; Matyjaszewski, K. *Macromolecules* **2000**, *33*, 2335–2339.
15. Louie, J.; Grubbs, R. H. *Chem. Commun.* **2000**, 1479–1480.
16. (a) Gibson, V. C.; O'Reilly, R. K.; Reed, W.; Wass, D. F.; White, A. J. P.; Williams, D. J. *Chem. Commun.* **2002**, 1850–1851. (b) Gibson, V. C.; O'Reilly, R. K.; Wass, D. F.; White, A. J. P.; Williams, D. J. *Dalton. Trans.* **2003**, 2824–2830. (c) O'Reilly, R. K.; Gibson, V. C.; Wass, D. F.; White, A. J. P.; Williams, D. J. *Polyhedron* **2004**, *23*, 2921–2928.
17. O'Reilly, R. K.; Gibson, V. C.; White, A. J. P.; Williams, D. J. *J. Am. Chem. Soc.* **2003**, *125*, 8450–8451.
18. Zhang, H.; Schubert, U. S. *Chem. Commun*. **2004**, 858–859.
19. Ibrahim, K.; Yliheikkilä, K.; Abu-Surrah, A.; Löfgren, B.; Lappalainen, K.; Leskelä, M.; Repo, T.; Seppälä, J. *Eur. Polym. J.* **2004**, *40*, 1095–1104.
20. Xue, Z.; Lee, B. W.; Noh, S. K.; Lyoo, W. S. *Polymer* **2007**, *48*, 4704–4714.
21. Ferro, R.; Milione, S.; Bertolasi, V.; Capacchione, C.; Grassi, A. *Macromolecules* **2007**, *40*, 8544–8546.
22. Niibayashi, S.; Hayakawa, H.; Jin, R.-H.; Nagashima, H. *Chem. Commun.* **2007**, 1855–1857.
23. Wang, G.; Zhu, X.; Zhu, J.; Cheng, Z. *J. Polym. Sci., Part A: Polym. Chem.* **2006**, *44*, 483–489.
24. Zhu, S.; Yan, D. *Macromol. Rapid Commun.* **2000**, *21*, 1209–1213.
25. Wang, Y.; Matyjaszewski, K. *Macromolecules* **2010**, *43*, 4003–4005.
26. (a) Teodorescu, M.; Gaynor, S. G.; Matyjaszewski, K. *Macromolecules* **2000**, *33*, 2335–2339. (b) Wang, Y.; Matyjaszewski, K. *Macromolecules* **2011**, *44*, 1226–1228.
27. Ishio, M.; Katsube, M.; Ouchi, M.; Sawamoto, M.; Inoue, Y. *Macromolecules* **2009**, *42*, 188–193.
28. Kanazawa, A.; Satoh, K.; Kamigaito, M. *Macromolecules* **2011**, *44*, 1927–1933.

29. Wang, J.-S.; Matyjaszewski, K. *J. Am. Chem. Soc*. **1995**, *117*, 5614–5615.

30. Pecec, V.; Barboiu, B. *Macromolecules* **1995**, *28*, 7970–7972.

31. Haddleton, D. M.; Jasieczek, C. B.; Hannon, M. J.; Shooter, A. J. *Macromolecules* **1997**, *30*, 2190–2193.

32. Granel, C.; Dobois, P.; Jérôme, R.; Teyssié, P. *Macromolecuels* **1996**, *29*, 8576–8582.

33. Uegaki, H.; Kotani, Y.; Kamigaito, M.; Sawamoto, M. *Macromolecules* **1997**, *30*, 2249–2253.

34. (a) Koumura, K.; Satoh, K.; Kamigaito, M. *Macromolecules* **2008**, *41*, 7359–7367. (b) Koumura, K.; Satoh, K.; Kamigaito, M. *Macromolecules* **2009**, *42*, 2497–2504. (c) Koumura, K.; Satoh, K.; Kamigaito, M. *J. Polym. Sci., Part A: Polym. Chem.* **2009**, *47*, 1343–1353. (d) Koumura, K.; Satoh, K.; Kamigaito, M. *Polym. J.* **2009**, *41*, 595–603.

35. (a) Bolm, C.; Legros, J.; Paih, J. L.; Zani, L. *Chem. Rev*. **2004**, *104*, 6217–6254. (b) Pearson, A. J. *Iron Compounds in Organic Synthesis*; Academic Press, London, U.K., 1994.

36. Wang, J.-S.; Matyjaszewski, K. *Macromolecules* **1995**, *28*, 7572–7573.

37. Moineau, G.; Dubois, Ph.; Jérôme, R; Senninger, T.; Teyssié, Ph. *Macromolecules* **1998**, *31*, 545–547.

38. Min, K.; Gao, H.; Matyjaszewski, K. *J. Am. Chem. Soc.* **2005**, *127*, 3825–3830.

39. Jakubowski, W.; Matyjaszewski, K. *Angew. Chem. Int. Ed.* **2006**, *45*, 4482–4486.

40. Matyjaszewski, K.; Jakubowski, W.; Min, K.; Tang, W.; Huang, J., Braunecker, W. A.; Tsarevsky, N. V.; *Proc. Natl. Acad. Sci. U.S.A*. **2006**, *42*, 15309–15314.

41. Percec, V.; Guliashvill, T.; Ladislaw, J. S.; Wistrand, A.; Stjerndahl, A.; Sienkowska, M. J.; Monteiro, M. J.; Sahoo, S. *J. Am. Chem. Soc.* **2006**, *128*, 14156–14165.

42. Luo, R.; Sen, A. *Macromolecules* **2008**, *41*, 4514–4518.

43. Chapter 1 of this thesis: Satoh, K.; Aoshima, H.; Kamigaito, M. *J. Polym. Sci., Part A: Polym. Chem.* **2008,** *46*, 6358–6363.

44. (a) Xue, Z.; Linh, N. T. B.; Noh, S. K.; Lyoo, W. S. *Angew. Chem. Int. Ed.* **2008**, *47*,

6426–6429. (b) Xue, Z.; Oh, H. S.; Noh, S. K.; Lyoo, W. S. *Macromol. Rapid Commun*. **2008**, *29*, 1887–1894. (c) Xue, Z.; He, D.; Noh, S. K.; Lyoo, W. S. *Macromolecules* **2009**, *42*, 2949–2957. (d) He, D.; Xue, Z.; Khan, M. Y.; Noh, S. K.; Lyoo, W. S. *J. Polym. Sci., Part A: Polym. Chem.* **2010,** 48, 144–151.

45. Wang, Y.; Kwak, Y.; Matyjaszewski, K. *Macromolecules* **2012**, *45*, 5911–5915.
46. Becer, C. R.; Hoogenboom, R.; Fournier, D.; Schubert, U. S. *Macromol. Rapid Commun*. **2007**, *28*, 1161–1166.
47. Kwak, Y.; Matyjaszewski, K. *Polym. Int.* **2009**, *58*, 242–247.
48. Khan, M. Y.; Xue, Z.; He, D.; Noh, S. K.; Lyoo, W. S. *Polymer* **2010**, *51*, 69–74.
49. He, D.; Noh, S. K.; Lyoo, W. S. *J. Polym. Sci., Part A: Polym. Chem.* **2011**, 49, 4594–4602.
50. Ando, T.; Kamigaito, M.; Sawamoto, M. *Macromolecules* **2000**, *33*, 2819–2824.
51. (a) Bamford, C. H.; Jenkins, A. D.; Johnston, R. *Nature* **1956**, *177*, 992. (b) Bamford, C. H.; Jenkins, A. D.; Johnston, R. *Proc. R. Soc*. **1957**, *239A*, 214–229.
52. (a) Brealey, J. G.; Uri, N. J. *Chem. Phys*. **1952**, *20*, 257–262. (b) Swanson, T. B.; Laurie, V. W. *J. Phys. Chem*. **1965**, *69*, 244–250.

Chapter 3

In-Situ Direct Mechanistic Transformation from $FeCl_3$-Catalyzed Living Cationic to Radical Polymerizations

Abstract

A trivalent iron chloride ($FeCl_3$) catalyst induced both living cationic and radical polymerizations of various monomers in the presence of an appropriate additive or ligand to yield polymers with controlled molecular weights and narrow molecular-weight distributions. The in-situ mechanistic transformation from a living cationic to a radical growing species during the styrene polymerization was achieved in a $FeCl_3$-based system with the simple addition of phosphine followed by an elevation of the reaction temperature. The growing cationic species was effectively converted into the radical species to produce a series of block copolymers that consist of styrene and various acrylic monomers.

Introduction

Since the discovery of living cationic polymerization,[1–5] reversible activation of dormant species has become a common method for controlled/living polymerizations, and reversible activation is now widely applicable for almost all chain-growth polymerizations.[6–9] Most living cationic polymerizations have been developed via the two-electron reversible activation of a covalent or dormant species, such as carbon–halogen and carbon–oxygen bonds. These dormant species are then transformed into the growing carbocationic species by various metal salts, including Sn(IV),[10] Ti(IV),[11] Zn(II),[12] Fe(III),[13] etc., which are usually in a higher oxidation state and thus possess considerable Lewis acidity.

As an analogy to living cationic polymerization, metal-catalyzed living radical polymerization or atom-transfer radical polymerization (ATRP) was discovered via the evolution of Kharasch or atom-transfer radical addition into radical polymerization, in which the dormant carbon–halogen bond is activated by a one-electron redox reaction of the metal center.[6,7] Effective transition-metal catalysts for this system include Ru(II),[14] Cu(I),[15–17] Fe(II)[18,19] etc., which are in a low oxidation state and thus able to release one electron to activate thedependin dormant covalent bond. Therefore, depending on the nature of the metal catalyst, a carbon–halogen bond can generate both the growing cationic and the radical species to induce cationic and radical polymerization, respectively.

Mechanistic transformation of the propagating species can expand the scope of polymerizable monomers during the polymerization. This technique is especially effective for the synthesis of block copolymers from different types of monomers via different active species.[20,21] Recently, dormant carbon–halogen bonds have been used for the preparation of block copolymers by a mechanistic transformation between living cationic and radical polymerizations via heterolytic and homolytic cleavage, respectively. For example, Lewis-acid-catalyzed living cationic polymerizations of cationically polymerizable monomers, such as β-pinene, isobutylene, and styrene, have been converted into living/controlled radical polymerizations of methyl acrylate

(MA), methyl methacrylate (MMA), and styrene by a switching of the catalysts to transition-metal complexes to yield block copolymers and vice versa.[22–25] However, most of the mechanistic transformations have been performed after the isolation of the halogen-capped polymer as the macroinitiator for the second-stage polymerization. For this technique, residues of the first metal catalysts must be rigorously removed because the metal catalysts for these two polymerizations are generally different.

Among the various metal catalysts for living polymerizations, iron complexes are highly promising because they are non-toxic, environmentally benign, abundant, and cost-effective. Iron(III) chloride ($FeCl_3$), a higher-oxidation-state species, has been employed as the Lewis acid to catalyze living cationic polymerizations of vinyl ether in combination with halide initiators.[13] As described in Chapter 1 and 2, the author have found that $FeCl_3$ also induces the living radical polymerization of styrene in conjunction with a halide initiator and an appropriate ligand such as tributylphosphine, contrary to the belief that the higher-oxidation-state iron(III) species would not be able to induce any radical polymerization without the intentional addition of reducing agents or radical initiators.[26] Although similar systems and their postulated mechanisms have been reported, discussions concerning the possible catalytic pathways still continue.[27–29]

This chapter is thus directed toward the in-situ mechanistic transformation of $FeCl_3$-catalyzed living cationic and radical polymerizations, both of which proceed by the reversible activation of C–Cl bonds by the same iron catalyst, for the synthesis of a series of block copolymers that comprise cationically and radically polymerizable monomers. The facile in-situ mechanistic transformation from cationic to radical polymerization was examined with the simple addition of phosphine or amine ligands to form the block copolymers in the same pot with the $FeCl_3$-based system (Scheme 1).

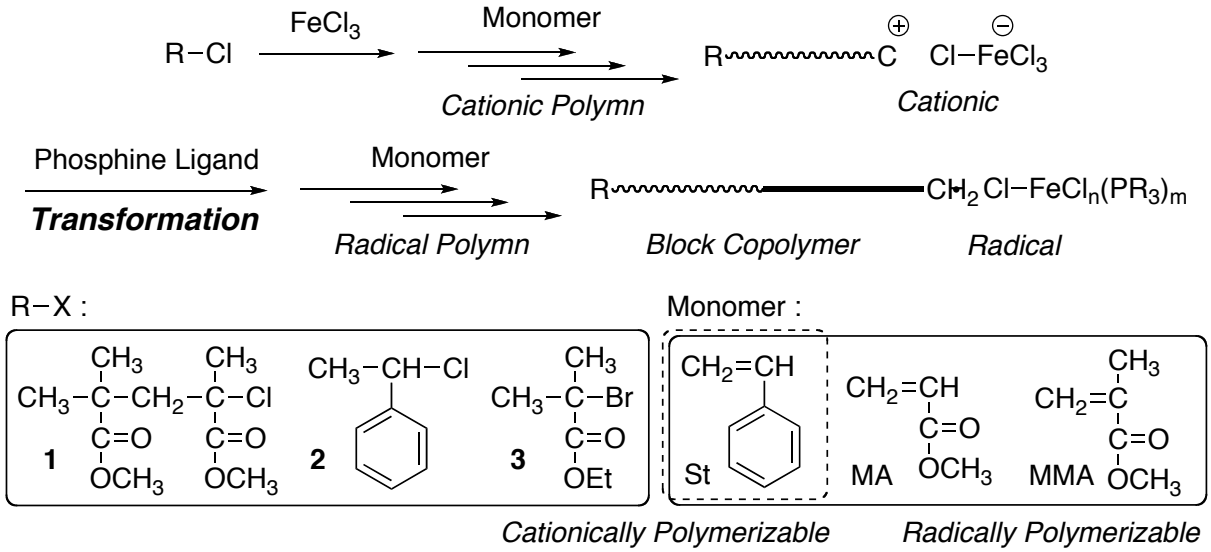

Scheme 1. Mechanistic Transformation from $FeCl_3$-catalyzed Living Cationic to Radical Polymerization

Experimental Section

Materials

Styrene (KISHIDA, 99.5%), methyl methacrylate (MMA; TCI; >99.8%) and methyl acrylate (MA; TCI; >99%) were distilled over calcium hydride under reduced pressure before use. $FeCl_3$ (Aldrich, >99.99%), $FeBr_3$ (Aldrich, 98%) and PPh_3 (Aldrich, 99%) were used as received and handled in a glove-box (VAC Nexus) under a moisture- and oxygen-free argon atmosphere (O_2 < 1 ppm). P*n*Bu_3 (KANTO, >98%) and P*t*Bu_3 (Aldrich, 98%) were used as received. N*n*Bu_3 (Wako, >98%), 1-chloroethylbenzene [MeCH(Ph)Cl (**2**)] (TCI, >97%), ethyl 2-bromoisobutyrate [$Me_2C(CO_2Et)Br$ (**3**)] (TCI, >98%) and chlorobenzene (Wako, >97%) were distilled from calcium hydride before use. $(MMA)_2$–Cl [$Me_2C(CO_2Me)CH_2C$-$(CO_2Me)(Me)Cl$ (**1**)] was prepared according to the literature.[30] Toluene (Kanto, >99.5%; H_2O<10 ppm), CH_2Cl_2 (Kanto, >99.5%; H_2O<10 ppm), diethyl ether (Et_2O; Kanto, >99.5%; H_2O<10 ppm) and methylcyclohexane (MCHx; Kanto, >98%; H_2O <0.1%) were dried and deoxygenized by passage through columns of Glass Contour Solvent Systems before use.

Polymerization

A typical example for the in-situ mechanistic transformation from the living cationic polymerization of styrene into the living radical polymerization of MA is given below. The cationic polymerization was initiated by addition of the CH_2Cl_2 solution (1.0 mL) of $FeCl_3$ (0.25 mmol; 0.041 g) and MA (5.0 mmol; 0.45 ml) into a monomer solution (4.0 mL), containing styrene (2.5 mmol; 0.29 mL), **2** (0.1 mmol; 0.17 mL of 0.59 M in CH_2Cl_2), and chlorobenzene (0.13 mL), in CH_2Cl_2/MCHx mixture (1.37/2.05 mL) at –40 °C. The total volume of the reaction mixture was thus 5.0 mL. When the conversion of styrene reached 92% (120 h, M_n = 2000, M_w/M_n = 1.21), the CH_2Cl_2/MCHx solution (1/1 v/v; 1.25 mL) of PPh_3 (2.5 mmol; 0.66 g) was directly added to the polymerization solution and maintained this at –40 °C of 12 h. The solution was then evenly charged in seven glass tubes, and the tubes were sealed by flame under a nitrogen atmosphere. The tubes were immersed in thermostatic oil bath at 80 °C. After an additional 200 h, the polymerization was terminated by cooling the reaction mixtures to –78 °C. The monomer conversions were determined from the concentration of the residual monomer measured by gas chromatography (> 99% for styrene) with chlorobenzene and ^{1}H NMR (37% for MA) with MCHx as the internal standard respectively. The quenched reaction mixture was diluted with toluene (ca. 30 ml), washed with dilute hydrochloric acid and water to remove complex residues, evaporated to dryness under reduced pressure, and vacuum-dried to give poly(styrene-*b*-MA) copolymer (M_n = 2700, M_w/M_n = 1.30).

Measurements

^{1}H NMR spectra were recorded on a JEOL ESC-400 spectrometer, operating at 400 MHz. The number-average molecular weight (M_n) and molecular weight distribution (MWD; M_w/M_n) of the polymers were measured by size-exclusion chromatography (SEC) using THF at a flow rate 1.0 mL/min at 40 °C on two polystyrene gel columns [Shodex KF-805L (pore size: 20–1000 Å; 8.0 mm i.d. × 30 cm)] that were connected to a JASCO PU-2080 precision pump and

a JASCO RI-2031 detector. The columns were calibrated against 10 standard polystyrene samples (Varian; M_p = 575–2783000, M_w/M_n = 1.02–1.23) for polystyrene and styrene-MA copolymers or 11 standard poly(MMA) samples (Varian; M_p = 202–1677000, M_w/M_n = 1.02–1.23) for poly(MMA).

Results and Discussion

1. Living Cationic and Radical Polymerizations Catalyzed by $FeCl_3$

Prior to the study of the mechanistic transformations during the polymerizations, each living cationic and radical polymerization of styrene was investigated using $FeCl_3$ as the catalyst (Figure 1). The cationic polymerization of styrene was first examined using $FeCl_3$ in conjunction with a chloride initiator [MeCH(Ph)Cl (**2**)] in a mixture of solvents (CH_2Cl_2/MCHx) at –40 °C. The polymerization proceeded smoothly and reached a nearly quantitative conversion in 85 h. As the polymerization proceeded, the SEC curves shifted to a higher-molecular-weight region but maintained their narrow MWDs (Figure 1). The M_n of the cationically obtained polystyrene increased in direct proportion to the monomer conversion. In addition, this value agreed well with the calculated value if one chloride initiator molecule was assumed to generate one living polymer chain (filled symbols), although the cationic polymerization was well controllable below 5,000 molecular weights as in the reported systems for styrene.[1–5] Thus, the Lewis-acidic $FeCl_3$ induces living cationic polymerization of styrene via the heterolytic cleavage of the C–Cl terminal.

As described in Chapter 1 and 2, trivalent $FeCl_3$ also catalyzes living radical polymerization of styrene in the presence of a phosphine ligand, which is contrary to a general belief that a higher-oxidation-state metal species should inhibit or retard this polymerization.[26] Coupled with tributylphosphine (P*n*Bu$_3$) as the ligand, $FeCl_3$ was used as a catalyst for the polymerization of styrene in conjunction with another chloride initiator $Me_2C(CO_2Me)$-

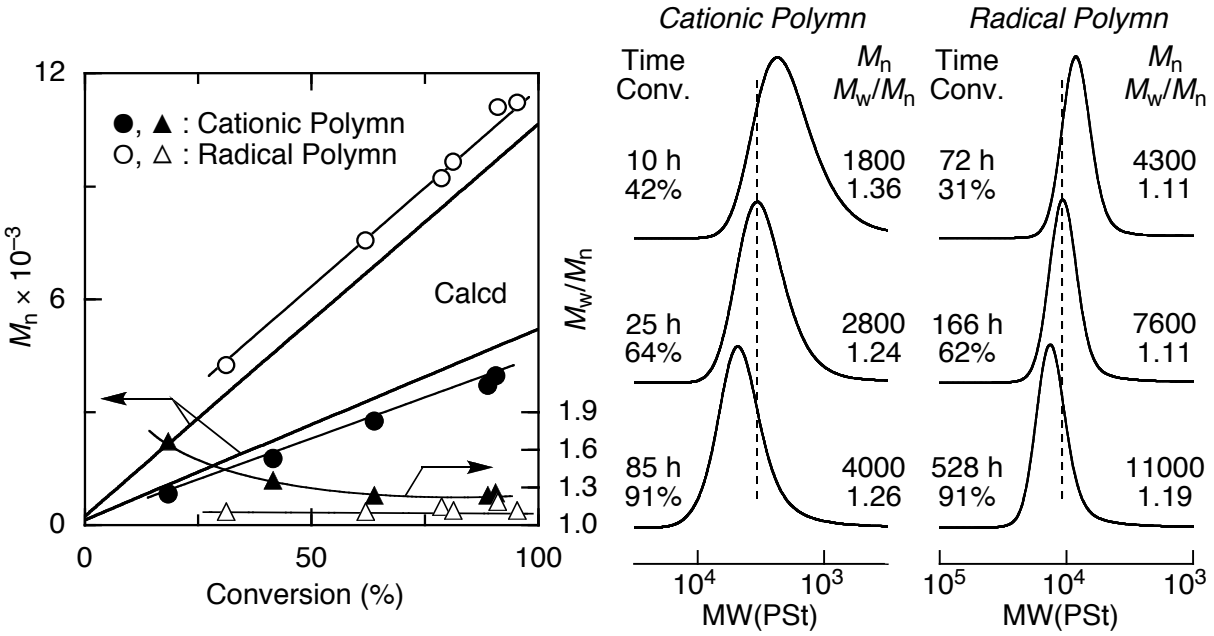

Figure 1. $FeCl_3$-catalyzed living radical and cationic polymerization of styrene in the presence (radical) or absence (cationic) of P*n*Bu$_3$: [styrene]$_0$ = 4.0 M, [**1**]$_0$ = 40 mM, [$FeCl_3$]$_0$ = 10 mM, [P*n*Bu$_3$]$_0$ = 20 mM in toluene at 100 °C (for radical polymerization), [styrene]$_0$ = 0.5 M, [**2**]$_0$ = 10 mM, [$FeCl_3$]$_0$ = 50 mM, [Et_2O]$_0$ = 300 mM in CH_2Cl_2/MCHx (1:1 v/v) at –40 °C (for cationic polymerization).

$CH_2C(CO_2Me)(Me)Cl$ (**1**), in toluene at 100 °C. The polymerization proceeded in a living fashion to produce polymers with controlled M_n and narrow MWDs ($M_w/M_n \sim 1.2$) (open symbols in Figure 1).

The radical polymerization in the presence of P*n*Bu$_3$ was significantly slower (91% conversion in 528 h) than the cationic polymerization that occurred in its absence (91% conversion in 85 h), even when this system was at a higher temperature. These results indicate that $FeCl_3$ effectively induces both the living radical and cationic polymerizations of styrene via activation of the C–Cl bonds in a reaction that is dependent on the various conditions and additives used.

2. $FeCl_3$-Catalyzed Living Radical Polymerization of (Meth)acrylic Monomers

The author also investigated the radical polymerizations of (meth)acrylic monomers, such as MMA and MA.[26b] Each radical polymerization of MMA and MA using $FeCl_3$ also proceeded with a range of ligands and halide initiators in toluene at 100 °C (Table 1). For the MMA polymerization, the use of **1** as the initiator gave controlled molecular weights irrespective of the phosphine or amine ligands used (entries 1–4), whereas **2** resulted in uncontrolled molecular weights because of slower initiation from the secondary C–Cl bond as compared to the tertiary bond of the producing PMMA (entry 5). Among the tested conditions, when **1** was coupled with the use of tri-*t*-butyl phosphine (P*t*Bu$_3$) or tributylamine (N*n*Bu$_3$) as the ligand, $FeCl_3$ afforded PMMA with the narrowest MWDs (M_w/M_n ~ 1.2). In contrast, in the MA polymerization, both **1** and **2** gave polymers with similarly controlled M_n values, which were similar to the calculated

Table 1. Living Radical Polymerization of MMA and MA with FeX_3/Ligand [a]

Run	Monomer	R–X	FeX_3	Ligand	Time (h)	Conv.[b] (%)	M_n[c]	M_n(calcd)[d]	M_w/M_n[d]
1	MMA	**1**	$FeCl_3$	P*n*Bu$_3$	36	90	7500	9300	1.36
2	MMA	**1**	$FeCl_3$	P*t*Bu$_3$	24	90	9200	9300	1.24
3	MMA	**1**	$FeCl_3$	PPh_3	130	92	7600	9500	1.47
4	MMA	**1**	$FeCl_3$	N*n*Bu$_3$	720	93	9500	9600	1.18
5	MMA	**2**	$FeCl_3$	P*t*Bu$_3$	150	84	14000	8600	1.35
6	MA	**1**	$FeCl_3$	PPh_3	52	92	8700	8200	1.68
7	MA	**2**	$FeCl_3$	PPh_3	140	97	9400	8500	1.68
8	MA	**3**	$FeBr_3$	PPh_3	145	86	8500	7600	1.15

[a] Polymerization conditions: $[MMA]_0$ = 2.0 M, $[R–X]_0$ = 20 mM, $[FeCl_3]_0$ = $[ligand]_0$ = 10 mM in toluene at 100 °C (for MMA). $[MA]_0/[R–X]_0$ = 100, $[FeX_3]_0$ = $[ligand]_0$ = 40 mM in toluene at 100 °C (for MA). [b] Determined by gas chromatography. [c] M_n(calcd) = MW(Monomer) × $[Monomer]_0/[R–X]_0$ × Conv. + MW(R–X). [d]Determined by SEC in THF (PMMA standard).

values, in conjunction with $FeCl_3$ and triphenylphosphine (PPh_3) (entries 6 and 7), whereas the MWDs were slightly broad. The combination of a bromide initiator (**3**) and $FeBr_3$ further improved the control of the MA polymerization to afford polymers with narrow MWDs (M_w/M_n = 1.15) (entry 8). Thus, the R–X/$FeCl_3$/PR'_3 or NR'_3 system proved effective for living radical polymerizations of not only styrene, but also of MMA and MA with an appropriate choice of the ligand and initiator.

3. In-situ Direct Mechanistic Transformation during Styrene Polymerization

The author subsequently examined the in-situ mechanistic transformation of the cationic to the radical growing species during the styrene polymerization. The living cationic polymerization of styrene was first investigated with $FeCl_3$ in CH_2Cl_2/MCHx at –40 °C. This experiment was then followed by the addition of P*n*Bu_3 and the elevation of the reaction temperature to 100 °C to continue the second polymerization via the radical intermediate in a single pot. When the cationic polymerization reached a nearly quantitative conversion (90% in 60 h), a fresh feed of styrene and P*n*Bu_3 was added to the polymerization mixture, which was kept at –40 °C for an additional 12 h and was then heated to 100 °C. Upon heating, the second-stage styrene polymerization resumed, likely via formation of the radical growing species.

Figure 2 shows the M_n values and SEC curves of the obtained polymer during the styrene polymerization. After the addition of the monomer and the phosphine ligand, the SEC curves further shifted to higher molecular weights while maintaining unimodal distributions, and the M_n increased with monomer conversion. The M_n slightly deviated from the calculated line in the later stages of the polymerization, which was likely because of a chain-transfer reaction, such as b-proton elimination at the C–Cl terminus of polystyrene, induced by the Lewis-acidic $FeCl_3$ in a polar solvent (CH_2Cl_2) at a high temperature. Similar results were reported in living radical polymerizations of styrene derivatives with the Fe(II) or Cu(II) complex coupled with an iodine or bromide initiator. Thus, the mechanistic transformation of the $FeCl_3$-catalyzed living cationic to

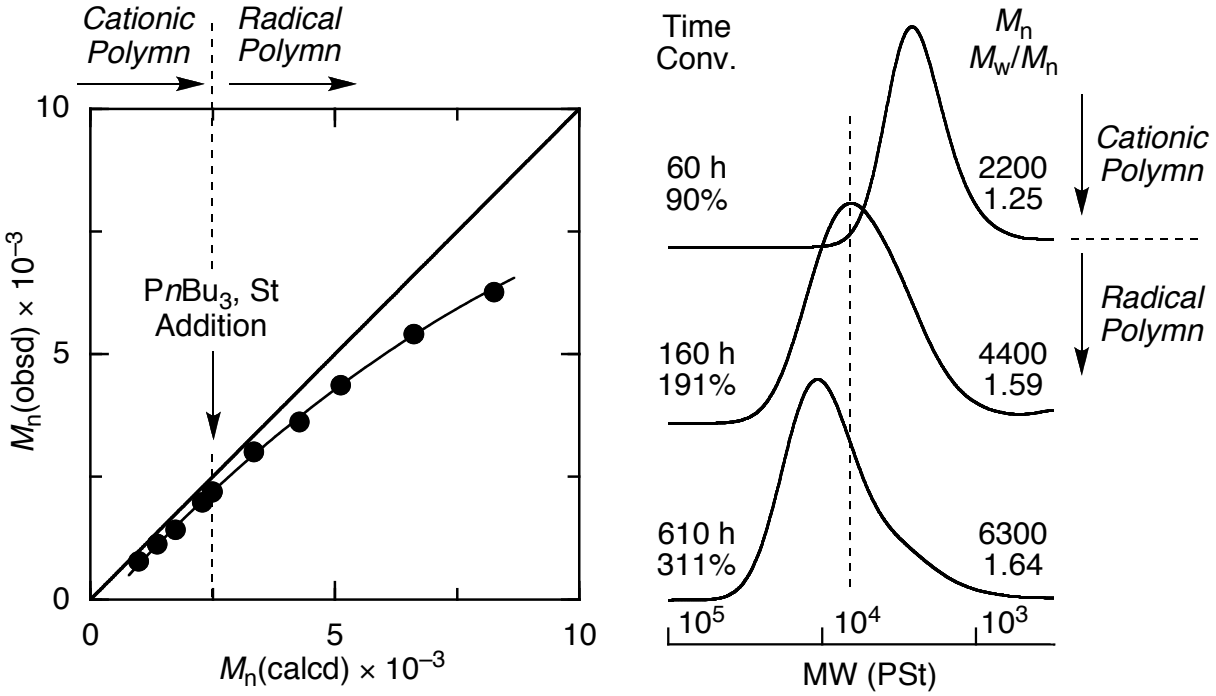

Figure 2. M_n, M_w/M_n and SEC curves of polystyrene obtained by the mechanistic transformation from living cationic to radical polymerization of styrene: $[styrene]_0$ = 0.5 M, $[styrene]_{add}$ = 2.0 M, $[\mathbf{2}]_0$ = 20 mM, $[FeCl_3]_0$ = 50 mM, $[P\textit{n}Bu_3]_{add}$ = 500 mM, $[Et_2O]_0$ = 300 mM in CH_2Cl_2/MCHx (1:1 v/v) at –40 °C to 100 °C.

radical polymerization of a single monomer, styrene, was achieved by the simple addition of the phosphine ligand and an elevation of the reaction temperature.

4. Synthesis of Styrene-MA Block Copolymers via Mechanistic Transformation

The synthesis of block copolymers consisting of styrene and MA was then examined via an in-situ mechanistic transformation with an R–Cl/$FeCl_3$/ligand system (Figure 3). The cationic polymerization of styrene was first performed with **2**/$FeCl_3$ in the absence or presence of MA (A and B, respectively).

Even in the presence of MA, the cationic styrene polymerization proceeded in a living fashion, although the rate of this reaction was slower compared with the rate of the reaction in

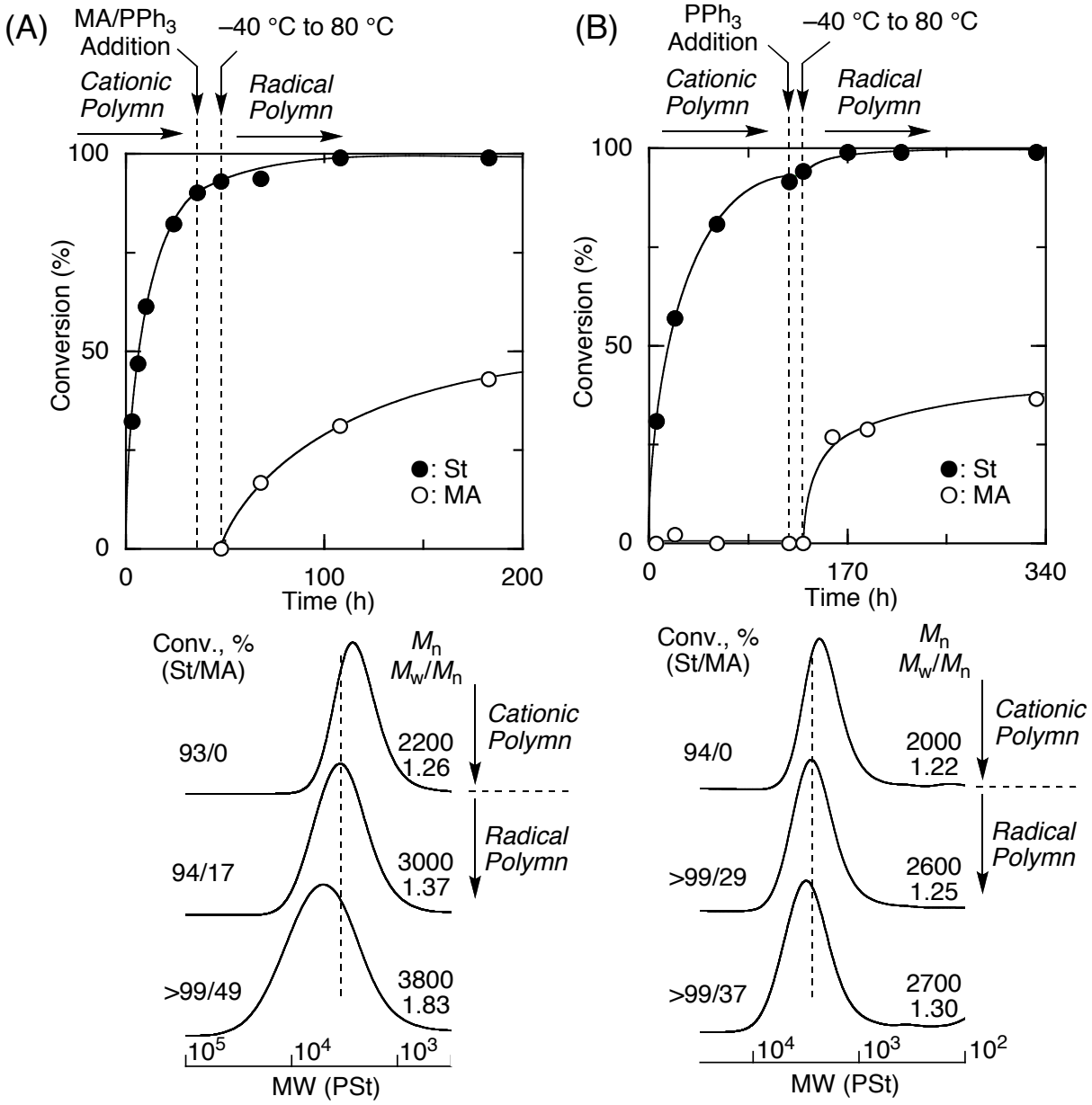

Figure 3. Time-conversion and SEC curves of poly(styrene-*b*-MA) obtained by the transformation from living cationic polymerization of styrene to living radical polymerization of MA in CH_2Cl_2/MCHx (1:1 v/v) at –40 °C to 80 °C: (A); $[styrene]_0$ = 0.5 M, $[MA]_{add}$ = 2.0 M, $[\mathbf{2}]_0$ = 20 mM, $[FeCl_3]_0$ = 50 mM, $[PPh_3]_{add}$ = 500 mM, $[Et_2O]_0$ = 300 mM, (B); $[styrene]_0$ = 0.5 M, [MA] = 1.0 M, $[\mathbf{2}]_0$ = 20 mM, $[FeCl_3]_0$ = 50 mM, $[PPh_3]_{add}$ = 500 mM.

which MA was absent, to afford polystyrenes with slightly narrower MWDs. This result shows that MA serves as a Lewis base to retard the cationic polymerization and to yield narrower MWDs. Immediately before the styrene was consumed, PPh_3, with or without MA, was added to the reaction mixture (Figures 3A and 3B, respectively). The mixture was maintained at –40 °C for an additional 12 h and heated to 80 °C. In both cases, the radical polymerization of MA took place smoothly after the addition and subsequent heating of the reaction mixture to produce the block copolymers. The SEC curves further shifted to high molecular weights, although the MWDs became slightly broader. More importantly, a narrower MWD was attained with procedure (B) in which only the addition of the ligand induced the in-situ mechanistic transformation from cationic to radical polymerization.

This in-situ mechanistic transformation was further utilized for the synthesis of block copolymers that consisted of polystyrene and random copolymers of styrene and MA blocks. In this synthesis, transformation by the ligand addition was conducted during the course of the cationic homopolymerization of styrene in the presence of MA to switch the reaction mechanism to a radical copolymerization of the residual styrene and MA. The living cationic polymerization of styrene was thus performed in the presence of MA at –40 °C, followed by the addition of PPh_3 at 61% styrene conversion in 22 h. After the addition of the phosphine ligand, the temperature was elevated to 80 °C, and the MA and the residual styrene were smoothly and simultaneously copolymerized. As shown in Figure 4, the SEC curves shifted to high molecular weights while retaining relatively narrow and unimodal MWDs ($M_w/M_n \sim 1.3$).

Thus, the $FeCl_3$-catalyzed living cationic polymerization of styrene can also be transformed into the radical (co)polymerization of MA, both of which proceed via activation of the dormant carbon–chlorine bond by the same metal catalyst, $FeCl_3$. The block copolymerization via this transformation not only proceeded well, but also gave tunable compositions of styrene and MA in the resulting block copolymer when a proper time was chosen for the addition of the ligands.

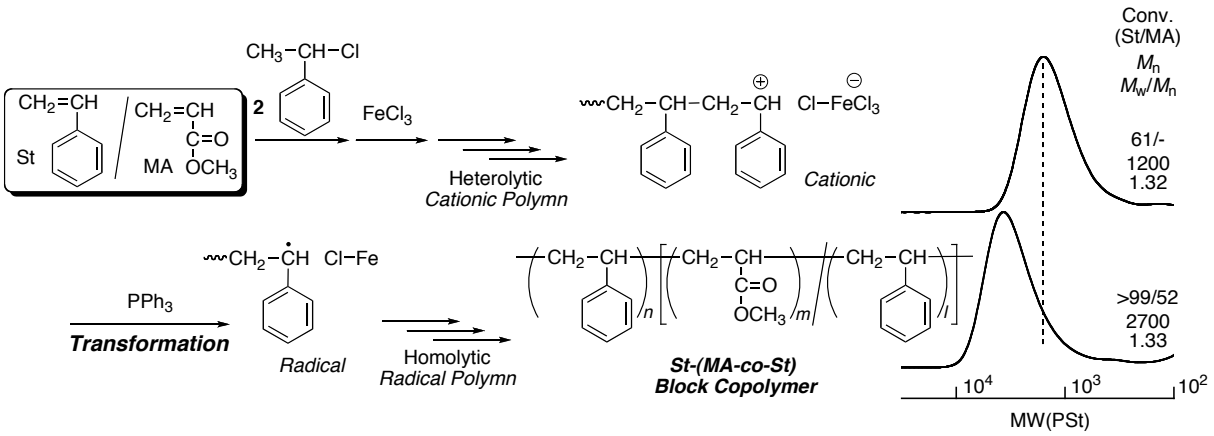

Figure 4. SEC curves of polystyrene and poly(styrene-*b*-MA) obtained by the transformation from living cationic polymerization of St to living radical copolymerization of MA: $[\text{styrene}]_0$ = 0.5 M, $[\text{MA}]_0$ = 1.0 M, $[\mathbf{2}]_0$ = 20 mM, $[FeCl_3]_0$ = 50 mM, $[PPh_3]_{add}$ = 500 mM, in CH_2Cl_2/MCHx (1:1 v/v) at –40 °C to 80 °C.

Figure 5 shows the ^{1}H NMR spectra of the polystyrene and block copolymers that were obtained with the $FeCl_3$-based system. The polymer obtained by the cationic polymerization of styrene in the presence of MA (Figure 5A) showed the characteristic signals of polystyrene without any concomitant MA units. In addition to the large absorptions that correspond to phenyl (*c*) and main-chain aliphatic (*a* and *b*) protons, small signals due to the end groups appeared, including a $–CH_3$ group (*a′*, 0.8–1.1 ppm) at the α-end and a CH(Ph)–Cl group (*b′*, 4.4 ppm) at the ω-end. The appearance of these signals was attributed to the chlorine atom at the growing terminal. Both of these groups are derived from the use of **2** as an initiator. The M_n value obtained from the peak intensity ratio of *b′* to c [M_n(NMR, ω-end) = 1900] was similar to that obtained by SEC [M_n(SEC) = 2100]. The functionality of the ω-end (*b′*: F_n = 0.91) was almost unity, which indicates that one polymer was generated from one initiator during the cationic polymerization.

As shown in Figures 5B and 5C, the polymers obtained after the mechanistic transformation showed the signals of the MA units, which are the methoxy (*f*) and main-chain aliphatic (*d* and *e*) protons, in addition to those of the styrene units. When styrene and MA were

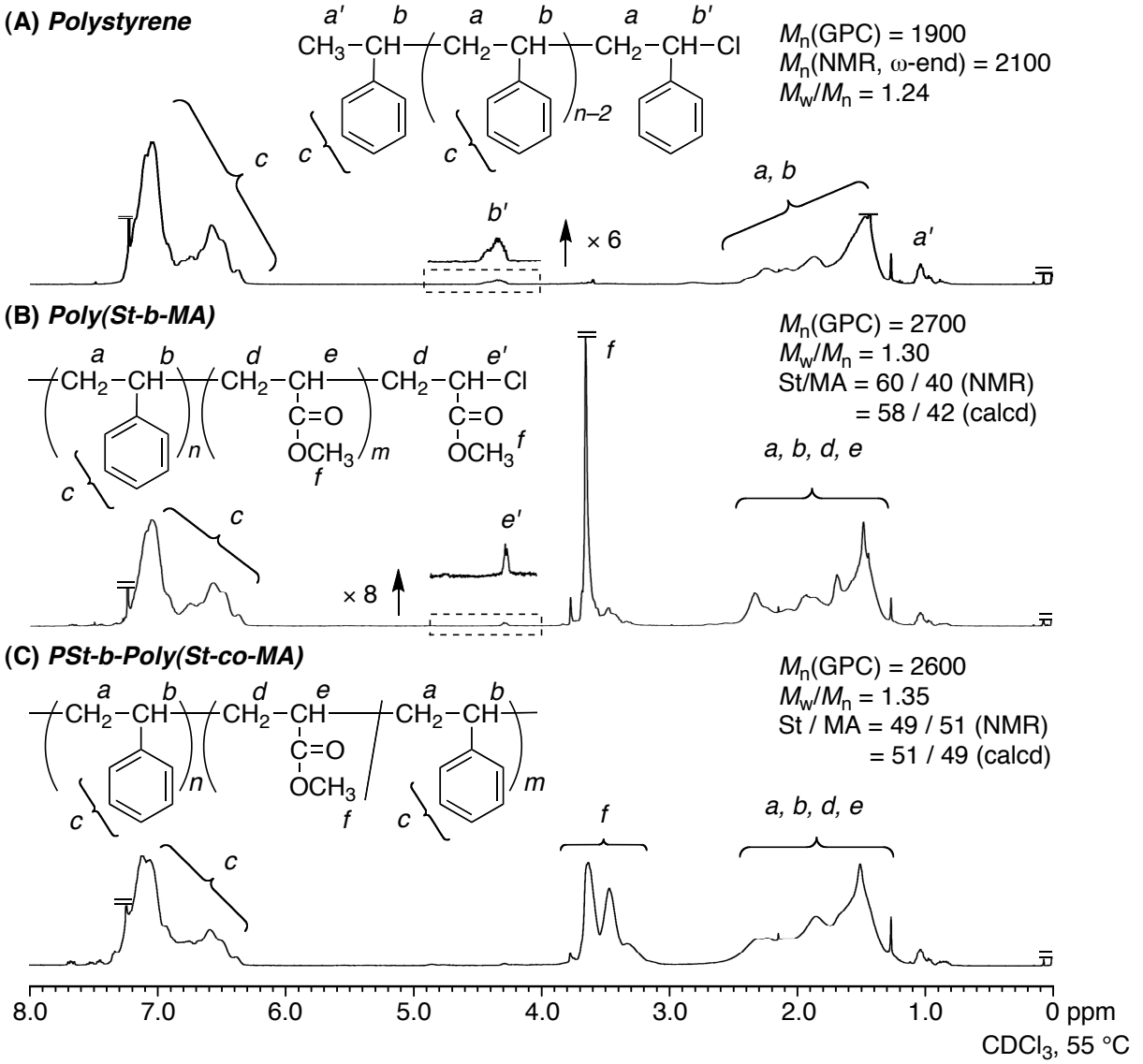

Figure 5. ^{1}H NMR spectra of (A) polystyrene, (B) poly(styrene-*b*-MA), and (C) polystyrene-*b*-poly (styrene-*co*-MA) obtained by the mechanistic transformation. See Figure 3B and 4 for synthesis conditions.

randomly copolymerized in the second stage of polymerization, the peak *f* became broader and split due to the comonomer sequences and cotacticity (Figure 5C). The signal of the methine proton (*b′*) at the chloride ω-terminal of polystyrene completely disappeared after the transformation, and, alternatively, a small signal (*e′*) appeared at 4.3 ppm, which was assigned to the methine proton [CH(CO_2Me)–Cl] at the terminal of the poly(MA) segment. In both spectra,

the unit ratios of styrene to MA calculated from the peak areas of *c* and *f* (60/40 and 49/51) agreed well with the calculated values from the monomer conversion and feed ratio (58/42 and 51/49, respectively).

5. Mechanistic Transformation for MMA-Containing Block Copolymer

A similar transformation from the cationic polymerization of styrene to the radical polymerization of MMA was also investigated. The transformation that occurred after the nearly complete consumption of styrene resulted in bimodal MWDs in the second-stage MMA radical polymerization. This result was attributed to a slower initiation of the MMA polymerization from the CH(Ph)–Cl terminal of polystyrene, as observed in the MMA homopolymerization with initiator **2** (see entry 5 in Table 1). In contrast, the addition of MMA and P*t*Bu$_3$ during the course of the cationic polymerization of styrene resulted in unimodal SEC curves that shifted to higher molecular weights in the second-stage radical copolymerization of styrene and MMA to form polystyrene-*b*-poly(styrene-*co*-MMA) copolymers (Figure 6).

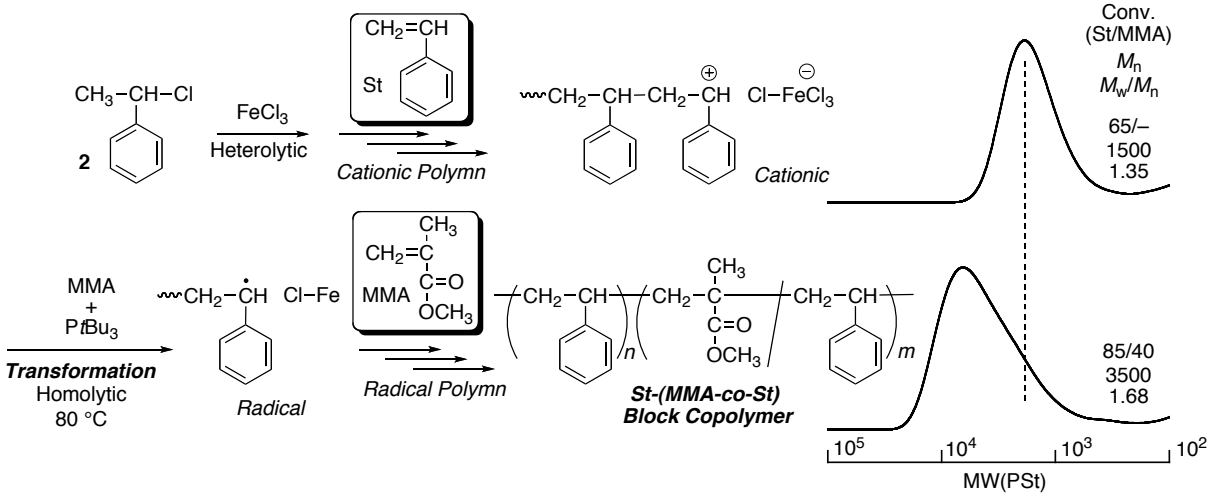

Figure 6. SEC curves of polystyrene and poly(styrene-*b*-MMA) obtained by the transformation from living cationic polymerization of styrene to living radical polymerization of MMA: $[\text{styrene}]_0$ = 0.5 M, $[\text{MMA}]_{add}$ = 2.0 M, $[\mathbf{2}]_0$ = 20 mM, $[FeCl_3]_0$ = 50 mM, $[P\textit{t}Bu_3]_{add}$ = 50 mM, $[Et_2O]_0$ = 300 mM in CH_2Cl_2/MCHx (1:1 v/v) at –40 °C to 80 °C.

This result suggests that radical cross-propagation between MMA and residual styrene yielded a more equal opportunity for propagation to almost all the polymer chains during the second-stage radical polymerizations because styrene can smoothly be polymerized both from the secondary CH(Ph)–Cl and tertiary C(CH_3)(CO_2Me)–Cl terminals.

The ^{1}H NMR spectrum of the polystyrene-*b*-poly(styrene-*co*-MMA) showed the characteristic signals of PMMA, i.e., the main-chain aliphatic (*d*), α-methyl (*e*), and methoxy (*f*) protons, in addition to the polystyrene signals (*a*–*c*) (Figure 7). Similar to the polystyrene-*b*-poly(styrene-*co*-MA) copolymer, a broadened methoxy group (*e*) was observed in the spectrum, which indicates that the obtained polymer contained the random copolymer segment. The styrene/MMA ratio, which was obtained from the peak areas of the phenyl (*c*) and methoxy (*e*) groups (38/62), was nearly identical to the calculated value from the monomer conversion and feed ratio (35/65). These results indicate that the mechanistic transformation of a radical copolymerization of MMA was achieved by addition of the appropriate ligand in the $FeCl_3$-based system.

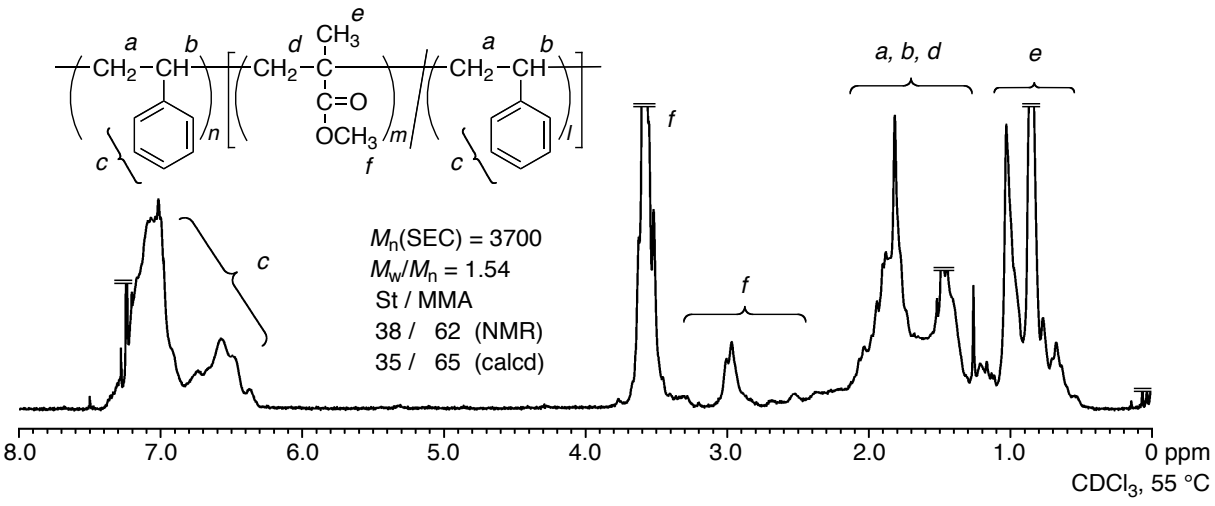

Figure 7. ^{1}H NMR spectrum of poylystyrene-*b*-poly(styrene-*co*-MMA) obtained in the same experiments as for Figure 6.

Conclusion

In this chapter, both the living cationic and radical polymerizations were achieved using higher-oxidation-state $FeCl_3$ as the catalyst under appropriate reaction conditions. As a result, the in-situ mechanistic transformation from the $FeCl_3$-mediated living cationic polymerization to the radical polymerization successfully occurred via the activation of the C–Cl terminal of polystyrene after the simple addition of the phosphine ligand and subsequent heating. This method could be further utilized for the one-pot synthesis of various block copolymers between cationically and radically polymerizable monomers.

References

1. Miyamoto, M.; Sawamoto, M.; Higashimura, T. *Macromolecules* **1984**, *17*, 265–268.
2. Faust, R.; Kennedy, J. P. *Polym. Bull.* **1986**, *15*, 317−323.
3. Sawamoto, M. *Prog. Polym. Sci.* **1991**, *16*, 111−172.
4. Puskas, J. E.; Kaszas, G. *Prog. Polym. Sci.* **2000**, *25*, 403−452.
5. Aoshima, S.; Kanaoka, S. *Chem. Rev.* **2009**, *109*, 5245−5287.
6. Kamigaito, M.; Ando, T.; Sawamoto, M. *Chem. Rev.* **2001**, *101*, 3689−3745.
7. Matyjaszewski, K.; Xia, J. *Chem. Rev*. **2001**, *101*, 2921−2990.
8. Hawker, C. J.; Bosman, A. W.; Harth, E. *Chem. Rev.* **2001**, *101*, 3661−3688.
9. Moad, G.; Rizzardo, E.; Thang, S. H. *Aust. J. Chem.* **2005**, *58*, 379−410.
10. Ishihama, Y.; Sawamoto, M.; Higashimura, T. *Polym. Bull.* **1990**, *24*, 201−206.
11. Kaszas, G.; Puskas, J. E.; Chen, C. C.; Kennedy, J. P. *Polym. Bull.* **1988**, *20*, 413−419.
12. Sawamoto, M.; Okamoto, C.; Higashimura, T. *Macromolecules* **1987,** *20***,** 2693−2697.
13. Kanazawa, A.; Hirabaru, Y.; Kanaoka, S.; Aoshima, S. *J. Polym. Sci., Part A: Polym. Chem.* **2006**, *44*, 5795−5800.
14. Kato, M.; Kamigaito, M.; Sawamoto, M. Higashimura, T. *Macromolecules* **1995**, *28*, 1271−1273.

15. Wang, J.-S.; Matyjaszewski, K. *J. Am. Chem. Soc.* **1995**, *117*, 5614−5615.

16. Percec, V.; Barboiu, B. , *Macromolecules* **1995**, *28*, 7970−7972.

17. Haddleton D. M.; Jasieczek, C. B.; Hannon, M. J.; Shooter, A. J. *Macromolecules* **1997**, *30*, 2190−2193.

18. Ando, T.; Kamigaito, M.; Sawamoto, M. *Macromolecules* **1997**, *30*, 4507−4510.

19. Matyjaszewski, K.; Wei, M.; Xia, J.; McDermott, N. E. *Macromolecules* **1997**, *30*, 8161−8164.

20. Yagci, Y.; Tasdelen, M. A. *Prog. Polym. Sci*. **2006**, *31*, 1133−1170.

21. Hadjichristidis, N.; Pitsikalis, M.; Iatrou, H. *Adv. Polym. Sci*. **2005**, *189*, 1−124.

22. (a) Coca, S.; Matyjaszewski, K. *Macromolecules* **1997,** *30,* 2808−2810. (b) Coca, S.; Matyjaszewski, K. *J. Polym, Sci., Part A: Polym. Chem.* **1997,** *35,* 3595−3601.

23. Chen, X.; Ivan, B.; Kops, J.; Batsberg, W. *Macromol. Rapid. Commun*. **1998**, *19*, 585−589.

24. Lu, J.; Liang, H.; Li, A.; Cheng, Q. *Eur. Polym. J*. **2004**, *40*, 397−402.

25. (a) Toman, L.; Janata, M.; Spěváček, J.; Vlček, P.; Látalová, P.; Masař, B.; Sikora, A. *J. Polym. Sci., Part A: Polym. Chem*. **2004**, *42*, 6096–6108. (b) Toman, L.; Janata, M.; Spěváček, J.; Vlček, P.; Látalová, P.; Sikora, A.; Masař, B. *J. Polym. Sci., Part A: Polym. Chem*. **2005**, *43*, 3823–3830.

26. (a) Chapter 1 of this thesis: Satoh, K.; Aoshima, H.; Kamigaito, M. *J. Polym. Sci., Part A: Polym. Chem*. **2008**, *46*, 6358−6363. (b) Chapter 2 of this thesis: Aoshima, H.; Kamigaito, M. *Polym. Chem.*, submitted.

27. Becer, C. R.; Hoogenboom, R.; Fournier, D.; Schubert, U. S. *Macromol. Rapid. Commun*. **2007**, *28*, 1161−1166.

28. (a) Xue Z.; Linh, N. T. B.; Noh, S. K.; Lyoo, W. S. *Angew. Chem., Int. Ed.* **2008**, *47*, 6426−6429. (b) Xue, Z.; He, D.; Noh, S. K.; Lyoo, W. S. *Macromolecules* **2009**, *42*, 2949−2957.

29. Kwak, Y.; Matyjaszewski, K. *Polym. Int.* **2009**, *58*, 242−247.

30. Ando, T.; Kamigaito, M.; Sawamoto, M. *Macromolecules* **2000**, *33*, 2819−2824.

Part II

Simultaneous Living Cationic and Radical Polymerization via Interconvertible Dual Active Species

Chapter 4

Interconvertible Dual Active Species during Vinyl Polymerization: Giving Jekyll-and-Hyde Nature to Dormant Covalent Bond

Abstract

The interconvertible living cationic and radical polymerization was investigated via dual activation of dormant C–S bonds in the presence of both Lewis acid and radical initiator. The copolymerization of isobutyl vinyl ether (IBVE) and methyl acrylate (MA) proceeded in the presence of trithiocarbonate as an initiator using both $EtAlCl_2$ and V-70, in which both IBVE and MA were simultaneously and quantitatively consumed. The M_n of the obtained copolymer agreed with the calculated value assuming that one molecule initiator generates one polymer chain. The NMR, HPLC, and MALDI-TOF-MS analyses revealed that the polymerization proceeded via interconvertible growing cationic and radical species to generate the copolymer consisting of the cationically and radically polymerizable segments.

Introduction

Chemical reaction often undergoes through a certain reactive intermediate, so-called active species, which forms on a pathway from starting materials to the stable product. The active species is generally short-lived, unstable, and not isolated, but actually occurs during the organic reactions. For example, numerous carbon-carbon bond forming reactions have been conducted via carbocation, carbanion including enolate ion, and carboradical in organic synthesis. These active species have been believed fundamentally incompatible each other and difficult to coexist. In the field of polymer chemistry, chain-growth polymerization of vinyl monomers has also been implemented via appropriate active species depending on the monomer structure to generate a polymer chain by repeating C–C bond forming reactions, which is mainly categorized into radical, cationic, anionic, or metal coordination polymerization.[1]

Meanwhile, tremendous developments have been achieved in polymer synthesis over the last couple of decades by living or "controlled/living" polymerization technique, which is defined as a system apparently free from side reactions, such as termination and chain transfer and can produce well-defined polymers with controlled molecular weights, molecular weight distributions (MWDs), and end-functionality.[2] Living polymerization was first introduced for styrene polymerization via anionic intermediate over 50 years ago.[3] Now that living or controlled polymerizations have been developed through various chemical intermediates, one can access numerous kinds of polymers with tailor-made architectures, such as block and graft copolymers, via living anionic,[4,5] cationic,[6] radical,[7–11] and coordinating[12] polymerizations. Some of these processes are based on a common strategy of the reversible deactivation process, that is, the introduction of a stable covalent bond at a polymer terminus referred as a dormant species that can be activated reversibly and intermittently into the short-lived growing species. Namely, most of the polymer chain ends are capped as dormant species so that the reversible formation of active species not only gives almost the same chance for propagation to all of the chains, but also reduces the probability of side reactions to afford polymers in a living fashion.

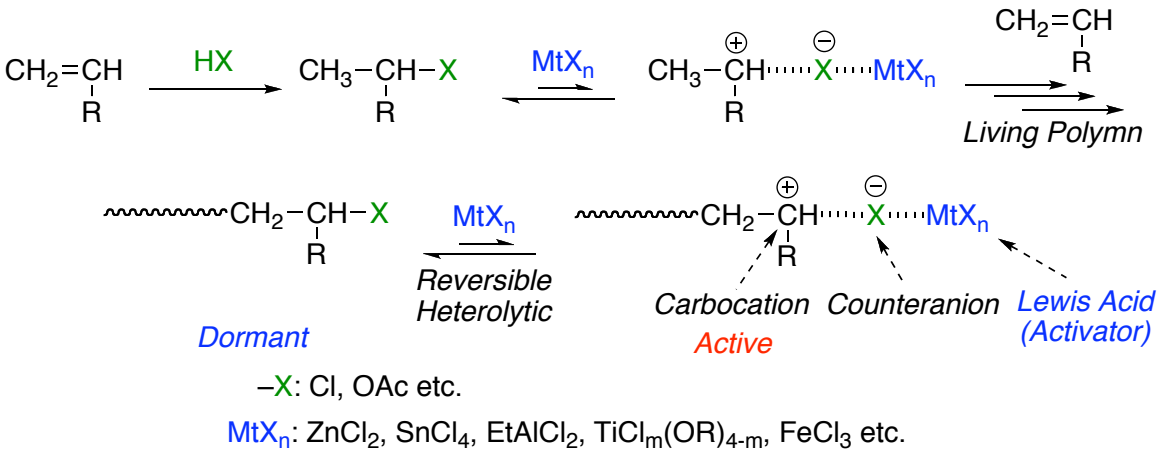

Scheme 1. Living Cationic Polymerization

Living carbocationic polymerization is often initiated with a combination of protonic acid and Lewis acid, in which the former first adds to the C=C bond in the monomer to form the dormant covalent bond and the latter was employed as the catalyst to reversibly activate the covalent bond into the growing cationic species and counteranion[6] (Scheme 1). A key to accomplish living cationic polymerization is the extension of the lifetime of the growing cations through the reversible interconversion of the active carbocation to dormant state. Thus, it is required to select a moderately nucleophilic and dissociative counteranion and a Lewis acid with moderate acidity. As the Lewis acid, metal chlorides, bromides, and alkoxides have been employed, while iodide, chloride, and acetate anions have been used as the counteranion.

There are now also several methods for living radical polymerization, in which the dormant covalent bonds are reversibly activated by appropriate stimulus to generate the growing radical species. Among various methods, RAFT polymerization, is one of the most versatile methods, which is mainly achieved using C–S bond as the dormant species coupled with radical species originating from radical initiator[11] (Scheme 2). The RAFT polymerization is initiated by the formation of a small amount of the oligomer radical chain generated from a radical initiator, such as AIBN, and the monomers. The radical species adds to the RAFT agent [R–SC(S)Z] to form the intermediate radical and then generates the fragment radical species (R·), which results in

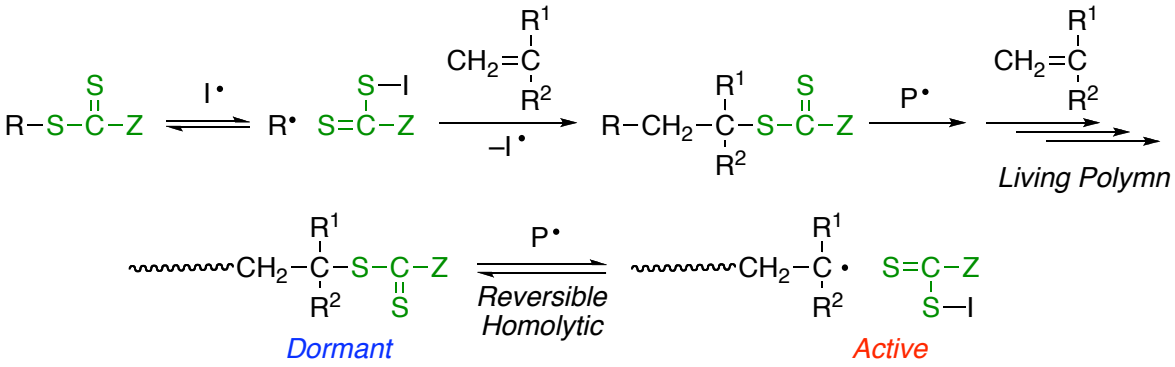

Scheme 2. RAFT Radical Polymerization

a polymer chain. The molecular weight of the resulting polymers can be basically determined by the feed ratio of the monomer to the RAFT agent while a slight amount the polymer chain is generated from the radical initiator. The design of the RAFT agents is important depending on the monomer structures, in which the dithiocarboxylates, such as dithiobenzoate (Z = Ph), dithiophenylacetate (Z = CH_2Ph), and trithiocarbonate (Z = SR) are effective for the controlled polymerizations of styrenes and (meth)acrylates, while xanthate (Z = OR) and dithiocarbamate (Z = NR_2) are suitable for vinyl acetate.

The difference between these two mechanisms is the activation of covalent bond through two electron heterolytic or one electron homolytic cleavage. However, a few known examples of tandem reaction with multiple active species has been reported to undergo just one-time and irreversible mechanistic transformation of the two active species to obtain block copolymers.[13–16]

Contrary to the long-time belief that chemical reactions including polymerization can take place via one chemical intermediate species inherently depending on the substrate or reactant structure, the author herein reports an unprecedented polymerization reaction that proceeds via interconvertible dual active species by giving Jekyll-and-Hyde nature to the dormant covalent bond to form one polymer chain; i.e., a stable C–S bond can be dissociated reversibly and non-specifically into either carbocationic or radical species (Scheme 3). This conceptually-new

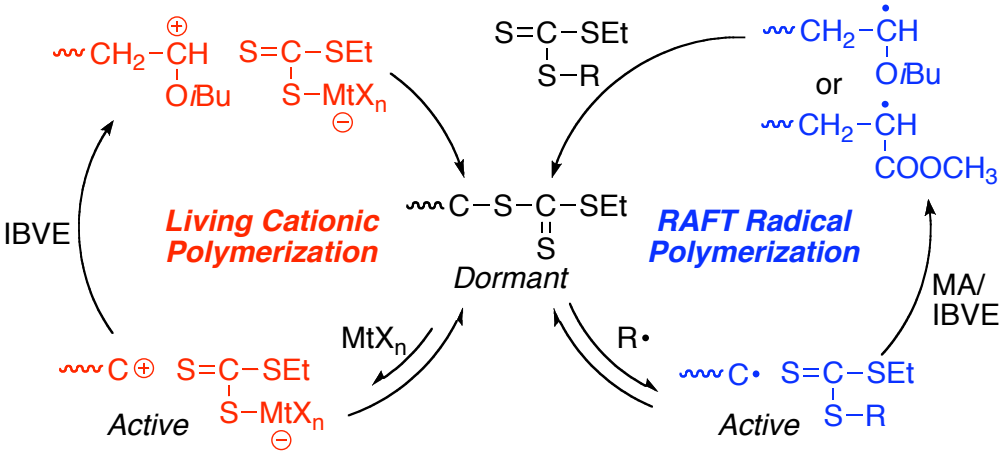

Scheme 3. Interconvertible Dual Active Species during Vinyl Polymerization

system will result in a polymer chain consisting of partitioned segments derived from cationically and radically polymerizable monomers, such as vinyl ether that give its homopolymer only by cationic polymerization and alkyl acrylate being polymerized only by radical or anionic polymerization.

Experimental Section

Materials

Isobutyl vinylether (IBVE) (TCI, 95%), methyl acrylate (MA, TCI, >99%), and were distilled over calcium hydride under reduced pressure before use. $EtAlCl_2$ (KANTO, 1.0 M solution in *n*-hexane) and $ZnCl_2$ (Aldrich, 1.0 M in Et_2O) was used as received. ethyl acetate (KANTO; >99%) was distilled over calcium hydride before use. 2,2-Azobis (4-methoxy-2,4-dimethylvaleronitrile) (V-70) (Wako, 95%) was purified by washing with acetone at –15 °C and was evaporated to dryness under reduced pressure. *S*-1-isobutoxyethyl *S'*-2-ethyl trithiocarbonate (BEETC) was synthesized according to the literature.[17] Toluene (Kanto, >99.5%; H_2O <10 ppm) was dried and deoxygenized by passage through columns of Glass Contour Solvent Systems before use.

Polymerization

The interconvertible living cationic and radical polymerization of IBVE and MA was carried out by the syringe technique under dry nitrogen in baked glass tubes equipped with a three-way stopcock. A typical example for the polymerization procedure is given below. The reaction was initiated by sequential addition of prechilled solutions of V-70 (0.026 mmol; 0.52 mL of 50 mM in toluene) and solution of $EtAlCl_2$ (0.26 mL of 25 mM in toluene) via dry syringes into a monomer solution (1.82 mL) containing IBVE (5.31 mmol), MA (5.31 mmol), BEETC (0.11 mmol), and ethyl acetate (2.66 mmol) in toluene at 20 °C. The total volume of the reaction mixture was 2.6 mL. After 140 h, the polymerization was terminated with methanol (1.0 mL) containing a small amount of triethylamine. Monomer conversion was determined from the concentration of residual monomer measured by ^{1}H NMR with ethyl acetate as an internal standard (IBVE; >99%, MA; 94%). The quenched reaction mixture was washed with dilute hydrochloric acid, and distilled water to remove initiator residues, evaporated to dryness under reduced pressure, and vacuum-dried to give the product polymers (M_n = 8900, M_w/M_n = 1.35).

Measurements

Monomer conversion was determined from the concentration of residual monomer measured by ^{1}H NMR spectroscopy with ethyl acetate as an internal standard. ^{1}H and ^{13}C NMR spectra were recorded on a JEOL ECS-400 spectrometer, operating at 400 MHz. MALDI-TOF-MS spectra were measured on a Shimadzu AXIMA-CFR Plus mass spectrometer (linear mode) with dithranol as the ionizing matrix and sodium trifluoroacetate as the ion source. HPLC analysis carried out at ambient temperature on silica column [TSKgel Silica-150; 4.6 mm i.d. × 25 cm; flow rate 0.5 mL/min] connected to a JASCO PU-2080 precision pump, a JASCO LG-2080-02 ternary gradient unit and an evaporative light scattering detector (PL-ELS 1000). The eluent composition for first 10 min contained 80% (v/v) hexane and 20% (v/v) THF, and then was gradually changed to a 20/80% (v/v) mixture of hexane and THF for next 10 min. The

number-average molecular weight (M_n) and the molecular weight distribution (M_w/M_n) of the product polymers were determined by size-exclusion chromatography (SEC) in THF at 40 °C on two polystyrene gel columns [Shodex KF-805 L (pore size: 20–1000 Å; 8.0 mm i.d. × 30 cm) × 2; flow rate 1.0 mL/min] connected to a JASCO PU-2080 precision pump and a JASCO RI-2031 detector. The columns were calibrated against 10 standard polystyrene samples (Varian; M_p = 575–2783000, M_w/M_n = 1.02–1.23).

Results and Discussion

1. Possibility of Interconvertible Cationic and Radical Living Polymerization

Recently, the author's group has found the possible living cationic polymerization via activation of C-S bond, and followed by one-time mechanistic transformation from radical to cationic species by the combination with RAFT radical polymerization for block copolymerization synthesis.[17] In this study, the author first copolymerized a mixture of isobutyl vinyl ether (IBVE) and methyl acrylate (MA) with a Lewis acid ($EtAlCl_2$) or a low-temperature radical initiator [2,2'-azobis(4-methocy-2,4-dimethylvaleronitrile): V-70] as the catalyst in conjunction with a trithiocarbonate (BEETC) as the initiator/RAFT agent for tuning copolymerization rate of cationic or radical polymerization, respectively (Figure 1).

When the IBVE/MA mixture was polymerized in the presence of BEETC using $EtAlCl_2$ alone in toluene at 20 °C, only IBVE was consumed quantitatively without any significant consumption of methyl acrylate indicating cationic polymerization (Figure 1A). Meanwhile, RAFT radical copolymerization proceeded using only V-70 with almost quantitative conversion of MA along with a lower consumption of IBVE (~30 %) (Figure 1B). It was of importance that the reaction rates for these polymerizations were not so different to promote the two mechanisms simultaneously. By SEC analysis of the obtained polymers, the cationic polymerization or RAFT radical copolymerization by using one of the catalysts proceeded in living fashions to give well-controlled polymers along with relatively narrow MWDs, in which the number-average

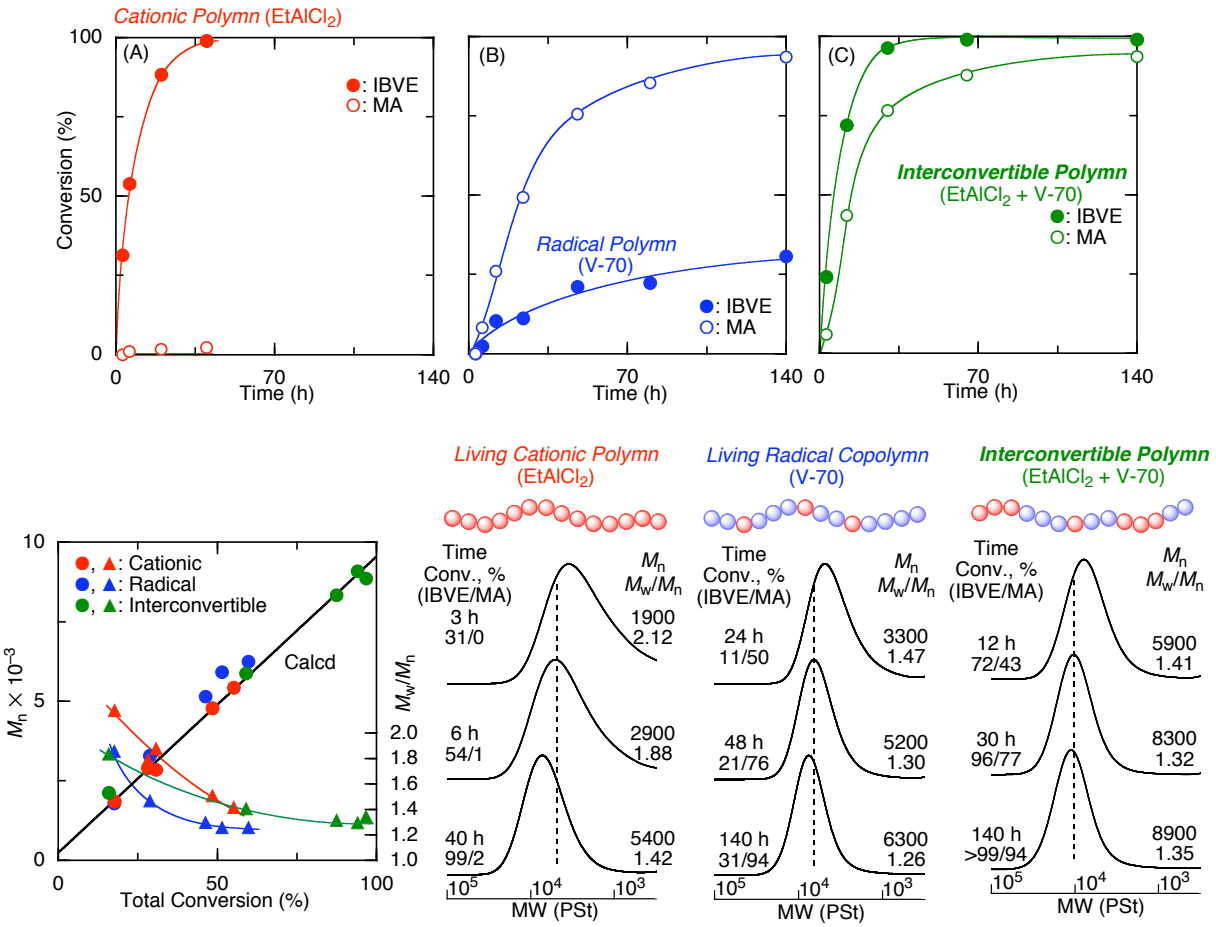

Figure 1. Copolymerization of IBVE and MA; $[IBVE]_0 = [MA]_0 = 2.0$ M, $[BEETC]_0 = 40$ mM, $[EtAlCl_2]_0 = 0$ or 2.5 mM, $[V\text{-}70]_0 = 0$ or 10 mM, $[EtOAc]_0 = 1.0$ M in toluene at 20 °C.

molecular weights (M_n) in both cases increased in direct proportion to the monomer conversions agreeing with the calculated values on the assumption that one trithiocarbonate molecules generates one polymer chain. Thus, it was confirmed that the C–S bond in the trithiocarbonate can not only be reversibly activated both cationically and radically into the two different active species, but also induce the two polymerization at almost same rate under an appropriate condition.

Now, the two catalysts were put in the reaction mixture at same time. In the presence of the two catalysts, both of the monomers were consumed simultaneously and quantitatively as shown in Figure 1C, in which non-radically homopolymerizable IBVE was consumed slightly faster than MA. Furthermore, the consumption rate of IBVE was almost the same as that only

with the Lewis acid, and that of MA was nearly the same as that in the radical copolymerization. Interestingly, the polymers obtained in the presence of both the two catalyst also exhibited unimodal and narrow MWDs as well, of which the M_ns also increased in direct proportion to the conversions and agreed well with the calculated values. Thus, the copolymerization with $EtAlCl_2$/V-70 also proceeded in a living fashion, suggesting the possibility of interconvertible and/or concurrent living cationic and radical polymerization via dual active species through the dormant C–S bonds originated from BEETC.

2. Analysis of Polymers obtained in Interconvertible Polymerization

To make this clear, the sequence structures of the copolymers were analyzed in detail by NMR spectroscopy (Figure 2 and 3). All these polymers gave characteristic signals of the main-chain units in the ^{1}H NMR spectra; i.e., aliphatic protons (*a*, *d*, and *e*), methine (*b*), and methylene protons (*c*) adjacent to oxygen for IBVE (I) units and aliphatic proton (*f*), a-proton to the carbonyl (*g*), and pendent methoxy proton (*h*) for MA (M) units, respectively. In particular, the poly(IBVE) (Figure 2A) exhibits signals assigned to the –CH–O group of the triad homo-sequence (I-I-I) at around 3.5 ppm (*b*), whereas the poly(IBVE-*co*-MA) obtained by radical copolymerization (Figure 2B) showed that of the alternating (M-I-M) sequence at around 3.1 ppm (*b'*) overlapped by methylene protons (*c'*) due to non-radically homo-polymerizability of IBVE. For the copolymer obtained with the both $EtAlCl_2$ and V-70 (Figure 2C), the ^{1}H NMR spectrum showed characteristic signals of both triad homo- (I-I-I) and alternating sequences (M-I-M) along with the peaks of MA units, in which the IBVE/MA composition, obtained from the peak intensity ratio (*e*/*g*), was in good agreement with the calculated values from the monomer feed ratios and conversion of each monomer. This suggests that the copolymer possess both sequences produced by cationic and radical polymerizations and not by alternating radical copolymerization.

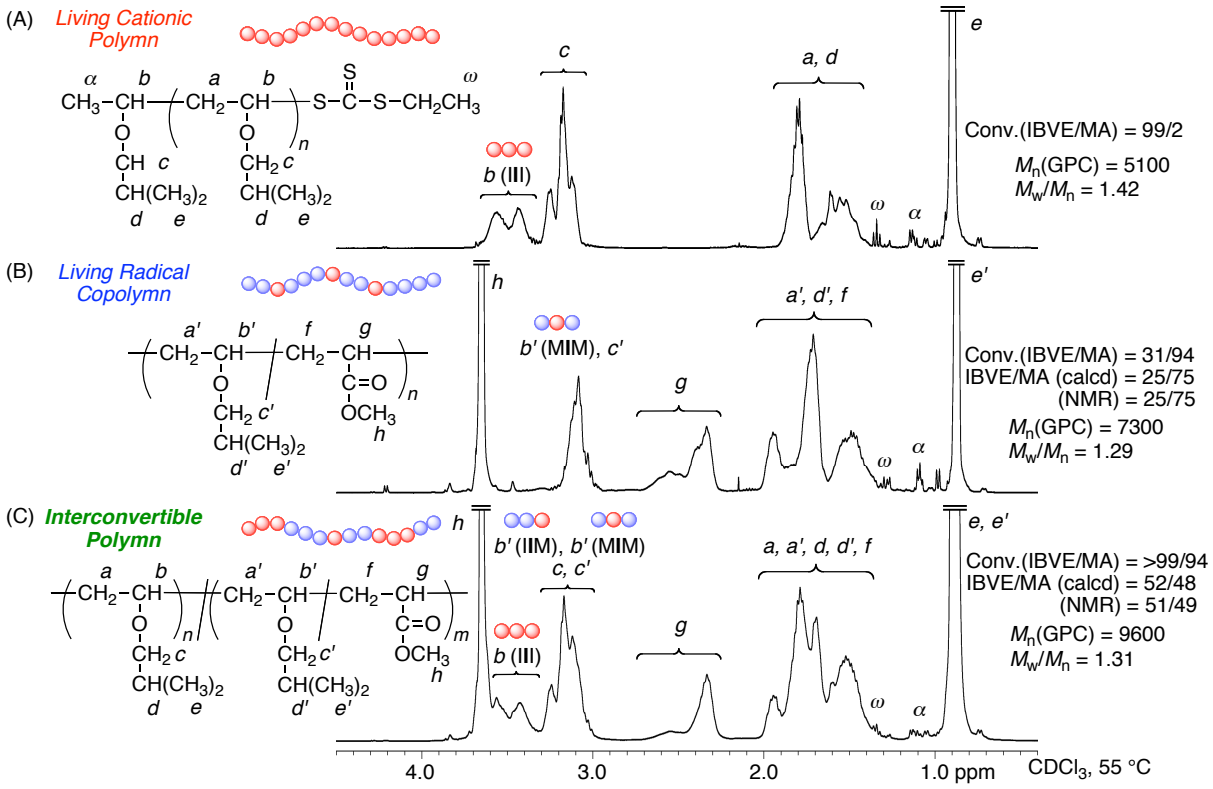

Figure 2. ^{1}H NMR spectra of the obtained copolymers obtained in the same experiments as for Figure 1.

In addition, ^{13}C NMR analyses gave more useful information about the sequences of the copolymers (Figure 3). In the spectrum obtained with the $EtAlCl_2$/V-70 system (Figure 3C), the splitting pattern of the carbonyl carbon in triad sequence of MA at around 175 ppm was predominant not by the alternating sequence (I-M-I) but by the homosequences of methyl acrylate (M-M-M), which was slightly different from that obtained in the normal RAFT copolymerization with V-70 alone (Figure 3B). This is totally different from the conventional Lewis acid-mediated alternating radical copolymerization to afford 1:1 alternating copolymers, in which much higher loading of the Lewis acid was required. Furthermore, the signals of methine (*b*) and methylene carbons (*c*) in IBVE units at around 75 ppm gave the information about the IBVE sequences, in which the copolymers obtained by $EtAlCl_2$/V-70 (Figure 3C) showed small signal attributed to I-I-M or its opposite, M-I-I, sequences, in addition to the peaks of homo I-I-I sequences from

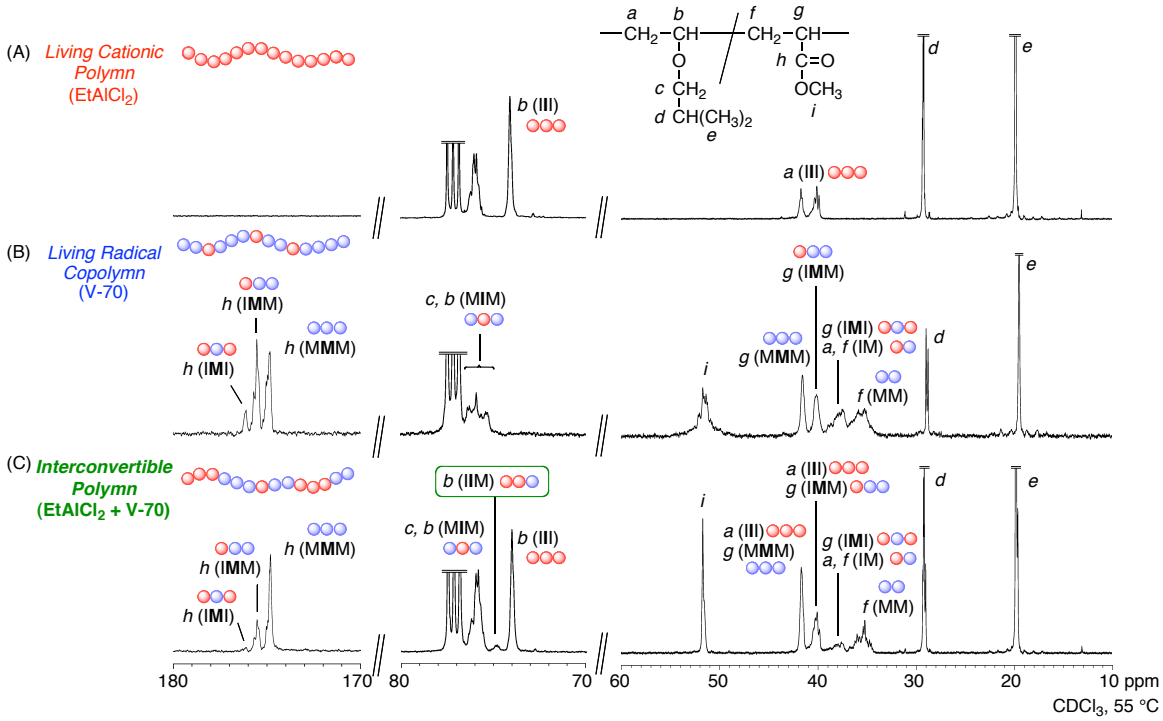

Figure 3. ^{13}C NMR spectra of the copolymers obtained in the same experiments as for Figure 1.

cationic process and alternating M-I-M derived from radical process as observed in Figures 3A and 3C, respectively. The occurrence of I-I-M (M-I-I) clearly indicates that the growing species was transformed from cation to radical, and vice versa, during the chain growth of the copolymer to form a segmented multiblock copolymer consisting of cationically- and radically-polymerized blocks. Figure 4A shows the contents of each sequence thus analyses by ^{13}C NMR as the function of monomer conversions. From the sequences, the contents of cationic and radical species at each conversion as well as the average numbers of the, i.e., interconversion per chain, could be calculated (Figure 4B). The contents of cationic and radical species were around 75% and 25% in the initial stage of the copolymerization, and they became closer to 50:50 as the polymerization proceeded. The numbers of interconversion increased as the polymerization proceeded and finally reached around 5 when the polymerization degree (DP) became about one hundred (DP = 96.9), in which the average monomer units in one cycle of the interconversion were also calculated to be 18.8 (cationic) and 22.8 (radical), respectively.

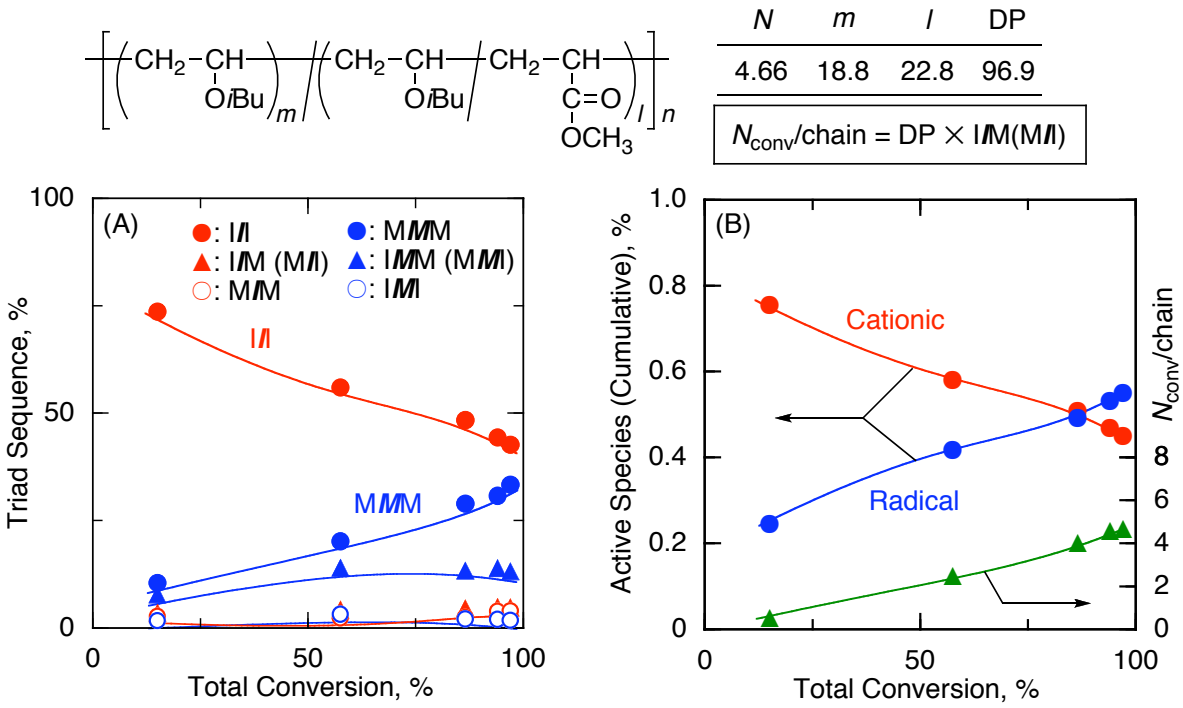

Figure 4. Dependence of triad sequence, cumulative active species composition and number of interconversion on the total conversion of monomers in simultaneous living radical/cationic polymerization

The polymerization probably proceeds via interconvertible carbocationic and carbon radical species generated from the trithiocarbonate, where the carbon–sulfur bond in BEETC was activated by $EtAlCl_2$ similarly to the living cationic polymerizations or by the reversible chain transfer of radical species similarly to the RAFT radical polymerization (Scheme 4). When the trithiocarbonate is activated by Lewis acid, it generates cationic propagating species to induce living cationic polymerization, and sooner or later, it is capped with trithiocarbonate to regenerate RAFT terminal. If the RAFT terminal is activated by radical species, it then generates growing radical species from the same chain to induce radical copolymerization of MA and IBVE, and then it is capped with trithiocarbonate moiety to regenerate RAFT terminal. By repeating the interconversion during the chain propagation, the single polymer chain with a segmented multiblock structure is produced by c.a. 5 interconversions during 100 monomer insertions.

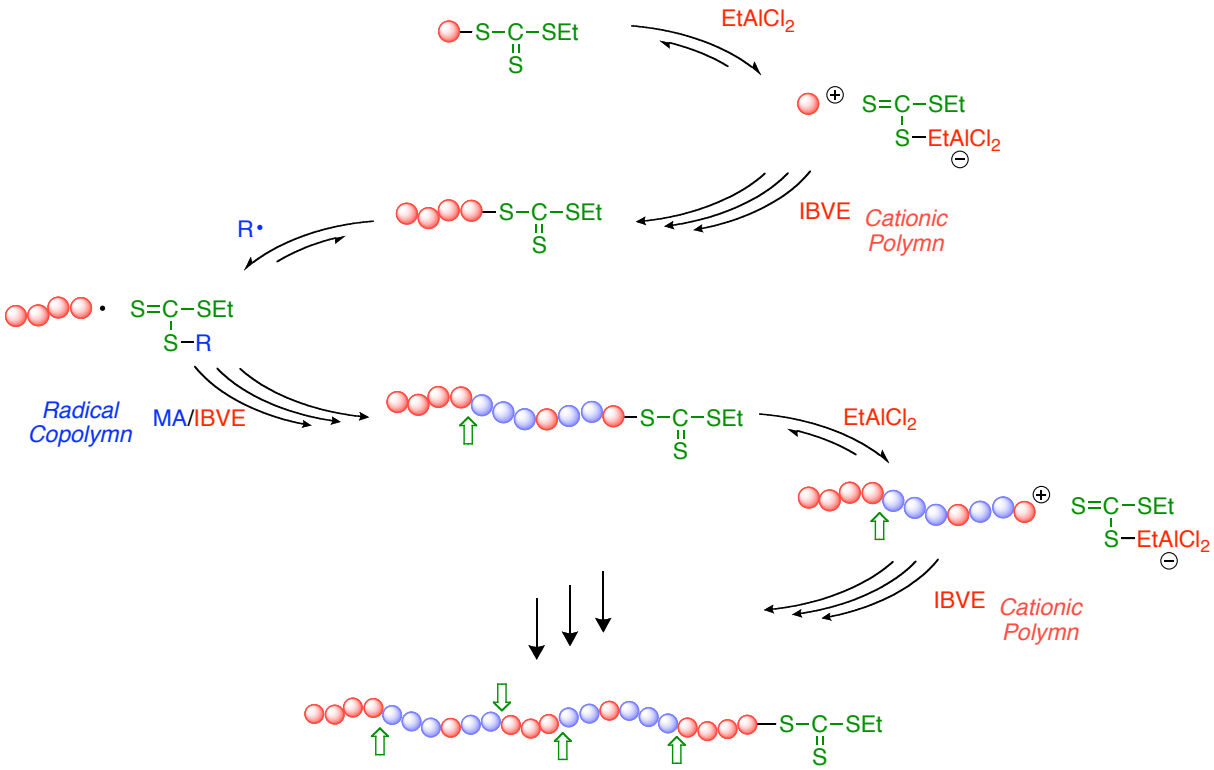

Scheme 2. Mechanism of Interconvertible Living Cationic and Radical Polymerization via Dual Active Species

The key to the interconvertible polymerization lies on the occurrence of terminal IBVE units capped with trithiocarbonate, which can be activated into both cationic and radical species depending on the catalysts.

Matrix-assisted laser desorption-ionization time-of-flight mass spectrometry (MALDI-TOF-MS) also supported these results. Figure 5 shows the MALDI-TOF-MS spectra of poly(IBVE) obtained with $EtAlCl_2$ and poly(IBVE-*co*-MA) with V-70 alone or $EtAlCl_2$/V-70 (Figure 5A–C, respectively). The spectra of the poly(IBVE) consists of the sharp peaks separated by a 100 Da corresponding to the molecular weights of IBVE monomer (Figure 5A), whereas the spectrum of the random copolymer by radical RAFT copolymerization exhibited complicated peaks separated by about 14 Da interval corresponding to the difference in molecular weights between IBVE and MA units (Figure 5B). On closer inspection, the latter spectrum

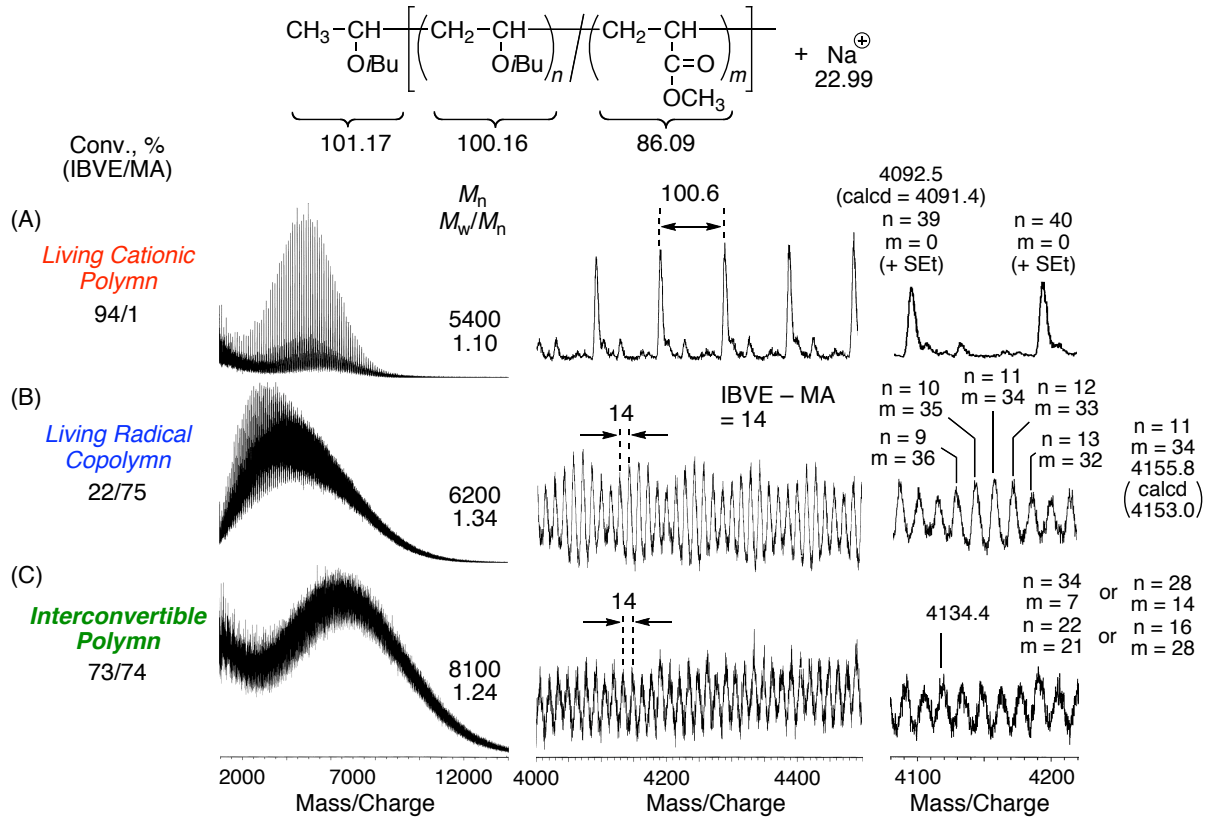

Figure 5. MALDI–TOF–MS spectra of the copolymers: $[IBVE]_0 = [MA]_0 = 2.0$ M, $[BEETC]_0 = 40$ mM, $[ZnCl_2]_0 = 2.5$ mM, $[V\text{-}70]_0 = 10$ mM, $[EtOAc]_0 = 1.0$ M in toluene at 20 °C.

showed statistical distributions according to the probability of IBVE/MA cross-propagation to afford a series of clustered peaks, each of which are for the copolymers consisting of the same total DP and agreed well with the calculated values for poly(IBVE-*co*-MA) with sodium ion. On the other hand, the spectrum obtained by interconvertible polymerization with $EtAlCl_2$/V-70 was also free from the peaks of the corresponding homopolymers and statistical peaks of copolymer, indicating totally random sequences (Figure 5C).

These polymers were also evaluated by HPLC analysis, in which a solvent mixture of THF and *n*-hexane with gradient compositions was employed as the eluent (Figure 6). The poly(IBVE) obtained by cationic polymerization with only $EtAlCl_2$ (Figure 6A) exhibited a sharp peak, which eluted faster than poly(IBVE-*co*-MA) by radical polymerization with only V-70 due to the higher polarity of MA units (Figure 6B). The copolymer obtained in the interconvertible

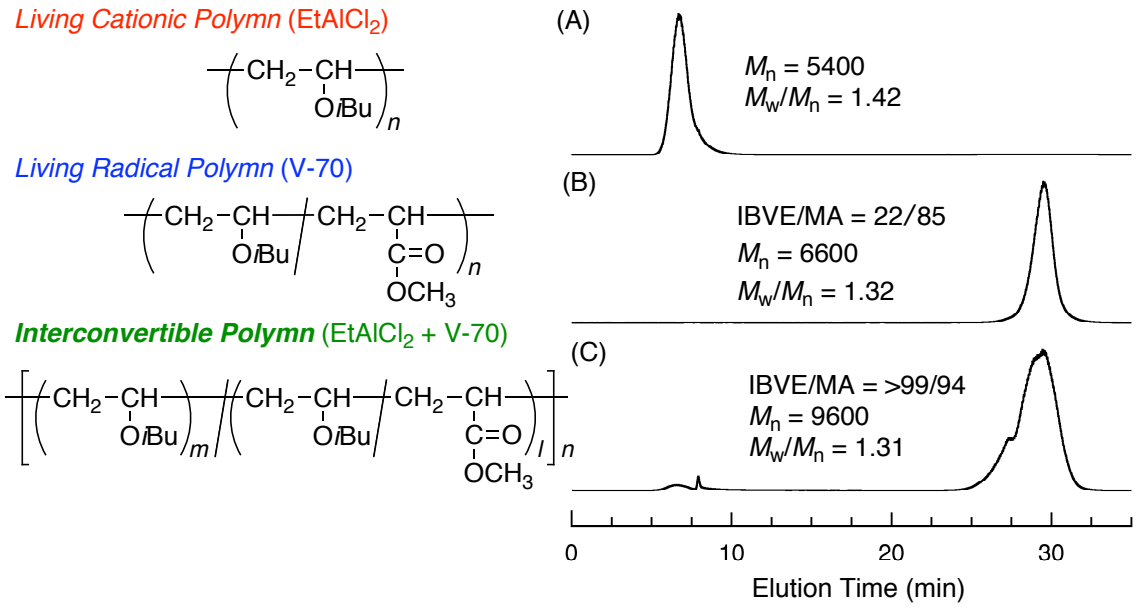

Figure 6. Chromatograms of the copolymers obtained in the same experiments as for Figure 1

polymerization showed broader peaks than that in radical copolymerization with almost no homopolymers of IBVE (Figure 6C). This also supports the occurrence of interconversion during the formation of the copolymer chain.

Conclusion

In conclusion, using reversible activation of RAFT terminal by Lewis acid and radical initiator, the author has succeeded in the interconvertible mechanistic transformation between radical and cationic polymerizations. This might be a new concept for vinyl monomer polymerizations beyond the conventional categories by propagating species.

References

1. Odian, G. *Principles of Polymerization, Fourth Edition*; John Wiley and Sons, Inc., Hoboken, New Jersey, 2004.
2. *Controlled and Living Polymerizations: From Mechanisms to Materials*; Müller A. H. E.; Matyjaszewski, K., Eds.; Wiley-VCH: Weilheim, Germany, 2008.
3. (a) Szwarc, M. *Nature* **1956**, *178*, 1168–1169. (b) Szwarc, M.; Levy, M.; Milkovich, R. *J. Am. Chem. Soc*. **1956**, *78*, 2656–2657.
4. (a) Hatada, K.; Kitayama, T. *Polym. Int*. **2000**, *49*, 11–47. (b) Baskaran, D. *Prog*. *Polym. Sci.* **2003**, *28*, 521–581. (c) Baskaran, D.; Müller, A. H. E. *Prog. Polym. Sci*. **2007**, *32*, 173–219.
5. Webster, O. W. *Adv. Polym. Sci.* **2004**, *167*, 1–34.
6. (a) Sawamoto, M. *Prog. Polym. Sci*. **1991**, *16*, 111–172. (b) Puskas. J.E.; Kaszas, G. *Prog. Polym. Sci*. **2000**, *25*, 403–452. (c) Goethals, E. J.; Prez, F. D. *Prog. Polym. Sci*. **2007**, *32*, 220–246. (d) Aoshima, S.; Kanaoka, S. *Chem. Rev*. **2009**, 129, 5245–5287.
7. (a) Hawker, C. J.; Bosman, A. W.; Harth, E. *Chem. Rev*. **2001**, *101*, 3661–3688. (b) Studer, A.; Schulte, T. *Chem. Rec*. **2005**, *5*, 27–35. (c) Sciannamea, V.; Jérôme, R.; Detrembleur, C. *Chem. Rev*. **2008**, *108*, 1104–1126. (d) Grubbs, R. B. *Polym. Rev*. **2011**, *51*, 104–137.
8. (a) Kamigaito, M.; Ando, T.; Sawamoto, M. *Chem. Rev*. **2001**, *101*, 3689–3745. (b) Kamigaito, M.; Ando, T.; Sawamoto, M. *Chem. Rec*. **2004**, *4*, 159–175. (c) Ouchi, M.; Terashima, T.; Sawamoto, M. *Acc. Chem. Res*. **2008**, *41*, 1120–1132. (d) Ouchi, M.; Terashima, T.; Sawamoto, M. *Chem. Rec*. **2009**, *109*, 4963–5050. (e) Kamigaito, M. *Polym. J.* **2010**, 42, 105–120.
9. (a) Matyjaszewski, K.; Xia, J. *Chem. Rev*. **2001**, *101*, 2921–2990. (b) Tsarevsky, N. V.; Matyjaszewski, K. *Chem. Rev*. **2007**, *107*, 2270–2299. (c) Braunecker, W. A.; Matyjaszewski, K. *Prog. Polym. Sci*. **2007**, *32*, 93–146. (d) di Lena, F.; Matyjaszewski, K. *Prog. Polym. Sci*. **2010**, *35*, 959–1021. (e) Matyjaszewski, K. *Macromolecules* **2012**, *45*, 4015–4039.

10. Rosen, B. M.; Percec, V. *Chem. Rev*. **2009**, *109*, 5069–5119.

11. (a) Moad, G.; Rizzardo, E.; Thang, S. H. *Aust. J. Chem.* **2005**, *58*, 379–410. (b) Moad, G.; Rizzardo, E.; Thang, S. H. *Polymer* **2008**, *49*, 1079–1131. (c) Moad, G.; Rizzardo, E.; Thang, S. H. *Acc. Chem. Res*. **2008**, *41*, 1133–1142. (d) Moad, G.; Rizzardo, E.; Thang, S. H. *Aust. J. Chem.* **2009**, *62*, 1402–1472. (e) Keddie, D. J.; Moad, G.; Rizzardo, E.; Thang, S. H. *Macromolcules* **2012**, *45*, 5321–5342.

12. Domski, G. J.; Rose, J. M.; Coates, G. W.; Bolig, A. D.; Brookhart, M. *Prog. Polym. Sci.* **2007**, *32*, 30–92.

13. (a) Yagci, Y.; Tasdelen, M. A. *Prog. Polym. Sci.* **2006**, *31*, 1133–1170. (b) Hadjichristidis, N.; Pitisikalis, M.; Iatrou, H. *Adv. Polym. Sci*. **2005**, *189*, 1–124.

14. (a) Yagci, Y.; Reetz, I. *Prog. Polym. Sci*. **1998**, *23*, 1485–1538. (b) Guo, H.-Q.; Kajiwara, A.; Morishima, Y; Kamachi, M. *Macromolecules* **1996**, *29*, 2354–2358. (c) Nomura, R.; Narita, M.; Endo, T. *Macromolecules* **1994**, *27*, 4853–4854.

15. (a) Coca, S.; Matyjaszewski, K. *Macromolecules* **1997**, *30,* 2808–2810. (b) Chen, X.; Ivan, B.; Kops, J.; Batsberg, W. *Macromol. Rapid. Commun*. **1998**, *19*, 585–589. (c) Lu, J.; Liang, H.; Li, A.; Cheng, Q. *Eur. Polym. J.* **2004**, *40*, 397–402. (d) Toman, L.; Janata, M.; Spěváček, J.; Vlček, P.; Látalová, P.; Masař, B.; Sikora, A. *J. Polym. Sci., Part A: Polym. Chem*. **2004**, *42*, 6096–6108. (e) Kumagai, S.; Nagai, K.; Satoh, K.; Kamigaito, M. *Macromolecules* **2010**, *43*, 7523–7531. (f) Chapter 3 of this thesis: Aoshima, H.; Satoh, K.; Kamigaito, M. *Macromol. Symp.* **2013**, *Macromol. Symp*. **2013**, *323*, 64–74.

16. (a) Masař, B.; Vlček, P.; Kříž, J. *J. Appl. Polym. Sci.* **2001**, *81*, 3514–3522. (b) Liu, F.; Liu, B.; Luo, B.; Ying, SK. *Chem. Res. Chin. U*. **2000**, *16*, 72–77.

17. Kumagai, S.; Nagai, K.; Satoh, K.; Kamigaito, M. *Macromolecules* **2010**, *43*, 7523–7531.

Chapter 5

Interconvertible Concurrent Living Cationic and Radical Polymerization of Various Monomers for Synthesis of Novel Copolymers

Abstract

The interconvertible cationic and radical polymerization of various monomers was investigated with a series of RAFT agent (**1**–**4**) in the presence of Lewis acids such as $EtAlCl_2$, $ZnCl_2$ and $FeCl_3$ and low-temperature radical initiator. The copolymerization of IBVE and MA proceeded simultaneously with $EtAlCl_2$ or $ZnCl_2$ in the presence of RAFT agent (**1** and **2**) in toluene at 20 °C to result in the copolymer consisting of both monomer segments with well-controlled molecular weight. In addition, the interconvertible polymerizations were achieved even at different monomer concentration or polymerization temperature. The ^{1}H and ^{13}C NMR analyses revealed that the multiblock copolymers were produced, of which the number of interconversion between cationic and radical species depended on these polymerization condition. The scope of radical polymerizable monomer for the interconvertible polymerization was expanded to other acrylates and methacrylates. Especially, although MMA has low radical copolymerizability with IBVE, interconvertible polymerization smoothly proceeded by the increasing the IBVE initial feed ratio.

Introduction

Most chemical reaction proceeds via intermediates, the so-called active species, which are generally instable, short-lived, and hardly isolated. In chain-growth polymerization, they are generated from initiator and add to the vinyl monomers consecutively to produce the polymer chains.[1] This polymerization is classified into cation, radical, anionic polymerization by the active species and can be transformed each another in theory by one- or two-electron oxidation or reduction of active species. In fact, the direct transformation during the polymerization, such as radical to cationic[2] and cationic to anionic[3] species, has been achieved by electron transfer to yield block copolymer. However, these transformations are irreversible, and the interconvertible one has seemed impossible because these active species considered incompatible and difficult to coexist.

Meanwhile, living polymerization is one of the most efficient methods for the control of the molecular weight as well as the polymer structure.[4] During past few decades, remarkable progress has been made in the living cationic and radical polymerization through the reversible equilibrium between the active species and stable covalent bond (dormant species).[5,11–15] This reversibility reduces the undesirable side reactions such as β-proton elimination and bimolecular termination to afford the precisely controlled polymer.

In the living cationic polymerization, the carbon-halogen bond or carbon-ester group are employed as dormant species and are reversibly converted into growing carbocation by Lewis Acid, including Zn(II),[6] Al(III),[7] Sn(IV),[8] Ti(IV),[9] and Fe(III)[10] etc. A key to accomplish living polymerization is the stabilization of the unstable carbocation via the nucleophilic interaction of the added base or counteranion originating from the initiator and Lewis acid. Thus, the judicious choice of the dormant species derived from initiator, Lewis acid, and additives are important for the controlled polymerization of various monomers.

Analogous to the cationic system, the one-electron reversible activation of dormant species led to develop numerous initiating system for living radical polymerizations, i.e.,

nitroxide-mediated radical polymerization (NMP),[11] transition metal-catalyzed living radical polymerization or atom transfer living radical polymerization (ATRP),[12–14] and reversible addition-fragmentation chain transfer (RAFT) polymerization.[15] Among them, RAFT system is one of the most useful polymerization from the aspect of a wide variety of controllable monomers and easily procedure. In this polymerization, the dormant carbon-dithioester group [R–SC(S)Z] reversibly formed growing radical species via the one-electron activation with another polymer radical or radical species derived from radical initiator. The design of RAFT agents depending on the monomer structure is most important for molecular weight control.

Along with the development of the living polymerization described above, the direct mechanistic transformation of active species have been achieved through dormant species to afford the well-defined block copolymer consisting of different monomer types.[16] As for the transformation between cationic and radical polymerization, the carbon-halogen employed as dormant species, which can generate different propagating species depending on the catalyst.[17,18] Recently, the author's group have found the living cationic polymerization of isobutyl vinyl ether (IBVE) via the two-electron activation of C–S bond in the trithiocarbonate by Lewis acid as well as the in-situ transformation from RAFT radical polymerization of methyl acrylate (MA) into living cationic polymerization of IBVE.[19]

Quite recently, the author evolved the in-situ mechanistic transformation into the simultaneous living cationic and radial polymerization of IBVE and MA through dormant C–S bond in chapter 4. This polymerization proceeded via interconvertible cationic and radical species, which can be reversibly and non-selectively generated by the activation of dormant C–S bond with Lewis acid and radical initiator, to result in a polymer chain consisting of cationic and radical polymerizable monomer segments.

In this study, the author investigated the interconvertible cationic and radical polymerization of IBVE and MA using several Lewis acid and RAFT agent under various conditions. The effect of the polymerization condition on the interconversion of active species

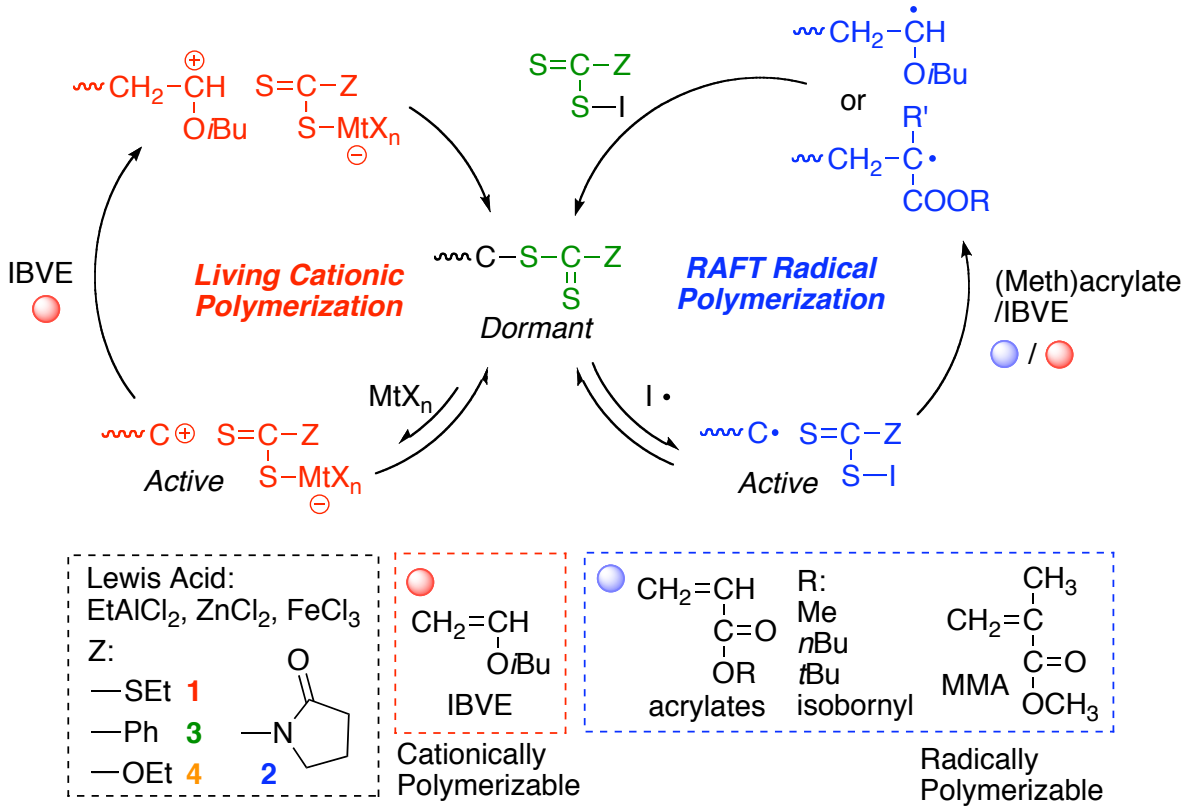

Scheme 1. Interconvertible Cationic and Radical Polymerization of IBVE and (Meth)acrylates under Various Conditions

and polymer structures were analyzed in detail by NMR analyses. The author also expanded a scope of radical polymerizable monomer such as other acrylates and methacrylates for the interconvertible polymerization (Scheme 1).

Experimental

Materials

Methyl acrylate (MA; TCI, >99%), *n*-butyl acrylate (*n*BA; TCI, >99%), *t*-butyl acrylate (*t*BA; TCI, >98%), isoboronyl acrylate (*i*BoA; TCI, >93%) and methyl methacrylate (MMA; TCI, >99.8%) were distilled over calcium hydride under reduced pressure before use. Isobutyl vinylether (IBVE; TCI, >99%), and ethyl acetate (KANTO; >99%) was distilled over calcium hydride before use. $EtAlCl_2$ (KANTO, 1.0 M solution in *n*-hexane), $ZnCl_2$ (Aldrich, 1.0 M

solution in diethyl ether), and $FeCl_3$ (Aldrich, >99.99%) were used as received. 2,2-Azobis(4-methoxy-2,4-dimethylvaleronitrile) (V-70) (Wako, 95%) was purified by washing with acetone at –15 °C and was evaporated to dryness under reduced pressure. *S*-1-isobutoxyethyl *S'*-2-ethyl trithiocarbonate (**1**) was synthesized according to the literature.[19] Toluene (Kanto, >99.5%; H_2O <10 ppm) and diethyl ether (Et_2O; Kanto, >99.5%; H_2O <50 ppm) was dried and deoxygenized by passage through columns of Glass Contour Solvent Systems before use.

Synthesis of *S*-1-isobutoxyethyl 2-Pyrrolidinone-1-carboditioate (2)

2 was synthesized by the reaction between sodium 2-pyrrolidone-1-carbodithioate and the HCl adduct of IBVE (IBVE–HCl). According to the reported method,[8] the IBVE-HCl was prepared by adding 1.0 M Et_2O solution of hydrogen chloride (66 mL, 66 mmol) dropwise into Et_2O solution of IBVE (7.83 mL, 60 mmol) at 0 °C. 2-Pyrrolidone-1-carodithioic acid was prepared from 2-pyrrolidone (11.4 mL, 0.15 mol), potassium hydroxide (13.2 g, 0.24 mol), and carbon disulfide (10.8 mL, 0.18 mol) in dry DMSO. Into a DMF solution of the acid (47 mmol) was added potassium carbonate (6.91g, 50 mol) under a dry nitrogen atmosphere and a small amount of water was removed by azeotropic drying with toluene. The IBVE–HCl solution (60 mmol) was then added dropwise at –78 °C over a period of 30 min. After stirring for 1 h at 0 °C and then over 2 h at ambient temperature, the reaction was quenched by diluting with Et_2O and the solution was washed with 5 wt% $NaHCO_3$ aqueous solution, brine and water. The solvent was removed by evaporation to give the crude product (7.46 g), and the product was purified by column chromatography on silica gel with *n*-hexane as an eluent. The dithiocarbamate **2** was obtained as yellow liquids (3.30g, 12.6 mmol, 26.9% yield). ^{1}H NMR ($CDCl_3$, r.t.): 0.90 (d, 6H, $OCH_2CH(CH_3)_2$, J = 6.4 Hz), 1.71 (d, 3H, CH_3CH, J = 6.4 Hz), 1.85 (m, 1H, $OCH_2CH(CH_3)_2$), 2.11 (m, 2H, $NCH_2CH_2CH_2C(O)$), 2.74 (t, 2H, $NCH_2CH_2CH_2C(O)$, J = 8.4 Hz), 3.28 and 3.51 (dd, 2H, $OCH_2CH(CH_3)_2$, J_{vic} = 6.4 and 6.9 Hz, J_{gem} = 9.2 Hz), 4.25 (m, 2H, $NCH_2CH_2CH_2C(O)$), and

5.77 (q, 1H, CH_3CH, J = 6.4 Hz).

Synthesis of *S*-1-isobutoxyethyl dithiobenzoate (3)

3 was synthesized by the reaction between sodium dithiobenzoate and the IBVE–HCl. Dithiobenzoic acid was prepared from 1.0 M THF solution of phenyl magnesium bromide (200 ml, 0.20 mol) and carbon disulfide (15 mL, 0.25 mol). Into Et_2O solution of sodium dithiobenzoate, which was prepared from the acid (60 mmol) and sodium hydride (3.12 g, 65 mmol), was added dropwise the IBVE–HCl solution (50 mmol) at –78 °C over a period of 30 min. After stirring for 1 h at 0 °C and then over 2 h at ambient temperature, the reaction was quenched by diluting with Et_2O and the solution was washed with 5 wt% $NaHCO_3$ aqueous solution, brine and water. The solvent was removed by evaporation to give the crude product (10.8 g), and a portion of the crude (3.05 g) was purified by column chromatography on silica gel with *n*-hexane as an eluent. The dithiocarbamate **2** was obtained as red liquids (2.62 g, 10.3 mmol). ^{1}H NMR ($CDCl_3$, r.t.): 0.91 (d, 6H, $OCH_2CH(CH_3)_2$, J = 6.4 Hz), 1.77 (d, 3H, CH_3CH, J = 6.0 Hz), 1.87 (m, 1H, $OCH_2CH(CH_3)_2$), 3.34 and 3.49 (dd, 2H, $OCH_2CH(CH_3)_2$, J_{vic} = 6.4 and 6.9 Hz, J_{gem} = 9.2 Hz), 5.83 (q, 1H, CH_3CH, J = 6.0 Hz), 7.38 (t, 2H, *m*-Ar*H*), 7.53 (t, 1H, *p*-Ar*H*), and 7.98 (d, 2H, *o*-Ar*H*).

Synthesis of *S*-1-isobutoxyethyl *O*-ethyl xanthate (4)

4 was synthesized by the reaction between potassium ethylxanthate and the IBVE–HCl. Into a Et_2O solution of potassium ethylxanthate (10.46 g, 58.7 mmol) was added dropwise the IBVE–HCl solution (50 mmol) at –78 °C over a period of 30 min. After stirring for 1 h at 0 °C and then over 2 h at ambient temperature, the reaction was quenched by diluting with Et_2O and the solution was washed with 5 wt% $NaHCO_3$ aqueous solution, brine and water. The solvent was removed by evaporation and the obtained product was purified by azeotropic drying with toluene. The xanthate **4** was obtained as pale yellow liquids (8.30 g, 37.3 mmol, 74.7% yield). ^{1}H NMR

($CDCl_3$, r.t.): 0.90 (d, 6H, $OCH_2CH(CH_3)_2$, J = 6.9 Hz), 1.43 (t, 3H, OCH_2CH_3, J = 6.9 Hz), 1.68 (d, 3H, CH_3CH, J = 6.4 Hz), 1.85 (m, 1H, $OCH_2CH(CH_3)_2$), 3.28 and 3.47 (dd, 2H, $OCH_2CH(CH_3)_2$, J_{vic} = 6.4 and 6.9 Hz, J_{gem} = 9.2 Hz), 4.65 (m, 2H, OCH_2CH_3), 5.59 (q, 1H, CH_3CH, J = 6.0 Hz).

Polymerization

The interconvertible living cationic and radical polymerization of IBVE and MA was carried out by the syringe technique under dry nitrogen in baked glass tubes equipped with a three-way stopcock. A typical example for the polymerization procedure is given below. The reaction was initiated by sequential addition of prechilled solutions of V-70 (0.026 mmol; 0.52 mL of 50 mM in toluene) and solution of $ZnCl_2$ (0.26 mL of 25 mM in Et_2O) via dry syringes into a monomer solution (1.82 mL) containing IBVE (5.31 mmol), MA (5.31 mmol), BEETC (0.11 mmol), and ethyl acetate (2.66 mmol) in toluene at 20 °C. The total volume of the reaction mixture was 2.6 mL. After 100 h, the polymerization was terminated with methanol (1.0 mL) containing a small amount of triethylamine. Monomer conversion was determined from the concentration of residual monomer measured by ^{1}H NMR with ethyl acetate as an internal standard (IBVE; 94%, MA; 91%). The quenched reaction mixture was washed with dilute hydrochloric acid, and distilled water to remove initiator residues, evaporated to dryness under reduced pressure, and vacuum-dried to give the product polymers (M_n = 8700, M_w/M_n = 1.25).

Measurements

Monomer conversion was determined from the concentration of residual monomer measured by ^{1}H NMR spectroscopy with ethyl acetate as an internal standard. ^{1}H and ^{13}C NMR spectra were recorded on a JEOL ECS-400 spectrometer, operating at 400 MHz. The number-average molecular weight (M_n) and the molecular weight distribution (M_w/M_n) of the product polymers were determined by size-exclusion chromatography (SEC) in THF at 40 °C on

two polystyrene gel columns [Shodex KF-805 L (pore size: 20–1000 Å; 8.0 mm i.d. × 30 cm) × 2; flow rate 1.0 mL/min] connected to a JASCO PU-2080 precision pump and a JASCO RI-2031 detector. The columns were calibrated against 10 standard polystyrene samples (Varian; M_p = 575–2783000, M_w/M_n = 1.02–1.23). The glass-transition temperature (T_g: midpoint of the transition) of the polymer was recorded on Q200 differential scanning calorimetry (TA Instruments Inc.). Certified indium and sapphire were used for temperature and heat flow calibration. All samples were first heated to 150 °C at 10 °C min^{-1}, equilibrated at this temperature for 5 min, and then cooled to –70 °C at 10 °C min^{-1}. After being held at that temperature for 5 min, the sample was then reheated to 150 °C at 10 °C min^{-1}. All T_g values were obtained from the second scan, after removing the thermal history.

The distribution of IBVE and MA-centered triad sequence were obtained from ^{1}H and ^{13}C NMR analyses. The cumulative growing cationic and radical species contents, F_{cum}(cationic) and F_{cum}(radical), calculated from the fraction of comonomer triad sequence by the following equation for each total monomer conversions.

$$F_{cum}(\text{cationic}) = \text{I-I-I} + \frac{1}{2}\ \text{I-I-M(M-I-I)}$$

$$F_{cum}(\text{radical}) = \text{M-M-M} + \text{I-M-M(M-M-I)} + \text{I-M-I} + \frac{1}{2}\ \text{I-I-M(M-I-I)}$$

The number of the interconversion between two active species per polymer chain (N_{conv}) and a average degree of polymerization via cationic and radical process per single mechanistic transformation (m and l, respectively) were estimated by the following equation

$$N_{conv} = \text{I-I-M(M-I-I)} \times DP_n$$

$$m = 2DP_n/N_{conv} \times F_{cum}(\text{cationic}),\ l = 2DP_n/N_{conv} \times F_{cum}(\text{radical})$$

where DP_n was calculated from the total monomer conversion.

Results and Discussions

1. Interconvertible Polymerization of IBVE and MA with Various Lewis Acids

The author first investigated that the interconvertible polymerization of an equimolar mixture of IBVE and MA with the combination of various Lewis acids ($EtAlCl_2$, $ZnCl_2$, and $FeCl_3$) and low-temperature radical initiator such as 2,2'-azobis(4-methocy-2,4-dimethylvaleronitrile) (V-70), in the presence of a 2-isobutoxyethyl trithiocarbonate-type RAFT agent (**1**) and ethyl acetate in toluene at 20 °C (Figure 1). The interconvertible polymerization with $EtAlCl_2$ and $ZnCl_2$ successfully promoted, where the both monomers were smoothly consumed in parallel with each other. In contrast, $FeCl_3$ induced only the consumption of IBVE to gave the poly(IBVE) homopolymer. This is due to the termination of growing radical species with $FeCl_3$ by forming C–Cl covalent bond.[20] Irrespective of Lewis acid, however, the number-average molecular weight (M_n) of the obtained polymer, which were based on the polystyrene calibration by SEC, were agreed well with the calculated

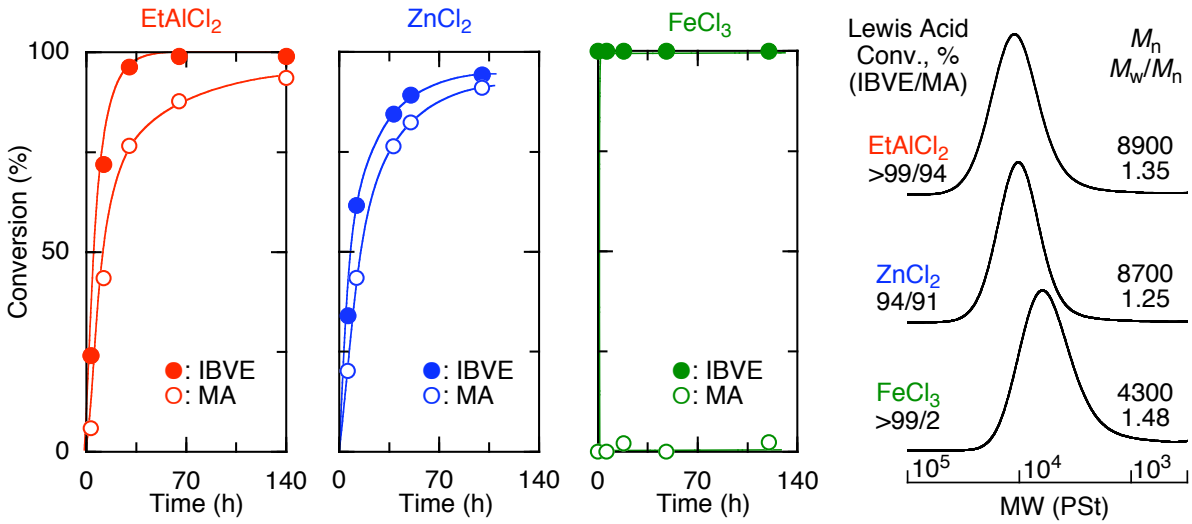

Figure 1. Interconvertible polymerization of IBVE and MA with various Lewis acid; $[IBVE]_0$ = 2.0 M, $[MA]_0$ = 2.0 M, $[\mathbf{1}]_0$ = 40 mM, $[\text{Lewis acid}]_0$ = 2.5 mM, $[\text{V-70}]_0$ = 10 mM, $[EtOAc]_0$ = 1.0 M in toluene at 20 °C.

values presuming that one molecule of **1** generates one polymer chain. The SEC curves were all unimodal and relatively narrow molecular weight distributions (MWDs), where the narrowest one was obtained with $ZnCl_2$.

The comonomer triad sequence of the copolymer produced with $EtAlCl_2$ and $ZnCl_2$ were analyzed by ^{1}H and ^{13}C NMR spectroscopies. In ^{13}C NMR spectra of the copolymers, the existence the split methine carbon (*b*) assigned to I-I-M (M-I-I) triad sequences (I = IBVE and M = MA) was confirmed at 70–80 ppm as shown later in Figure 4A. It suggests the occurrence of transformation from cationic into radical species and vice versa, since the I-I and I-M (M-I) sequences generate only via cationic and radical process, respectively.

Figure 2 shows a plot of the cumulative growing cationic and radical species contents, F_{cum}(cationic) and F_{cum}(radical), calculated from the fraction of comonomer triad sequence. The difference between these cumulative contents with $ZnCl_2$ was lower than that with $EtAlCl_2$ in the initial stage of the polymerization, although the set of cumulative contents finally closed to half.

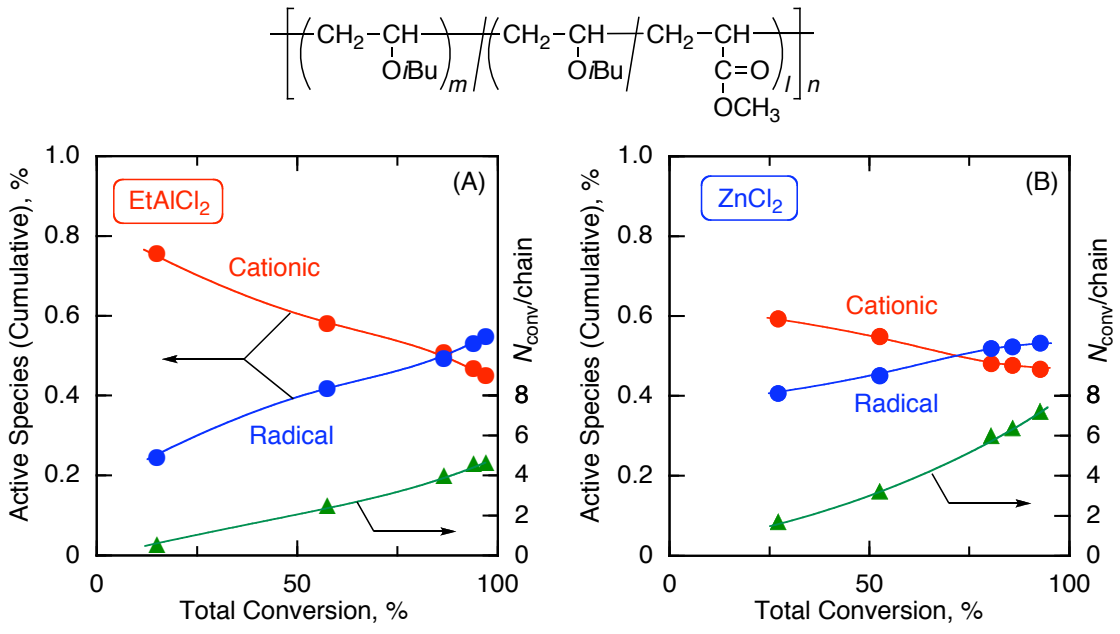

Figure 2. Dependence of cumulative active species composition [F_{cum}(cation) and F_{cum}(radical)] and numbers of the interconversion between active species per polymer chain (N_{conv}) on the total conversion of monomers for the polymerization in Figure 1.

Furthermore, the numbers of the interconversion between two active species per polymer chain (N_{conv}) were estimated from the fraction of I-I-M (M-I-I) triad sequences. The N_{conv} increased in the proportion to monomer conversion and were estimated to be 4.66 ($EtAlCl_2$) and 7.24 ($ZnCl_2$) during the insertion of approximately 100 monomer units. Namely, the segment lengths via each active species are about 20 (m = 18.8, l = 22.8 for $EtAlCl_2$) and 12 monomer units (m = 12.0, l = 13.6 for $ZnCl_2$), where m and l are the average degree of cationic and radical polymerization per single mechanistic transformation, respectively. These results indicated that the appropriate choice of Lewis acid was not only achieved the interconvertible cationic and radical polymerization but also tuned the N_{conv} and the degree of polymerization via each active species.

2. Effect of RAFT Agent on the Interconvertible Polymerization of IBVE and MA

To investigate the effects of the RAFT agent, a series of 2-isobutoxyethyl dithioester derivatives [$CH_3CH(OiBu)SC(S)Z$], which possesses the effective Z groups for the controlled/living radical polymerization of MA such as 2-pyrrolidonyl **(2)**,[21] phenyl **(3)**,[22] and *O*-ethyl **(4)**,[23] were employed for interconvertible polymerization of IBVE and MA with $ZnCl_2$ and V-70 in toluene at 20 °C (Figure 3). Both monomers were smoothly and simultaneously consumed with all RAFT agents except for **3**. With dithiobenzoate **3**, IBVE was consumed quantitatively without the consumption of MA to result in poly(IBVE) homopolymer via cationic process. Even in the MA radical homopolymerization, MA was not consumed in the presence of **3** and V-70. These results suggest that the terminal IBVE-dithiobenzoate group is ineffective for the RAFT radical polymerization because the significant stable its intermediate radical, formed by the addition of other radical species, does not fragment and produce the growing radical species any more. In all cases, the M_n values increased in the direct proportion to the monomer conversion and agreed well with the calculated values. The copolymer with **2** and **3** had unimodal and relatively narrow MWDs. However, the polymer with **4** possessed the bimodal and broad MWDs, indicating the slow interconverion as described in following section.

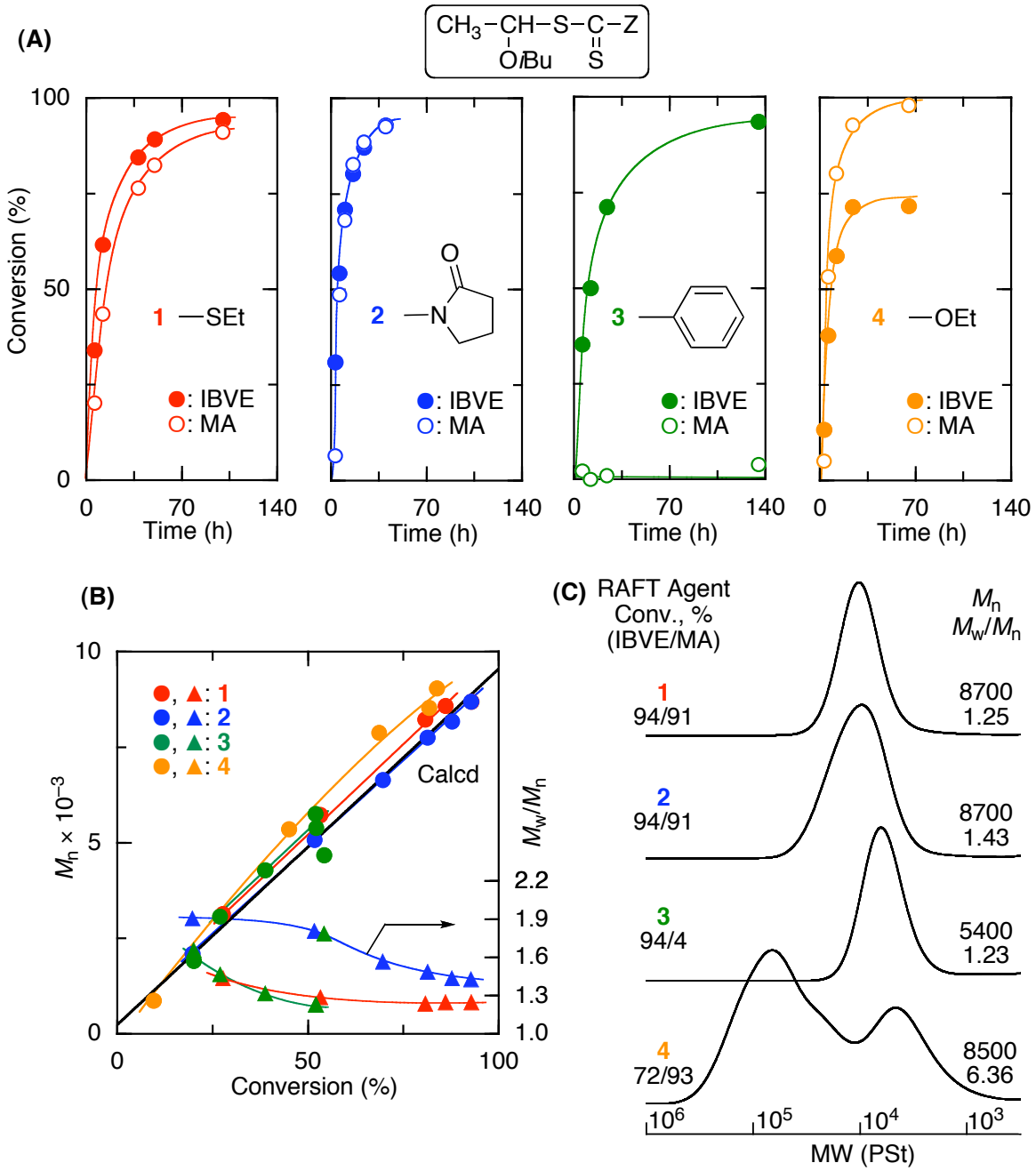

Figure 3. Interconvertible polymerization of IBVE and MA with various RAFT agents; $[IBVE]_0$ = 2.0 M, $[MA]_0$ = 2.0 M, [RAFT Agent]$_0$ = 40 mM, $[ZnCl_2]_0$ = 2.5 mM, $[V\text{-}70]_0$ = 10 mM, $[EtOAc]_0$ = 1.0 M in toluene at 20 °C.

The structure of the copolymer obtained with **2** and **4** were evaluated by NMR spectroscopies and were compared to that with **1**. Figure 4A showed the ^{13}C NMR spectra of the

region for the main-chain methine carbon (*b*) of IBVE unit at 70–80 ppm. The copolymer obtained with dithiocarbamate **2** also exhibited the characteristic peak of I-I-M (M-I-I) sequence, although the peak intensities was lower than those with trithiocarbonate **1**. The N_{conv} value with **2** increased more gradually than with **1** as the polymerization proceeded and finally was 3.06 (Figure 4B and entry 3 in Table 1). However, the copolymer with **4** showed almost no peak of I-I-M (M-I-I) sequence and gave the low N_{conv} (<0.83) (entry 4 in Table 1). This is probably because the IBVE xanthate terminal, which can be a transformation point of active species, is not generate easily due to the slow addition of growing radical species to xanthate group. As a results, the cationic polymerization and the radical copolymerization separately proceeded without transformation to result in the bimodal SEC curve as shown in Figure 3. These results suggested that the design of RAFT agent also played critical role in the interconvertible polymerization.

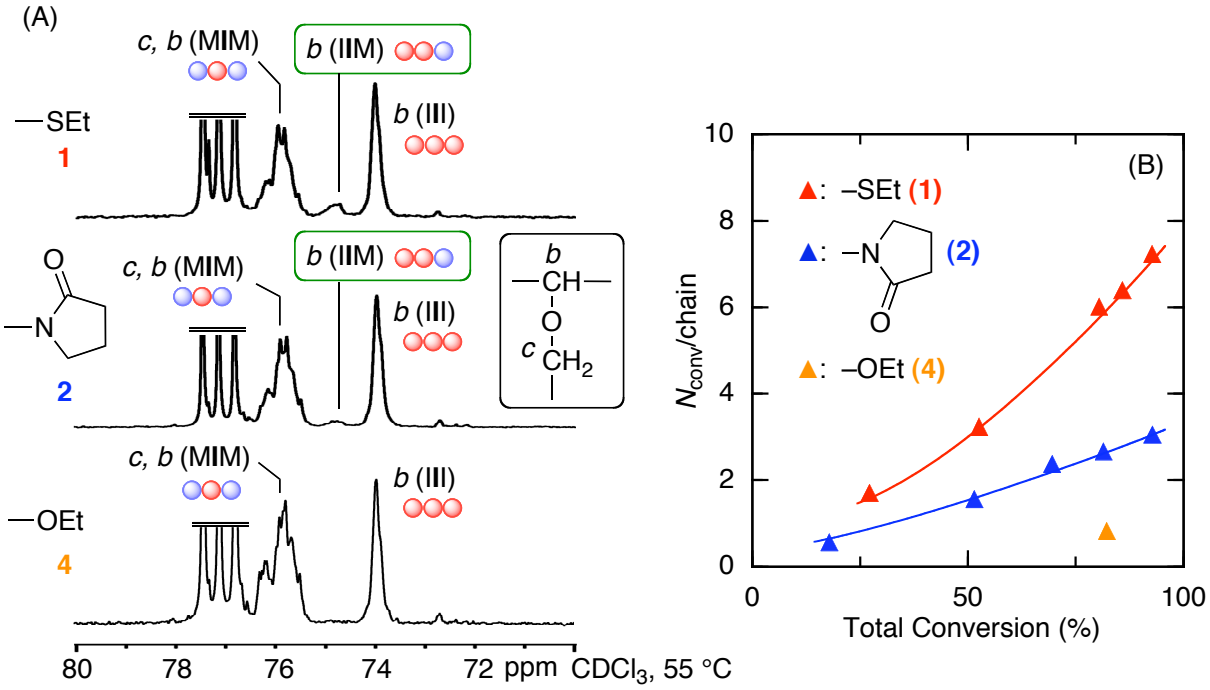

Figure 4. ^{13}C NMR spectra of the obtained copolymers (A) and dependence of N_{conv} on the total monomer conversion (B) in the interconvertible polymerization of IBVE and MA with various RAFT agents. See Figure 3 for the polymerization conditions.

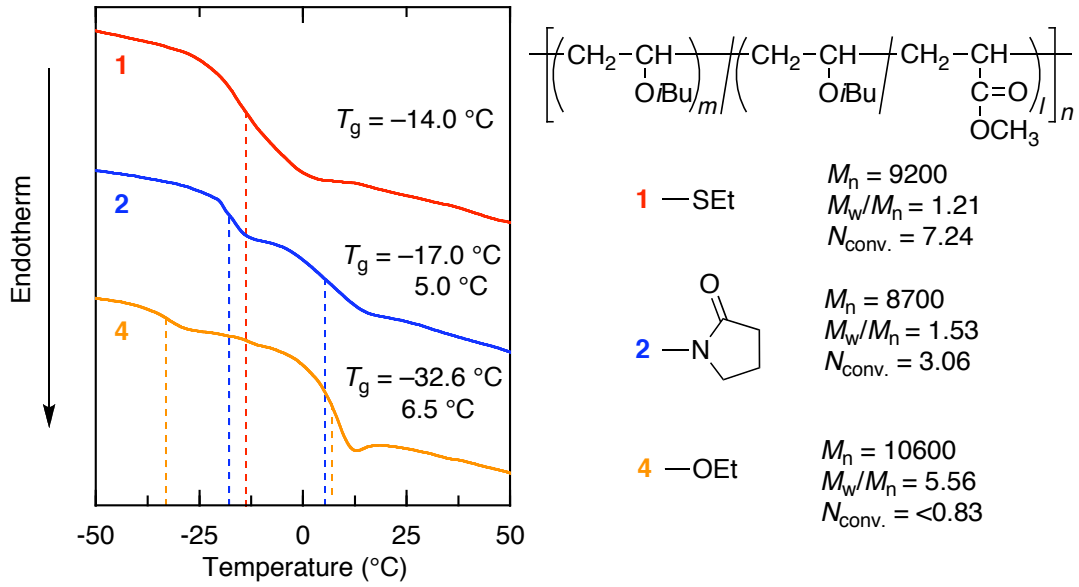

Figure 5. Differential scanning calorimetry (DSC) curves of the obtained copolymer by the interconvertible polymerization with various RAFT agent in Figure 3

The thermal properties of the obtained copolymers with the almost same molecular weights but with different number of the interconversion were evaluated by differential scanning calorimetry (DSC) under a nitrogen atmosphere (Figure 5). The copolymer with low N_{conv} values (3.06 and <0.83) showed two glass transition temperatures (T_g) around –15 ~ –35 °C and 5 °C, corresponding to poly(IBVE) and poly(IBVE-*r*-MA), respectively. In contrast, only one T_g was observed at –14 °C with high $N_{conv.}$ values (7.24), because the length of cationically and radically polymerizable segments become shorter as the N_{conv} values increase and are miscible each other. This results also proved that a series of multiblock copolymers were prepared via interconvertible polymerization with various RAFT agent.

3. Effect of $[M]_0$ and Temperature on the Interconvertible Polymerization of IBVE and MA

The effects of the polymerization conditions were investigated for the interconvertible polymerization of IBVE and MA using **1**/$ZnCl_2$/V-70 initiating system with varying temperature (20 or 40 °C) or the concentration of monomers ($[IBVE]_0 = [MA]_0$ = 0.5 or 2.0 M, $[M_{total}]_0/[\mathbf{1}]_0$ =

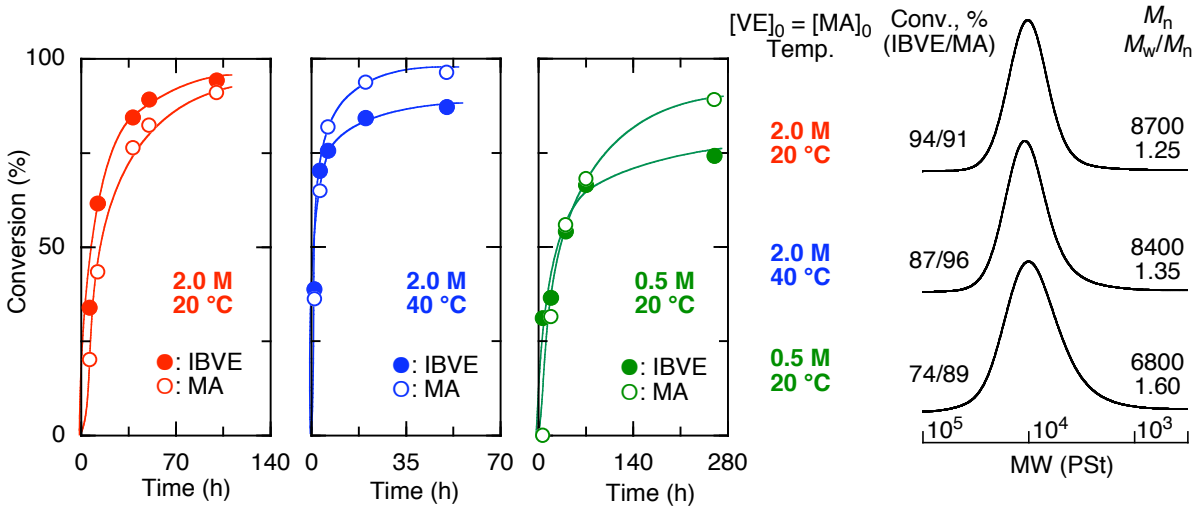

Figure 6. Interconvertible Polymerization of IBVE and MA under Various Conditions; $[IBVE]_0 = [MA]_0 = 0.5$ or 2.0 M, $[\mathbf{1}]_0 = 10$ or 40 mM, $[ZnCl_2]_0 = 2.5$ mM (for 20 °C) or 4.0 mM (for 40 °C), $[V\text{-}70]_0 = 2.5$ mM ($[M]_0 = 0.5$ M) or 10 mM ($[M]_0 = 2.0$ M) in toluene at 20 °C or 40 °C.

100) (Figure 6). Even at the higher temperature (40 °C) or the lower concentration of monomers (0.5 M), the adjusted amount of Lewis acid and radical initiator induced the simultaneous consumption of the both monomers to give the copolymers with well-controlled molecular weights.

The NMR analyses of the obtained copolymers revealed that the N_{conv} also was affected by the polymerization condition (Figure 7A). Compared to the initial condition ($[IBVE]_0 = [MA]_0 = 2.0$ M at 20 °C, $N_{conv} = 7.26$), the elevation of polymerization temperature resulted in the slightly higher N_{conv} (7.47) whereas the decrease of monomer concentration led the lower N_{conv} (4.98). In addition, the polymerization condition, which gave the polymer with higher N_{conv} values, showed the narrower MWDs (Figure 7B). The similar trend was also observed in the polymerization with various Lewis acid and RAFT agent. This suggests that the fast exchange between the dormant and active species contributed to a large number of interconversion between cationic and radical species.

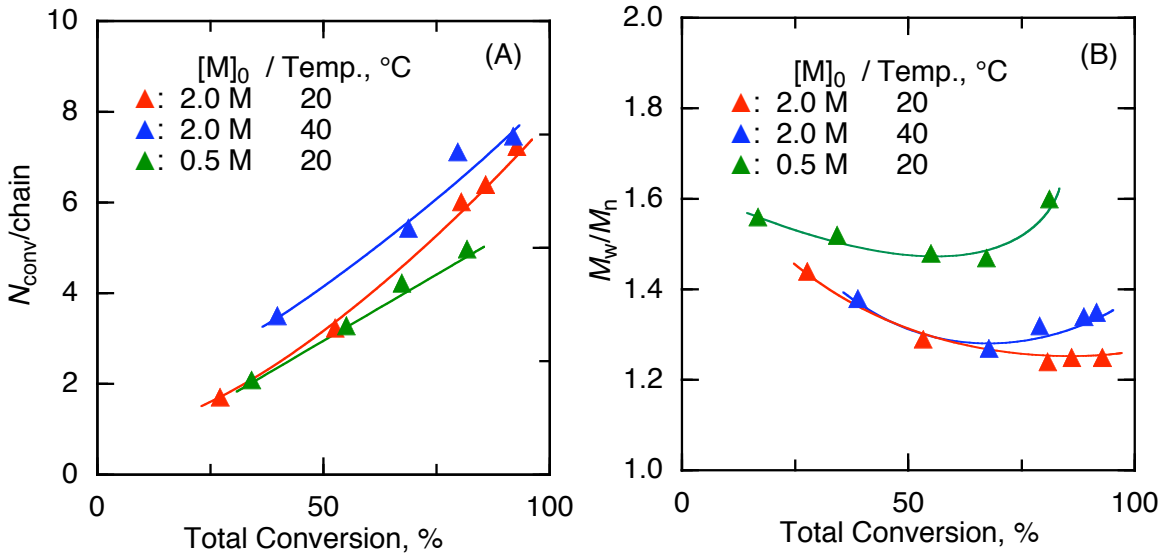

Figure 7. Dependence of N_{conv} (A) and M_w/M_n (B) on the total monomer conversion for the polymerization in Figure 5.

Table 1 also summarizes the analysis results of the polymer obtained by interconvertible polymerization with various initiating system under different conditions. Especially, the N_{conv} values can be changed from 3.06 to 7.47, depending on the Lewis acid, RAFT agent, monomer concentration, and polymerization temperature. Thus, the synthesis of multiblock copolymers having well-defined poly(IBVE) and poly(IBVE-*r*-MA) segment were accomplished by interconvertible polymerization via dual active speices.

Table 1. Interconvetible Living Cationic and Radical Polymerization of IBVE and MA[a]

Entry	$[M]_0$ (M)	RAFT agent	temp. (°C)	Lewis acid	M_w/M_n[b]	DP_n[b]	N_{conv}	*m* (cationic)	*l* (radical)
1	2.0	**1**	20	$EtAlCl_2$	1.35	96.9	4.66	18.8	22.8
2	2.0	**1**	20	$ZnCl_2$	1.24	92.7	7.24	12.0	13.6
3	2.0	**2**	20	$ZnCl_2$	1.43	92.8	3.06	23.8	36.4
4	2.0	**4**	20	$ZnCl_2$	6.36	82.2	<0.83	-	-
5[c]	2.0	**1**	40	$ZnCl_2$	1.35	91.2	7.47	7.6	17.0
6[d]	0.5	**1**	20	$ZnCl_2$	1.60	81.7	4.98	12.3	20.5

[a]$[M]_0 = [IBVE]_0 = [MA]_0$, $[RAFT\ agent]_0$ = 40 mM, $[Lewis\ Acid]_0$ = 2.5 mM, $[V\text{-}70]_0$ = 10 mM in toluene. [b]Determined by monomer conversion. [c]$[ZnCl_2]_0$ = 4.0 mM. [d]$[V\text{-}70]_0$ = 2.5 mM.

4. Interconvertible Polymerization of IBVE and Various Acrylates

A series of other acrylate such as *n*-butyl (*n*BA), *t*-butyl (*t*BA), and isoboronyl acrylate (*i*BoA) were then employed with IBVE for interconvertible polymerization with **1**/Lewis acid/V-70 systems in toluene at 20 °C (Figure 8). Regardless of the substituents in the monomer, the acrylates were almost quantitatively consumed. The consumption rates of IBVE were similar with that of *n*BA and *i*BoA, while the consumption of IBVE with *t*BA ceased around 30% after the depletion of the counterpart comonomer as in the conventional radical copolymerizations. This is probably due to the deactivation of Lewis acid by the reaction with *t*-butyl ester moiety. These results indicated that the interconvertible polymerization was achieved for various acrylates with IBVE, although the *t*BA was not suitable.

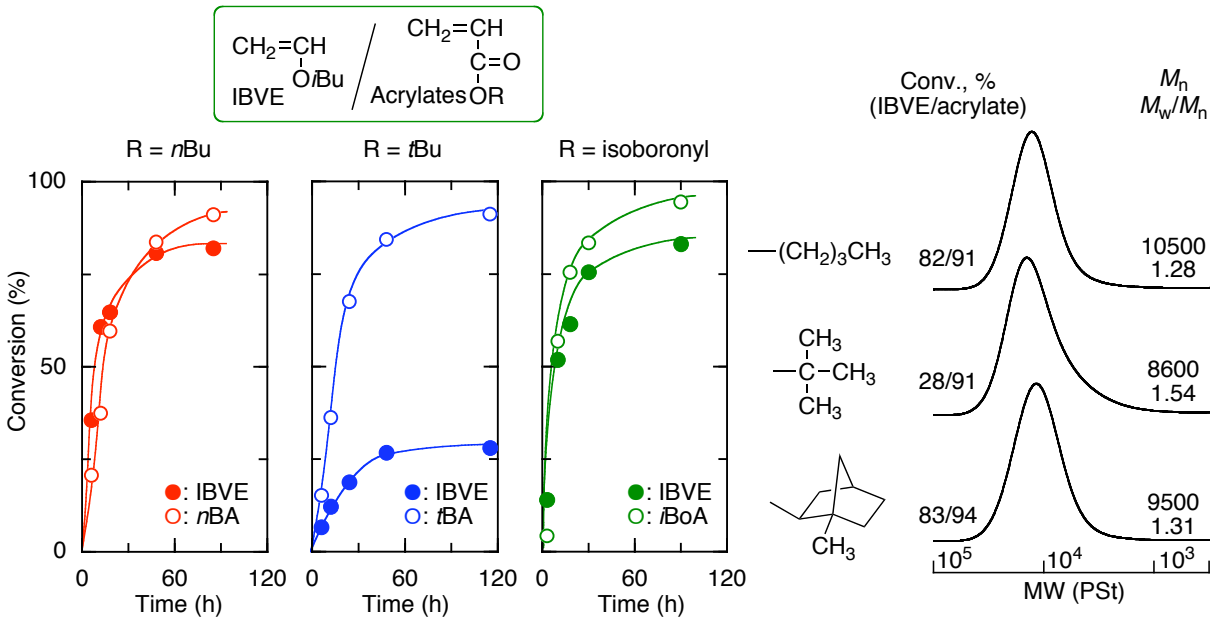

Figure 8. Interconvertible polymerization of various acrylates with IBVE in toluene at 20 °C; $[IBVE]_0 = [acrylates]_0$, $[nBA]_0 = [tBA]_0 = 2.0$ M, $[iBoA]_0 = 1.5$ M, $[M_{total}]_0/[\mathbf{1}]_0 = 100$, $[ZnCl_2]_0 = 2.5$ mM (for *n*BA and *t*BA), $[EtAlCl_2]_0 = 2.5$ mM (for *i*BoA), $[V\text{-}70]_0 = 10$ mM, $[EtOAc]_0 = 1.0$ M.

5. Interconvertible Polymerization of IBVE and MMA

Finally, MMA was used as comonomer instead of acrylates for the interconvertible polymerization with IBVE. The copolymerization of IBVE and MMA ($[IBVE]_0/[MMA]_0$ = 1/1) was investigated with **1**/$ZnCl_2$/V-70 system in toluene at 20 °C (Figure 9A). As was observed in the polymerization of IBVE and acrylates, MMA was quantitatively and simultaneously consumed with IBVE to give the polymer with the controlled molecular weight. However, the yielded polymer showed the bimodal and broad MWDs, suggesting that the slow interconversion of active species. This is likely due to the lower radical copolymerizability of IBVE with MMA than with MA.

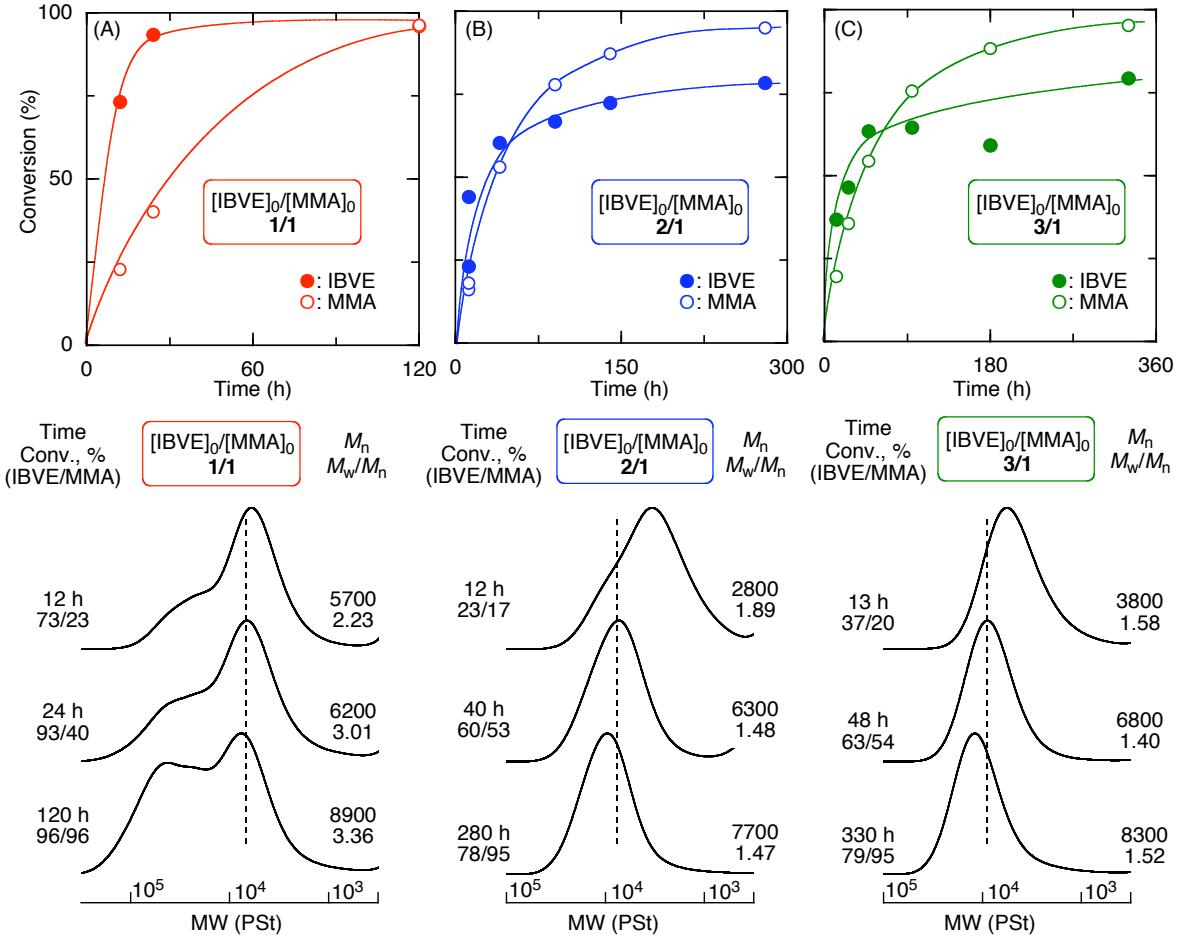

Figure 9. Interconvertible polymerization of IBVE and MMA with various initial monomer feed ratio in toluene at 20 °C; $[M_{total}]_0$ = 4.0 M, $[IBVE]_0/[MMA]_0$ = 1/1, 2/1, and 3/1, $[\mathbf{1}]_0$ = 40 mM, $[ZnCl_2]_0$ = 1.25 mM, $[V\text{-}70]_0$ = 20 mM, $[EtOAc]_0$ = 1.0 M (for $[IBVE]_0/[MMA]_0$ = 1/1) or 2.0 M.

In order to increase the opportunities for the transformation of active species, the polymerization examined at a higher IBVE initial feed ratio $[IBVE]_0/[MMA]_0$ = 2/1 or 3/1 (Figure 9B and C). Irrespective of the feed ratio, two monomers were copolymerized simultaneously. The SEC curves of the obtained copolymer became unimodal and shifted to the higher molecular weights retaining the relatively narrow MWDs. Thus, the interconvertible polymerization of IBVE and MMA was accomplished by the effective generation of trithiocarbonate IBVE terminal through the change of the monomer feed ratio.

The obtained copolymer ($[IBVE]_0/[MMA]_0$ = 2/1) was analyzed by ^1H and ^{13}C NMR spectroscopies and compared to the spectra of PMMA and poly(IBVE-*r*-MMA) with a high incorporation of IBVE units, which were prepared by the radical polymerization and copolymerization with $EtAl(ODBP)_2$, respectively. Figure 10A, C, and D showed the ^{13}C NMR spectra of the regions for carbonyl carbon at 175–180 ppm. The observed peak split due to the tacticity and triad sequence. In the spectrum of poly(IBVE-*r*-MMA) (B), the peaks assigned to I-M-M (M-M-I) and alternating I-M-I sequences were confirmed in addition to the same peaks as PMMA homopolymer (A). On the other hand, the spectrum of the poly(IBVE-*co*-MMA) (C) obtained via interconvertible polymerization was similar to that of PMMA homopolymer although the copolymer incorporated much IBVE units (IBVE/MMA = 60/40 calculated from ^1H NMR). Furthermore, the characteristic methine proton peaks (*b*) attributed to continual I-I-I sequence was observed at 3.3–3.5 ppm in ^1H NMR spectrum (F). These result support that the interconvertible polymerization proceeded successfully to afford the polymer consisting of both IBVE and MMA repeating units.

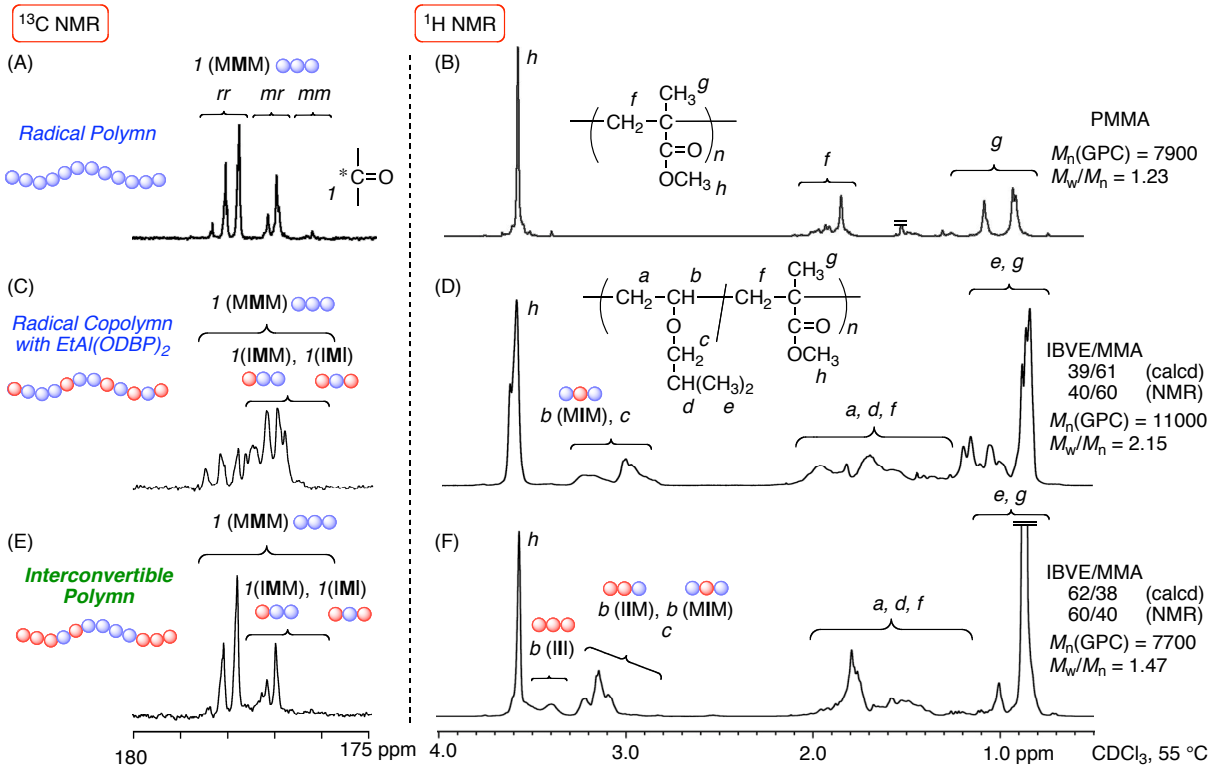

Figure 10. ^{1}H and ^{13}C NMR spectra of PMMA obtained by RAFT radical polymerization (A and B), poly(IBVE-*r*-MMA) obtained by radical copolymerization with EtAl(ODBP)$_2$ (C and D), and poly(IBVE-*co*-MMA) obtained by interconvertible polymerization ([IBVE]$_0$/[MMA]$_0$ = 2/1) (E and F).

Conclusion

The interconvertible cationic and radical polymerization proceeded via dual active species for IBVE and a series of (meth)acrylate with various RAFT agent in the presence of Lewis acids and radical initiator. The number of the interconversion between two species per polymer chain and the length of the cationically and radically segments can be tuned by the choice of the initiating system and the polymerization condition. The author believes that the interconvertible polymerization will make a large contribution to polymer synthesis beyond the traditional limitation by active species.

References

1. Odian, G. *Principles of Polymerization, Fourth Edition*; John Wiley and Sons, Inc., Hoboken, New Jersey, 2004.
2. (a) Yagci, Y.; Reetz, I. *Prog. Polym. Sci*. **1998**, *23*, 1485–1538. (b) Guo, H.-Q.; Kajiwara, A.; Morishima, Y; Kamachi, M. *Macromolecules* **1996**, *29*, 2354–2358.
3. Nomura, R.; Narita, M.; Endo, T. *Macromolecules* **1994**, *27*, 4853–4854.
4. *Controlled and Living Polymerizations: From Mechanisms to Materials*; Müller A. H. E.; Matyjaszewski, K., Eds.; Wiley-VCH: Weilheim, Germany, 2008.
5. (a) Sawamoto, M. *Prog. Polym. Sci*. **1991**, *16*, 111–172. (b) Puskas. J.E.; Kaszas, G. *Prog. Polym. Sci*. **2000**, *25*, 403–452. (c) Goethals, E. J.; Prez, F. D. *Prog. Polym. Sci*. **2007**, *32*, 220–246. (d) Aoshima, S.; Kanaoka, S. *Chem. Rev*. **2009**, 129, 5245–5287.
6. Sawamoto, M.; Okamoto, C.; Higashimura, T. *Macromolecules* **1987**, *20*, 2693–2697.
7. Aoshima, S.; Higashimura, S. *Polym. Bull*. **1986**, *15*, 417–423.
8. Kamigaito, M.; Sawamoto, M.; Higashimura, T. *Macoromolecules* **1993**, *26*, 1643–1649.
9. Kaszas, G.; Puskas, J. E.; Chem, C. C.; Kennedy, J. P. *Polym. Bull*. **1988**, *20*, 413–419.
10. Kanazawa, A.; Hirabaru, Y.; Kanaoka, S.; Aoshima, S. *J. Polym. Sci., Part A: Polym. Chem.* **2006**, *44*, 5795–5800.
11. (a) Hawker, C. J.; Bosman, A. W.; Harth, E. *Chem. Rev*. **2001**, *101*, 3661–3688. (b) Studer, A.; Schulte, T. *Chem. Rec*. **2005**, *5*, 27–35. (c) Sciannamea, V.; Jérôme, R.; Detrembleur, C. *Chem. Rev*. **2008**, *108*, 1104–1126. (d) Grubbs, R. B. *Polym. Rev*. **2011**, *51*, 104–137.
12. (a) Kamigaito, M.; Ando, T.; Sawamoto, M. *Chem. Rev*. **2001**, *101*, 3689–3745. (b) Kamigaito, M.; Ando, T.; Sawamoto, M. *Chem. Rec*. **2004**, *4*, 159–175. (c) Ouchi, M.; Terashima, T.; Sawamoto, M. *Acc. Chem. Res*. **2008**, *41*, 1120–1132. (d) Ouchi, M.; Terashima, T.; Sawamoto, M. *Chem. Rec*. **2009**, *109*, 4963–5050. (e) Kamigaito, M. *Polym. J*. **2010**, 42, 105–120.
13. (a) Matyjaszewski, K.; Xia, J. *Chem. Rev*. **2001**, *101*, 2921–2990. (b) Tsarevsky, N. V.;

Matyjaszewski, K. *Chem. Rev*. **2007**, *107*, 2270–2299. (c) Braunecker, W. A.; Matyjaszewski, K. *Prog. Polym. Sci*. **2007**, *32*, 93–146. (d) di Lena, F.; Matyjaszewski, K. *Prog. Polym. Sci*. **2010**, *35*, 959–1021. (e) Matyjaszewski, K. *Macromolecules* **2012**, *45*, 4015–4039.

14. Rosen, B. M.; Percec, V. *Chem. Rev*. **2009**, *109*, 5069–5119.
15. (a) Moad, G.; Rizzardo, E.; Thang, S. H. *Aust. J. Chem.* **2005**, *58*, 379–410. (b) Moad, G.; Rizzardo, E.; Thang, S. H. *Polymer* **2008**, *49*, 1079–1131. (c) Moad, G.; Rizzardo, E.; Thang, S. H. *Acc. Chem. Res*. **2008**, *41*, 1133–1142. (d) Moad, G.; Rizzardo, E.; Thang, S. H. *Aust. J. Chem.* **2009**, *62*, 1402–1472. (e) Moad, G.; Rizzardo, E.; Thang, S. H. *Aust. J. Chem.* **2012**, *65*, 985–1076.
16. (a) Yagci, Y.; Tasdelen, M. A. *Prog. Polym. Sci.* **2006**, *31*, 1133–1170. (b) Hadjichristidis, N.; Pitisikalis, M.; Iatrou, H. *Adv. Polym. Sci*. **2005**, *189*, 1–124.
17. (a) Coca, S.; Matyjaszewski, K. *Macromolecules* **1997**, *30,* 2808–2810. (b) Coca, S.; Matyjaszewski, K. *J. Polym. Sci., Part A: Polym. Chem*. **1997**, *35*, 3595–3601. (b) Chen, X.; Ivan, B.; Kops, J.; Batsberg, W. *Macromol. Rapid. Commun*. **1998**, *19*, 585–589. (c) Lu, J.; Liang, H.; Li, A.; Cheng, Q. *Eur. Polym. J*. **2004**, *40*, 397–402. (d) Chapter 3 of this thesis; Aoshima, H.; Satoh, K.; Kamigaito, M. *Macromol. Symp.* **2013**, *323*, 64–74.
18. (a) Toman, L.; Janata, M.; Spěváček, J.; Vlček, P.; Látalová, P.; Masař, B.; Sikora, A. *J. Polym. Sci., Part A: Polym. Chem*. **2004**, *42*, 6096–6108. (b) Toman, L.; Janata, M.; Spěváček, J.; Vlček, P.; Látalová, P.; Sikora, A.; Masař, B. *J. Polym. Sci., Part A: Polym. Chem*. **2005**, *43*, 3823–3830.
19. Kumagai, S.; Nagai, K.; Satoh, K.; Kamigaito, M. *Macromolecules* **2010**, *43*, 7523–7531.
20. (a) Bamford, C. H.; Jenkins, A. D.; Johnston, R. *Nature* **1956**, *177*, 992. (b) Bamford, C. H.; Jenkins, A. D.; Johnston, R. *Proc. R. Soc.* **1957**, *239A*, 214–229.
21. Rizzardo, E.; Chiefari, J.; Mayadunne, RTA.; Moad, G.; Thang, SH. *ACS Symp. Ser*. **2000**, *768*, 278–296.

22. Chong, B. Y. K.; Le, T. P. T.; Moad, G.; Rizzardo, E.; Thang, S. H. *Macromolecules* **1999**, *32*, 2071–2074.

23. Charmot, D.; Corpart, P.; Adam, H.; Zard, S. Z.; Biadatti, T.; Bouhadir, G. *Macromol. Symp.* **2000**, *150*, 23–32.

Part III

Direct Mechanistic Transformation from Living Anionic into Radical Polymerization

Chapter 6

Direct Mechanistic Transformations from Isotactic or Syndiotactic Living Anionic Polymerizations of Methyl Methacrylate into Metal-Catalyzed Living Radical Polymerizations

Abstract

The mechanistic transformations from living anionic polymerizations into living radical polymerizations were examined after halogenating the growing terminal during the stereospecific living anionic polymerization of methyl methacrylate (MMA), directly forming a macroinitiator with a covalent carbon–halogen terminal for subsequent transition metal-catalyzed living radical polymerizations. The quantitative halogenation of the living isotactic or syndiotactic PMMA anion, prepared using *t*BuMgBr in toluene or diphenylhexyllithium (DPHLi) in THF, respectively, was achieved using CCl_3Br or CCl_4 as a halogen source in the presence of strong Lewis bases, such as 1,8-diazabicyclo[5.4.0]undec-7-ene, to generate stereoregular PMMA with a C–X (X = Br or Cl) bond. The halogenated terminal was then transformed into the radical species through a one-electron redox reaction of the ruthenium catalysts to allow the living radical polymerization of styrene or MMA, resulting in block copolymers that consisted of stereoregular PMMA and polystyrene segments or stereoblock PMMAs.

Introduction

A large number of controlled/living polymerizations currently exists,[1] some of which have versatile uses in various vinyl monomers as often observed in recently developed controlled/living radical polymerizations. Not many of these controlled/living polymerizations enable additional control, such as stereoregularity of the polymers or highly precise control of the molecular weights and chain-end groups, as is sometimes observed in ionic and coordination polymerizations. A combination of the latter systems with the former general methods could broaden the scope of well-defined synthetic polymers that not only possess additional specificity but also versatility (e.g., a variety of block copolymers that retain stereoregular structures).

Since the discovery of the living anionic polymerization of styrene in 1956, various vinyl monomers, including non-polar conjugated monomers and polar monomers such as methacrylic monomers, have been successfully polymerized in a controlled fashion using various designed anionic initiating systems.[2] Among these systems, the stereospecific living anionic polymerization of methyl methacrylate (MMA) has been achieved using *t*BuMgBr in toluene or diphenylhexyllithium (DPHLi) in THF to generate highly isotactic or syndiotactic polymers, respectively, with controlled molecular weights.[3,4] Both of these polymerizations proceed via the enolate-growing species associated with the specific metal countercations. In addition to their highly controlled structures, these polymers exhibit interesting properties, including glass transition temperatures that vary from 50 °C to 130 °C depending on the polymers' tacticities[5] and the formation of stereocomplexes between the iso- and syndiotactic polymers with melting points over 150 °C.[6]

Over the last two decades, tremendous progress has been attained in controlled/living radical polymerizations, enabling the control of molecular weights and the synthesis of a wide variety of well-defined polymers such as block, graft, and star polymers from a number of vinyl monomers.[7] Among this variety of methods, metal-catalyzed living radical polymerization, or atom transfer living radical polymerization (ATRP), is one of the most widely employed strategies.

This technique is based on the reversible activation of a dormant carbon–halogen bond, which can be easily introduced into low and high molecular weight initiators, via a one-electron redox reaction of the transition metal catalysts into the growing radical species.[7a,b] However, the initiating system cannot principally control the stereochemistry of the resulting polymers due to the absence of the substantial interactions between the halogen or metal catalyst and the growing radical species, similar to all of the other controlled/living radical polymerizations that proceed via the reversible activation of the dormant species. Although stereochemical control has become possible even in radical polymerization[8] by using bulky monomers, polar solvents, or Lewis acid additives, the regularity is moderate and lower than those attained in stereospecific anionic polymerization reactions.

A direct mechanistic transformation of the propagating species between different living polymerizations can expand the scope of polymerizable monomers per chain and now represents one of the most efficient methods of synthesizing well-defined block copolymers that consist of different monomer types.[9] In addition, recent advances in direct mechanistic transformation have been achieved through the use of common dormant species, which can generate different propagating species depending on the stimulus, such as covalent carbon–halogen and related bonds via heterolytic and homolytic cleavage by Lewis acids and transition metal catalysts for living cationic and radical polymerizations, respectively.[10]

Because anionic living polymerizations can allow for highly well-controlled polymers when compared to the radical processes mentioned above, a mechanistic transformation that switches from anionic to radical polymerization should provide a highly efficient strategy for novel block copolymer syntheses. However, a direct mechanistic transformation from a carbanion into a carbon radical species has been limited[11] in comparison to many reports regarding an indirect method[9,12] (i.e., the initiating moiety for living radical polymerization is introduced at the functionalized chain end obtained after the modification of the anionic polymerization terminal).

Halogenation of a carbanion can be achieved and is widely employed in organic synthesis.[13] Thus, this study aims for the straightforward halogenation of the living anionic species, especially the enolate chain end in the stereospecific living anionic polymerization of MMA, into the carbon–halogen terminal for successive transition metal-catalyzed living radical polymerization via a mechanistic transformation. This chapter demonstrates the quantitative halogenation of the growing terminal in the isotactic and syndiotactic living anionic polymerizations of MMA to produce halogen-capped polymers. Furthermore, the subsequent ruthenium-catalyzed living radical polymerizations of styrene or MMA blocking from the halogen-capped stereoregular PMMA to generate novel block copolymers (Scheme 1) are reported and quantitated here.

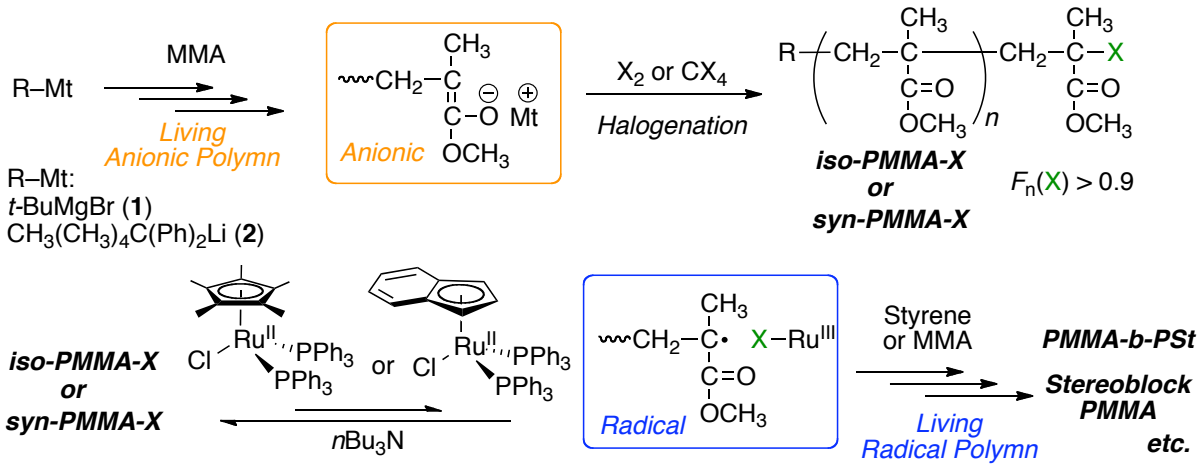

Scheme 1. Mechanistic Transformation from Living Anionic Polymerization into Metal-Catalyzed Living Radical Polymerization.

Experimental Section

Materials

Methyl methacrylate (MMA; TCI, >99.8%), styrene (KISHIDA, 99.5%), 1,8-diazabicyclo[5.4.0]undec-7-ene (DBU; TCI, >98.0%), 1,1,3,3-tetramethylguanidine (TMG; TCI, >99.0%), *N,N,N',N'*-tetramethylenediamine (TMEDA; TCI, >98.0%), *N,N,N',N'',N''*-penta- methyldiethylenetriamine (PMDETA; TCI, >98%), 1,1,4,7,10,10-hexamethyltriethylenetetramine (HMTETA; Aldrich, 97%), and N*n*Bu_3 (Wako, >98%) were distilled over calcium hydride under reduced pressure before use. CCl_3Br (TCI, >98%), CCl_4 (Kanto, >99.9%), and Et_3N (KISHIDA, >99.0%) were distilled over calcium hydride before use. RuCp*Cl(PPh_3)$_2$, Ru(Ind)Cl(PPh_3)$_2$ (both provided from Wako), and CBr_4 (TCI, >99.0%) were used as received and handled in a glovebox (MBraun Labmaster sp) under a moisture- and oxygen-free argon atmosphere (O_2, < 1 ppm). 1,4-Dioxane-Br_2 complex (TCI, >95.0%) was used as received. *t*BuMgBr and diphenylhexyllithium (DPHLi) were prepared according to the literature.[3c,4b] Toluene (Kanto, >99.5%; H_2O <10 ppm) and tetrahydrofuran (THF; Kanto, >99.5%; H_2O <0.001%) were dried and deoxygenized by passage through columns of Glass Contour Solvent Systems before use.

Stereospecific Living Anionic Polymerization of MMA and Subsequent Halogenation. The reactions were carried out by syringe techniques under dry argon in baked glassware equipped with a three-way stopcock. A typical example for living anionic polymerization of MMA with the *t*BuMgBr/toluene system and subsequent bromination of the living PMMA anion with CCl_3Br/DBU is given below. The polymerization was initiated by adding MMA (1.15 mL, 10.8 mmol) slowly via dry syringe into the prechilled initiator solution (6.9 mL), containing *t*BuMgBr (0.43 mmol, 1.50 mL, 289 mM in Et_2O) and toluene (5.4 mL), at –78 °C. The total volume of the reaction mixture was thus 8.05 mL. After stirring for 25 h, the THF solution (6.4 mL) of CCl_3Br (17.2 mmol, 1.69 mL) was added to the reaction mixture. After 2 h, into the reaction

mixture was then added DBU (2.15 mmol, 0.32 mL) and the reaction temperature was gradually raised to 0 ºC. After additional 23 h, the reaction was quenched by 1 mL of argon-bubbled methanol. The quenched solution was diluted with ca. 30 mL of toluene and washed with dilute hydrochloric acid and water, evaporated to dryness under reduced pressure, and vacuum-dried to give the product polymers (PMMA–X). The obtained polymer was precipitated into hexane twice, filtered, vacuum-dried, and employed as macroinitiator for mechanistic transformation described below.

Ruthenium-Catalyzed Living Radical Polymerization Initiated from PMMA–X. The polymerizations were also carried out by syringe techniques under dry argon or nitrogen in baked glassware equipped with a three-way stopcock. A typical example for the ruthenium-catalyzed living radical polymerization of styrene initiated from the isotactic PMMA–Br is given below. To the glass tube containing RuCp*Cl(PPh_3)$_2$ (12.7 mg, 0.016 mmol), PMMA–Br (M_n = 2900, 0.466 g, 0.16 mmol), styrene (1.83 mL, 16.0 mmol), tetraline (0.1 mL), toluene (1.19 mL), and a stock solution of nBu$_3$N (0.40 mL, 401 mM in toluene) were added sequentially. The solution was evenly charged in eight glass tubes, and the tubes were sealed by flame under a nitrogen atmosphere. The tubes were immersed in thermostatic oil bath at 80 °C. In predetermined intervals, the polymerization was terminated by cooling the reaction mixtures to –78 °C. The monomer conversions were determined from the concentration of the residual monomer measured by ^{1}H NMR with tetraline as the internal standard (450 h, 94% conversion). The quenched reaction mixture was diluted with toluene (30 ml), washed with dilute citric acid and water to remove complex residues, evaporated to dryness under reduced pressure, and vacuum-dried to give the product polymers (0.11 g; M_n = 14,800, M_w/M_n = 1.15).

Measurements.

^{1}H and ^{13}C NMR spectra were recorded on a JEOL ESC-400 spectrometer, operating at 400 and 100 MHz for ^{1}H and ^{13}C, respectively. The number-average molecular weight (M_n) and molecular weight distribution (M_w/M_n) of the polymers were measured by size exclusion chromatography (SEC) using THF at a flow rate 1.0 mL/min at 40 °C on two polystyrene gel columns [Shodex KF-805L (pore size: 20–1000 Å; 8.0 mm i.d. × 30 cm)] that were connected to a JASCO PU-2080 precision pump and a JASCO RI-2031 detector. The columns were calibrated against standard poly(MMA) samples (Varian; M_p = 202–1677000, M_w/M_n = 1.02–1.23). The triad tacticity of the polymer was determined by the area of the carbonyl C=O carbons at 175–180 ppm in the ^{13}C NMR spectrum of the PMMA side chain.

Results and Discussion

1. Halogenation of Living Anionic PMMA Terminal

The author investigated the halogenation of a growing enolate species by quenching the stereospecific anionic living polymerization of MMA using several halogenating agents in the presence and absence of Lewis base additives. The stereospecific living anionic polymerization of MMA was first performed using previously reported systems, i.e., *t*BuMgBr in toluene or diphenylhexyllithium (DPHLi) in THF at –78 °C. In both cases, the polymers obtained after quenching with methanol as control experiments possessed controlled molecular weights, agreeing well with the calculated values, assuming that one molecule of the organometallic compound generates one living polymer chain, and narrow molecular weight distributions (MWDs) (M_w/M_n ~ 1.1) (entries 1 and 15 in Table 1). In addition to the livingness, the Mg/toluene-based system produced highly isotactic PMMA (*mm*/*mr*/*rr* = 91/8/1), while the Li/THF-based system produced syndiotactic PMMA (*mm*/*mr*/*rr* = 1/25/74), as reported in the literature.[3,4]

Table 1. Halogenation of Living Anionic PMMA Terminal [a]

entry	initiator/solvent	Halogenating Agent	additive	M_n [b]	M_w/M_n [b]	F_n(C–X) [c]
1	*t*BuMgBr/ toluene [d]	None	none	2400	1.14	–
2		Br_2		2300	1.23	0.46
3		CBr_4		2500	1.16	0.89
4		CCl_3Br		2500	1.17	0.90
5		CCl_4		2500	1.16	0.39
6		CBr_4	DBU	2500	1.18	1.00
7		CCl_3Br		2400	1.19	1.04
8		CCl_4		2800	1.19	0.90
9		CCl_3Br	TMG	2400	1.16	1.02
10		CCl_4		2600	1.19	0.95
11		CCl_3Br	Et_3N	2500	1.18	0.90
12			TMEDA	2500	1.24	0.99
13			PMDETA	2400	1.17	0.96
14			HMTETA	2600	1.19	0.86
15	DPHLi/THF [e]	None	none	2800	1.14	–
16		CCl_3Br		2900	1.14	0.95
17		CCl_4		2900	1.18	0.96
18		CCl_3Br	DBU	2700	1.12	0.94
19		CCl_4		3200	1.18	0.95

[a] $[M]_0/[I]_0$ = 25, $[I]_0/[\text{halogenating agent}]_{add}/[\text{additive}]_{add}$ = 1/40/5. [b] Determined by SEC using PMMA standards in THF. [c] Obtained from M_n(SEC)/M_n(NMR). [d] $[MMA]_0$ = 1.35 M, polymerization: 25 h (–78 °C), halogenation: 2 h (–78 °C) and then 23 h (–78 ~ 0 °C). [e] $[MMA]_0$ = 0.85 M, polymerization: 0.25 h (–78 °C), halogenation: 2 h (–78 °C), and then 23 h (–78 ~ 0 °C).

The author then examined a reaction to end-cap the living PMMA anions using an excess amount of Br_2, CBr_4, and CCl_3Br for bromination and CCl_4 for chlorination as the halonium cation source (40 eq. to the anionic initiator). These reactions result in forming carbon–halogen bonds at the terminal along with the formation of a metal halide or metal trihalomethide and further possible decomposition into a carbene species in the case of polyhalogenated compounds. When the anionic polymerization was nearly completed, these

halogenating agents were added directly to the polymerization mixture, which was maintained at –78 °C for 2 h and then gradually warmed to 0 °C for an additional 23 h to complete the end-capping reaction. In addition, the halogenation was also investigated in the presence of a series of Lewis bases, including 1,8-diazabicyclo[5.4.0]undec-7-ene (DBU), 1,1,3,3-tetramethylguanidine (TMG), Et_3N, *N,N,N',N'*-tetramethylenediamine (TMEDA), *N,N,N',N'',N''*-pentamethyldiethykenetriamine (PMDETA), and 1,1,4,7,10,10-hexamethyl-triethylenetetramine (HMTETA), which are used for similar end-functionalization reactions of the PMMA anion.[14] As shown in Table 1, the obtained polymers exhibited narrow MWDs and controlled M_n values that agreed well with the calculated values regardless of the initiating systems, the halogenating agents, and the additives.

Figure 1 presents the ^{1}H NMR spectra of the isotactic (A–C) and syndiotactic PMMAs (D–F) with hydrogen terminals obtained by quenching with methanol (A and D) and by using CCl_4 (B and E) or CCl_3Br (C and F) in the presence of DBU or TMG. The polymers gave signals characteristic of repeating PMMA units, i.e., methoxy (*c*), methylene (*a*), and α-methyl (*b*) protons, which exhibited typical spectral patterns depending on their tacticities. The polymers obtained using *t*BuMgBr (A–C) exhibited primarily *mm* α-methyl (1.2 ppm) and double-doublet methylene (1.5 and 2.2 ppm) protons, while those obtained using DPHLi (D–F) exhibited primarily *rr* α-methyl (0.9 ppm) and singlet methylene (1.8 ppm) protons.

In addition to these large peaks, small signals that were ascribed to the halide ω-end (C–X), such as $–OCH_3$ (c_2 or c_3, 3.8 ppm) and $–CH_2–$ (a_2 or a_3, 2.5–2.8 ppm) groups adjacent to chlorine (B and E) or bromine atoms (C and F), respectively, were observed. In contrast, the hydrogen terminal only exhibited the indicative C–H peak (*d*, 2.5 ppm) (A and D). The terminal halogen functionality [F_n(C–X)] at the ω-end was thus determined by comparing the M_n(NMR) values obtained from the peak intensity ratios of c_2 or c_3 to *c* against the M_n(SEC) measured by SEC based on the PMMA calibration [F_n(C–X) = M_n(SEC)/M_n(NMR)].

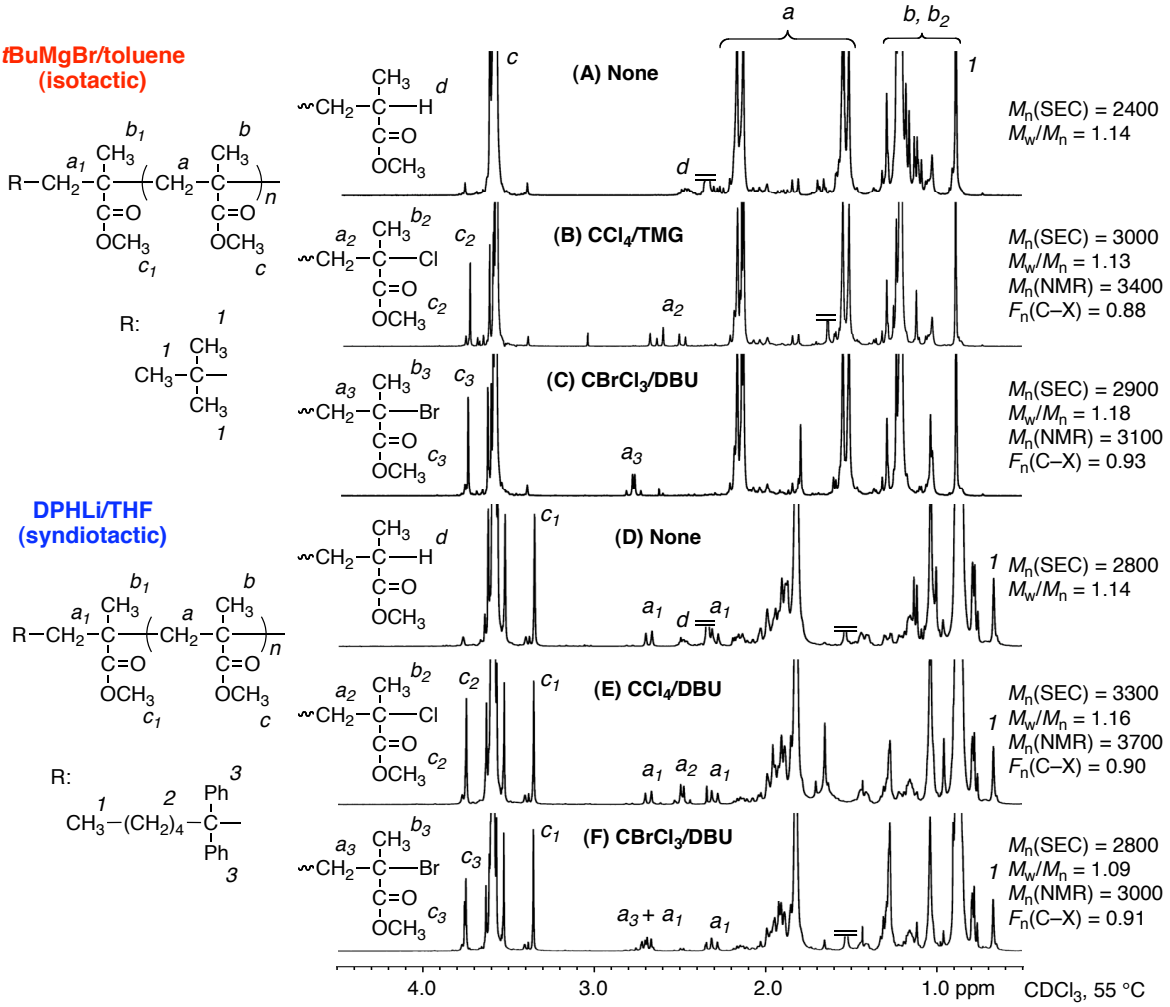

Figure 1. ^{1}H NMR spectra of PMMA-X (X = H, Cl and Br) obtained with *t*-BuMgBr in toluene (A–C) or diphenylhexyllithium in THF (D–F) at –78 °C using methanol (A and D), CCl_4 (B and E), or CCl_3Br (C and F) as the quenching agent in the presence of DBU or TMG (for halogenation).

The functionality depends on both the halogenating agents and the additives; Br_2 resulted in a lower functionality, as has been reported in non-stereospecific living anionic polymerizations of MMA,[11a] while the polyhalogenated compounds totally provided higher functionalities. The functionality of the terminal carbon–halogen bond obtained with the DPHLi/THF system was almost one regardless of the polyhalogenated compounds (entries 16 and 17 in Table 1). The *t*BuMgBr/toluene system mostly resulted in lower functionalities (entries 2–5),

especially for the least reactive halogenating agent, CCl_4. The lower functionality produced using *t*BuMgBr/toluene was most probably due to aggregation of the growing anionic species in the less polar solvent toluene. However, the functionality was improved with the addition of Lewis bases to enable nearly quantitative conversions into the C–X bonds. The functionalities of bromide with CCl_3Br or CBr_4 in the presence of such additives were near unity (entries 6, 7, 9 12, and13), and that of the chloride with CCl_4 was much higher (entries 8 and 10) than that in the absence of the additives. These additives probably coordinated with the magnesium or lithium countercation to result in both the disaggregation of the growing chain ends and the reactivity enhancement of the PMMA anion.

2. Ruthenium-Catalyzed Living Radical Polymerization from PMMA–X

Isotactic or syndiotactic PMMA–Br, which were obtained after halogenation of the stereoregular living anionic PMMA with CCl_3Br/DBU, were then employed as the macroinitiators for the living radical polymerization of styrene catalyzed by $RuCp^*Cl(PPh_3)_2$ with the *n*Bu_3N additive in toluene at 80 °C (Figure 2). In both cases, styrene was smoothly consumed to provide block copolymers consisting of isotactic or syndiotactic PMMA and polystyrene segments, and the SEC curves shifted to higher molecular weights while maintaining narrow MWDs. A small shoulder at high styrene conversions can be attributed to small amount of coupling reaction between the propagating radical chain-end of styrene. The monomer compositions of the obtained products were determined using ^{1}H NMR and were in good agreement with those calculated from the initial feed ratio of styrene to macroinitiator and the monomer conversions (Figure 3). These results also indicated efficient direct conversions of the growing living anionic species (~~~C^-) into covalent carbon–bromine bonds (~~~C–Br) that can be activated into the growing radical species using the transition metal complex in the subsequent metal-catalyzed living radical polymerizations.

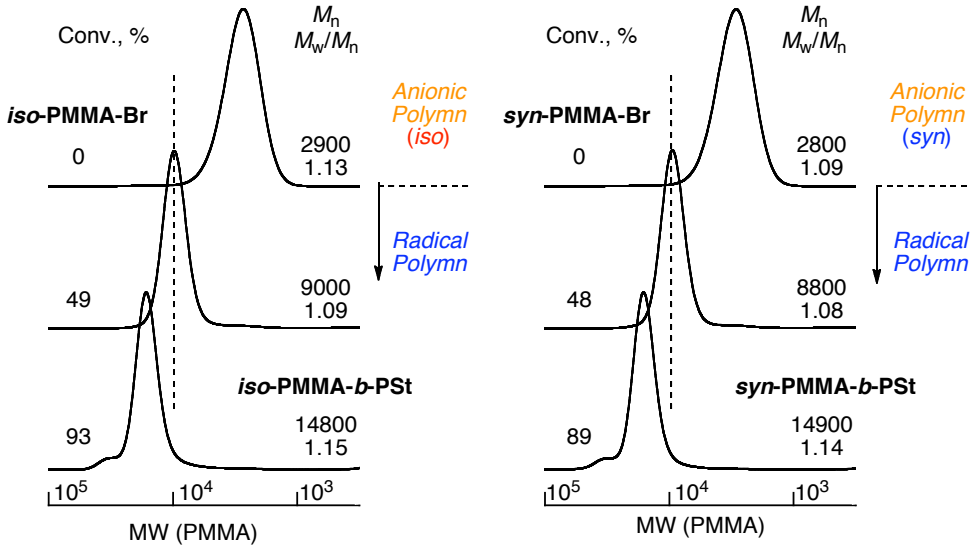

Figure 2. SEC curves of isotactic or syndiotactic PMMA-Br and PMMA-*b*-PSt obtained via the transformation from stereospecific living anionic polymerization of MMA to metal-catalyzed living radical polymerization of styrene: $[\text{styrene}]_0$ = 4.0 M, $[\text{PMMA–Br}]_0$ = 40 mM, $[\text{RuCp*Cl(PPh}_3)_2]_0$ = 4 mM, $[n\text{Bu}_3\text{N}]_0$ = 40 mM in toluene at 80 °C.

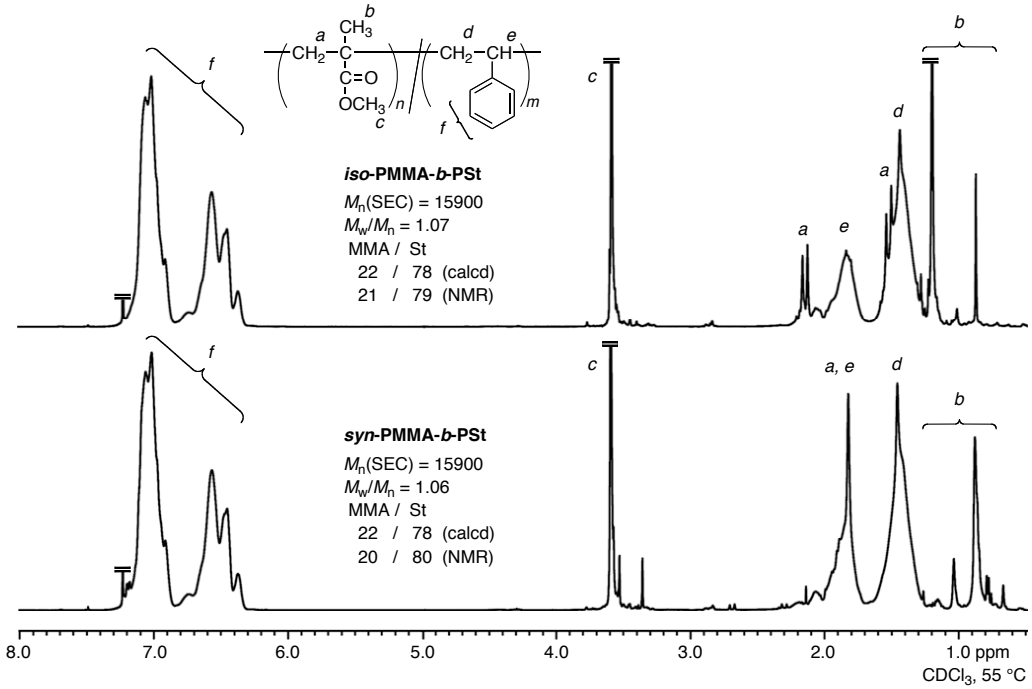

Figure 3. ^{1}H NMR spectra of isotactic or syndiotactic PMMA-*b*-polystyrene obtained via the transformation from living anionic polymerization of MMA to metal-catalyzed living radical polymerization of styrene (the same experiments as for Figure 2). See entries 7 and 16 in Table 1 for the synthetic conditions of isotactic and syndiotactic PMMA–Br.

A similar block ruthenium-catalyzed living radical polymerization of MMA was also attained via direct mechanistic transformation using isotactic or syndiotactic PMMA–X (X = Cl and Br) and Ru(Ind)Cl(PPh_3)$_2$ to produce stereoblock PMMAs. The tacticities of the stereoblock PMMAs were changed from highly isotactic or syndiotactic enchainment, produced by stereospecific anionic polymerization, into moderate syndiotactic enchainment by radical polymerization (Figures 4 and 5). Although stereoblock PMMAs have already been prepared through living anionic,[15] coordination,[16] and radical[17] polymerizations without converting the polarity of the growing chain end, this result can broaden the scope of producing stereoblock copolymers with different tacticities.

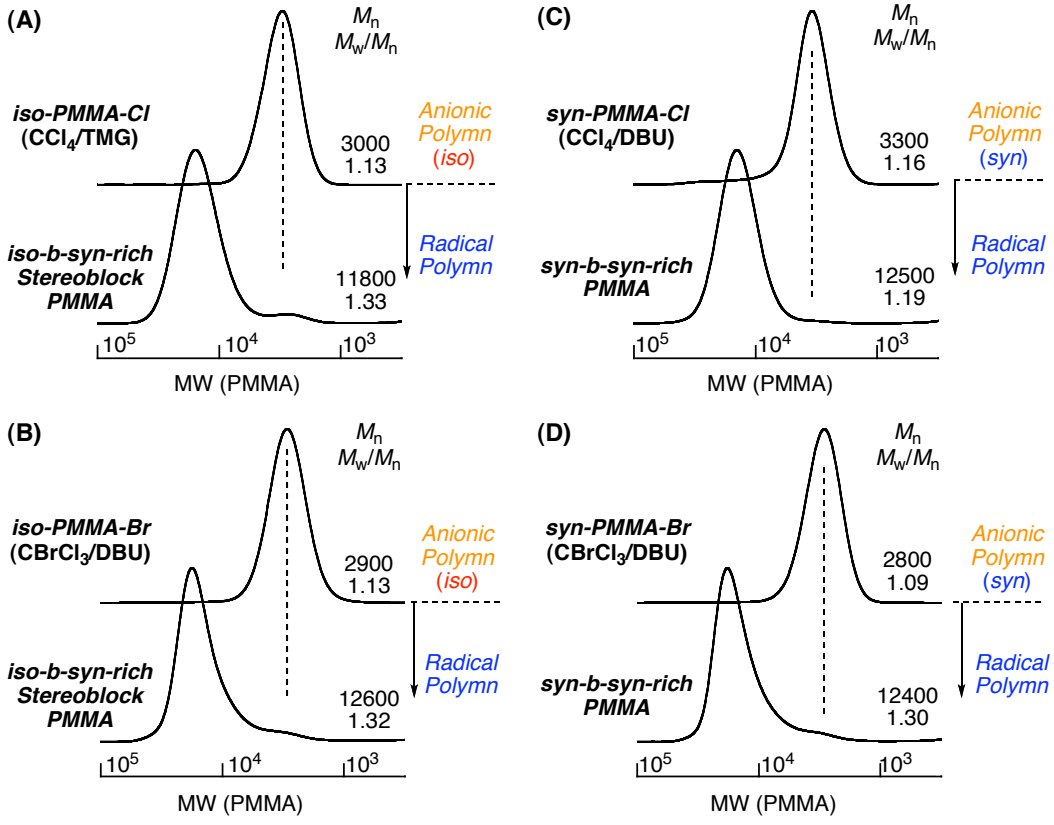

Figure 4. SEC curves of stereoblock PMMAs obtained by ruthenium-catalyzed living radical polymerization from isotactic PMMA–Cl (A), –Br (B) and syndiotactic PMMA–Cl (C), –Br (D): $[MMA]_0$ = 4.0 M, $[PMMA–X]_0$ = 40 mM, $[Ru(Ind)Cl(PPh_3)_2]_0$ = 4 mM, $[nBu_3N]_0$ = 40 mM in toluene at 80 °C. See entries 10, 7, 19, and 18 in Table 1 for the synthetic conditions of stereospecific PMMA–X in (A), (B), (C), and (D), respectively.

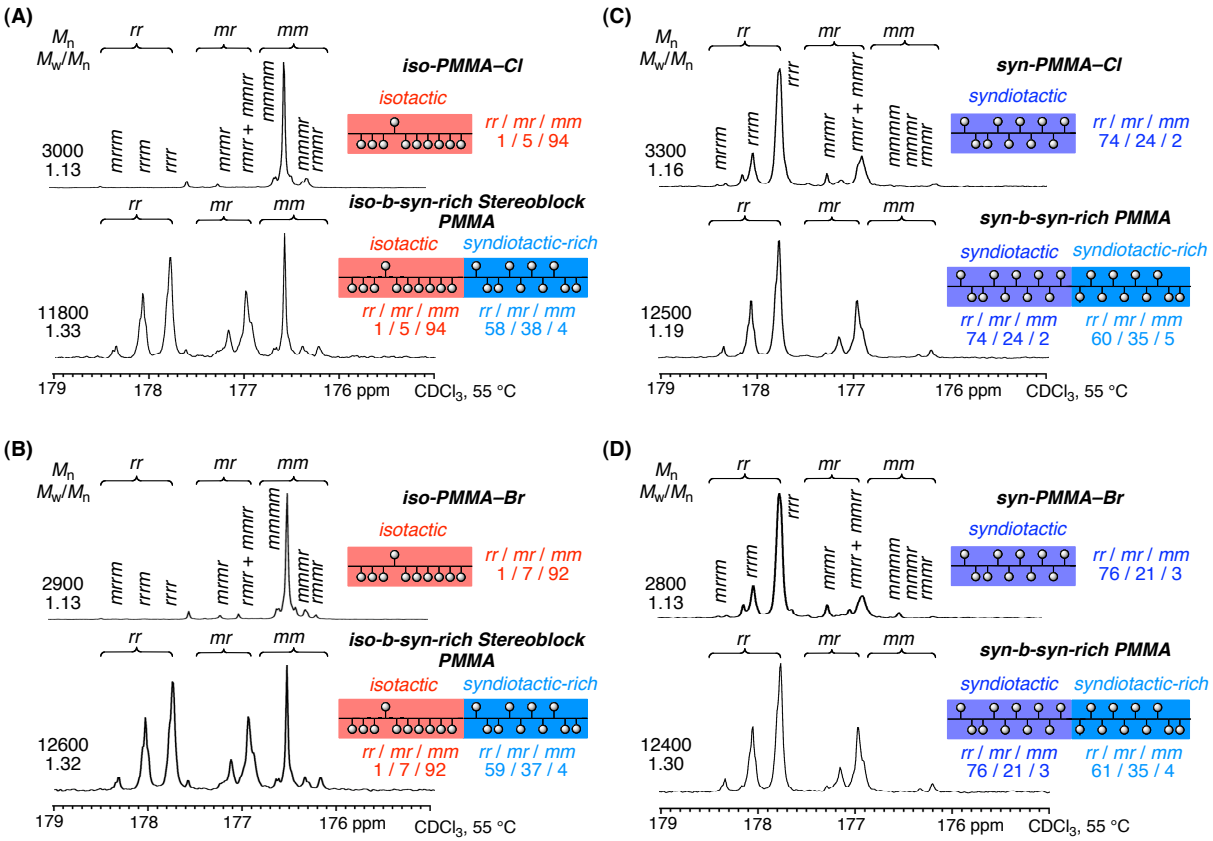

Figure 5. ^{13}C NMR spectra for the carbonyl carbons of isotactic or syndiotactic PMMA–X (X = Cl and Br) and stereoblock PMMAs obtained in the same experiment as for Figure 4

Conclusion

In summary, this study succeeded in the quantitative halogenation of the stereospecific living anionic PMMA-growing species by using appropriate halogenating agents and additives to produce highly isotactic or syndiotactic PMMAs with a covalent carbon–halogen terminal, which can be directly employed in subsequent metal-catalyzed living radical polymerizations. Thus, the direct mechanistic transformation from stereospecific living anionic polymerization into living radical polymerization was accomplished to produce block copolymers consisting of stereoregular PMMA segments and other radically polymerized segments, such as polystyrene and PMMA, with moderate syndiotacticity. This method not only developed a novel direct synthesis strategy for various block copolymers between living anionic and radical polymerizations, but it also

would construct novel higher-ordered structures or provide novel polymeric materials that originate from possible stereocomplex formations using block copolymers.

References

1. *Controlled and Living Polymerizations: From Mechanisms to Materials*; Müller A. H. E.; Matyjaszewski, K., Eds.; Wiley-VCH: Weilheim, Germany, 2008.
2. (a) Hatada, K.; Kitayama, T.; Ute, K. *Prog. Polym. Sci.* **1988**, *13*, 189–276. (b) Baskaran, D.; Müller, A. H. E. *Prog. Polym. Sci.* **2007**, *32*, 173–219.
3. (a) Goode, W. E.; Owens, F. H.; Fellmann, R. P.; Snyder, W. H.; Moore, J. E. *J. Polym. Sci.* **1960**, *46*, 317–331. (b) Nishioka, A.; Watanabe, H.; Abe, K.; Sono, Y. *J. Polym. Sci.* **1960**, *48*, 241–272. (c) Hatada, K.; Ute, K.; Tanaka, K.; Kitayama, T.; Okamoto, Y. *Polym. J.* **1985**, *17*, 977–980.
4. (a) Freyss, D.; Rempp, P.; Benoit, H. *J. Polym. Sci., Polym. Lett.* **1964**, *2*, 217–222. (b) Cao, Z-K.; Okamoto, Y.; Hatada, K. *Koubunshi Ronbunshu* **1986**, *12*, 857–861. (c) Ohata, M.; Ikeda, S.; Akatani, S.-i.; Isono, Y. *Macromolecules* **1992**, *25*, 5131–5136.
5. (a) Karasz, F. E.; MacKnight, W. J. *Macromolecules* **1968**, *1*, 537–540. (b) Allen, P. E. M.; Host, D. M.; Truong, V. T.; Williams, D. R. G. *Eur. Polym. J.* **1985**, *21*, 603–610. (c) Kitayama, T.; Masuda, E.; Yamaguchi, M.; Nishiura, T.; Hatada, K. *Polym. J.* **1992**, *24*, 817–827.
6. (a) Spěváček, J.; Schneider, K. *Adv. Colloid Interface Sci.* **1987**, *27*, 81–150. (b) te Nijenhuism K. *Adv. Polym. Sci.* **1997**, 130, 67–81. (c) Hatada, K.; Kitayama, T. *Polym. Int.* **2000**, *49*, 11–47.
7. (a) Kamigaito, M.; Ando, T.; Sawamoto, M. *Chem. Rev.* **2001**, *101*, 3689–3745. (b) Matyjaszewski, K.; Xia, J. *Chem. Rev.* **2001**, *101*, 2921–2990. (c) Hawker, C. J.; Bosman, A. W.; Harth, E. *Chem. Rev.* **2001**, *101*, 3661–3688. (d) Moad, G.; Rizzardo, E.; Thang, S. H. *Aust. J. Chem.* **2005**, *58*, 379–410.

8. (a) Habaue, S.; Okamoto, Y. *Chem. Rec.* **2001**, *1*, 46–52. (b) Satoh, K.; Kamigaito, M. *Chem. Rev.* **2009**, *109*, 5120–5156.

9. (a) Yagci, Y.; Tasdelen, M. A. *Prog. Polym. Sci.* **2006**, *31*, 1133–1170. (b) Hadjichristidis, N.; Pitsikalis, M.; Iatrou, H. *Adv. Polym. Sci*. **2005**, *189*, 1–124.

10. (a) Coca, S.; Matyjaszewski, K. *Macromolecules* **1997**, *30,* 2808–2810. (b) Chen, X.; Ivan, B.; Kops, J.; Batsberg, W. *Macromol. Rapid. Commun*. **1998**, *19*, 585–589. (c) Lu, J.; Liang, H.; Li, A.; Cheng, Q. *Eur. Polym. J*. **2004**, *40*, 397–402. (d) Toman, L.; Janata, M.; Spěváček, J.; Vlček, P.; Látalová, P.; Masař, B.; Sikora, A. *J. Polym. Sci., Part A: Polym. Chem*. **2004**, *42*, 6096–6108. (e) Kumagai, S.; Nagai, K.; Satoh, K.; Kamigaito, M. *Macromolecules* **2010**, *43*, 7523–7531. (f) Chapter 3 of this thesis: Aoshima, H.; Satoh, K.; Kamigaito, M. *Macromol. Symp.* **2013**, *Macromol. Symp*. **2013**, *323*, 64–74.

11. (a) Masař, B.; Vlček, P.; Kříž, J. *J. Appl. Polym. Sci.* **2001**, *81*, 3514–3522. (b) Liu, F.; Liu, B.; Luo, B.; Ying, SK. *Chem. Res. Chin. U*. **2000**, *16*, 72–77.

12. (a) Hazer, B.; Çakmak, I.; Küçükyavuz, S.; Nugay, T. *Eur. Polym. J*. **1992**, *28*, 1295–1297. (b) Acar, M. H.; Matyjaszewski, K. *Macromol. Chem. Phys.* **1999**, *200*, 1094–1100.

13. (a) Zefirov, N. S.; Makhon'kov, D. I. *Chem. Rev.* **1982**, *82*, 615–624. (b) Abele, E.; Lukevics, E. *Org. Prep. Proced. Int.* **1999**, *31*, 359–377.

14. (a) Hatada, K.; Kitayama, T.; Ute, K.; Masuda, E; Shinozaki, T.; Yamamoto, M. *Polym. Bull.* **1989**, *21*, 165–172. (b) Kitayama, T.; Nakagawa, O.; Kishiro, S.; Nishimura, T.; Hatada, K. *Polym. J*. **1993**, *25*, 707–720.

15. (a) Doherty, M. A.; Hogen-Esch, T. E. *Macromol. Chem.* **1986**, *187*, 61–69. (b) Kitayama, T.; Fujimoto, N.; Yanagida, T.; Hatada, K. *Polym. Int.* **1994**, *33*, 165–170.

16. (a) Bolig, A. D.; Chen, E. Y.-X. *J. Am. Chem. Soc*. **2002**, *124*, 5612–5613. (b) Chen, E. Y.-X.; Cooney, M. J. *J. Am. Chem. Soc*. **2003**, *125*, 7150–7151.

17. (a) Ishitake, K.; Satoh, K.; Kamigaito, M.; Okamoto, Y. *Angew. Chem. Int. Ed.* **2009**, *48*, 1991–1994. (b) Ishitake, K.; Satoh, K.; Kamigaito, M.; Okamoto, Y. *Macromolecules*

2011, *44*, 9108–9117. (c) Ishitake, K.; Satoh, K.; Kamigaito, M.; Okamoto, Y. *Polym. Chem.* **2012**, *3*, 1750–1757.

List of Publications

Papers

Chapter 1

"Iron(III) Chloride/R–Cl/Tributylphosphine for Metal-Catalyzed Living Radical Polymerization: A Unique System with a Higher Oxidation State Iron Complex"

Kotaro Satoh, Hiroshi Aoshima, Masami Kamigaito

J. Polym. Sci., Part A: Polym. Chem., **2008**, *46*, 6358-6363.

Chapter 2

"A Simple Combination of Higher Oxidation State FeX_3 and Phosphine and Amine Ligand for Living Radical Polymerization of Styrene and (Meth)acrylates:"

Hiroshi Aoshima, Kotaro Satoh, Tomonari Umemura, Masami Kamigaito

Polym. Chem., submitted.

Chapter 3

"In-Situ Direct Mechanistic Transformation from $FeCl_3$-Catalyzed Living Cationic to Radical Polymerizations"

Hiroshi Aoshima, Kotaro Satoh, Masami Kamigaito

Macromol. Symp. **2013**, *323*, 64–74.

Chapter 4

"Interconvertible Dual Active Spices during Vinyl Polymerization: Giving Jekyll-and-Hyde Nature to Dormant Covalent Bond"

Kotaro Satoh, Hiroshi Aoshima, Mineto Uchiyama, Masami Kamigaito

in preparation

Chapter 5

"Interconvertible Concurrent Cationic and Radical Polymerization of Various Monomers for Synthesis of Novel Copolymers"

Hiroshi Aoshima, Kotaro Satoh, Masami Kamigaito

in preparation

Chapter 6

"Direct Mechanistic Transformation from Isotactic or Syndiotactic Living Anionic Polymerizations of Methyl Methacrylate into Metal-Catalyzed Living Radical Polymerizations"

Hiroshi Aoshima, Kotaro Satoh, Masami Kamigaito

ACS Macro Lett. **2013**, *2*, 72–76.

Acknowledgments

This thesis presents the studies that the author carried out from 2007 to 2013 at Department of Applied Chemistry, Graduate School of Engineering, Nagoya University under the direction of Professor Masami Kamigaito.

First of all, the author would like to express his deepest and sincere gratitude to Professors Masami Kamigaito for his constant guidance and encouragement throughout the course work. The author is also deeply grateful to Associate Professor Kotaro Satoh for his helpful and convincing suggestions, stimulating discussions, and his kind guidance in experimental techniques. Very sincere thanks to Dr. Kanji Nagai for his help and advice.

The author would like to express his special thanks to Professors Eiji Yashima and Kenichiro Itami for their valuable comments and suggestions as his dissertation committee members.

It is pleasure to express his appreciation to Drs. Tomoyuki Ikai, Kazuhiko Koumura, Tor Kit Goh, Arihiro Kanazawa, Masato Mizutani, and Kenji Ishitake. The author is sincere thanks to Messrs. Masaru Matsuda, Shinya Kumagai, Kazunori Mukunoki, Daisuke Ito, Tsuyoshi Hamada, Dong-Hyoung Lee, Kenta Ishiduka, Yuya Terao, Satoshi Motoda, Mineto Uchiyama, Satoshi Okazaki, Takamasa Soejima, Masato Handa, Toshifumi Kondo, Jing M. Ren and all colleagues for useful suggestion and sharing his pleasant student life.

The author is deeply indebted to all ‘‘ORION’’ members; Professors Yoshio Okamoto (Nagoya University and Harbin Engineering University), Mitsuo Sawamoto (Kyoto University), Yoshitsugu Hirokawa (The University of Shiga Prefecture), Sadahito Aoshima (Osaka University), and Eiji Yashima (Nagoya University), and all members of their groups for their

meaningful discussion and kind encouragements. The author especially wishes to thank Dr. Muneki Ishio (Kuraray, Co., Ltd), Dr. Shohei Ida (The University of Shiga Prefecture), Dr. Kazuhiro Nakatani (Mitsubishi Chemical Co., Ltd), Hiroaki Shimomoto (Ehime University), Mr. Yasushi Ishido (Osaka University), and Mr. Yu Shinke (Osaka University) for friendly association and useful discussion.

The author also acknowledges Dr. Yuka Takasaki and Associate Professor Tomonari Umemura (Nagoya University) for the measurements of inductively coupled plasma mass (ICP-MS) spectrometry in Chapter 2.

The author is very grateful to the Fellowships of the Global COE program ‘‘Elucidation and Design of Materials and Molecular Functions’’ (2010-2012), Program for Leading Graduate Schools ‘‘Integrative Graduate Education and Research Program in Green Natural Sciences’’ (2012-2013), and the Research Fellowship of the Japan Society for the Promotion of Science for Young Scientists (2012-2013).

Finally, the author wishes to express his deep appreciation to his parents, Mr. Tamio Aoshima and Mrs. Setsuko Aoshima, his brother, Mr. Tsutomu Aoshima, and his sister, Ms. Sumiyo Aoshima for their constant care and affectionate encouragement.

January 2013

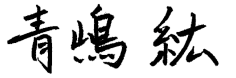

Hiroshi AOSHIMA